

EXPERIMENTAL INVESTIGATIONS ON SINGLE/TWO PHASE CARBON DIOXIDE BASED NATURAL CIRCULATION LOOPS

Thesis

Submitted in partial fulfillment of the requirement for the degree of

DOCTOR OF PHILOSOPHY

by

THIPPESWAMY L. R.

(135022ME13F10)



DEPARTMENT OF MECHANICAL ENGINEERING
NATIONAL INSTITUTE OF TECHNOLOGY KARNATAKA
SURATHKAL, MANGALORE – 575025

DECEMBER 2020

DECLARATION

I hereby declare that the Research Thesis entitled “**Experimental investigations on single/two phase carbon dioxide based natural circulation loops**” which is being submitted to the **National Institute of Technology Karnataka**, Surathkal in partial fulfillment of the requirements for the award of the Degree of **Doctor of Philosophy in Mechanical Engineering** is a *bonafide report of the research work carried out by me*. The material contained in this Research Thesis has not been submitted to any University or Institution for the award of any degree.

Register Number : 135022ME13F10

Name of the Research Scholar : THIPPESWAMY L. R.

Signature of the Research Scholar :

Department of Mechanical Engineering

Place: NITK, Surathkal

Date: 29/12/2020

C E R T I F I C A T E

I hereby *declare* that the Research Thesis entitled “**Experimental investigations on single/two phase carbon dioxide based natural circulation loops**” which is being submitted to the **National Institute of Technology Karnataka, Surathkal**, in partial fulfillment of the requirements for the award of the Degree of **Doctor of Philosophy in Mechanical Engineering** is a *bonafide report of the research work carried out by me*. The material contained in this Research Thesis has not been submitted to any University or Institution for the award of any degree.

R e s e a r c h G u i d e

Dr. AJAY KUMAR YADAV

Assistant Professor

Department of Mechanical Engineering

National Institute of Technology Karnataka, Surathkal

Chairman-DRPC

Department of Mechanical Engineering

National Institute of Technology Karnataka, Surathkal

Date: 29/12/2020

DEDICATED TO
MY BELOVED
FAMILY MEMBERS
&
ALL OF MY TEACHERS

ACKNOWLEDGMENT

It is a great pleasure for me to express my deep sense of gratitude to my supervisor **Dr. Ajay Kumar Yadav**, for his excellent, inspiring guidance, valuable suggestions and encouragement rendered throughout the course of my thesis work. I am thankful to Professor **Dr. Shrikantha S. Rao**, Professor and Head, Department of Mechanical Engineering, for the support and providing facilities required for the successful completion of this research work. I take this opportunity to acknowledge the former HODs, Mechanical engineering, **Dr. Gangadharan K.V. and Dr. Narendranath S.**, for their support and encouragement. I wish to thank my RPAC members **Dr. N. Gnanasekaran** and **Dr. Harshavardhan**, for their valuable suggestions during my research work assessment meet. My special thanks to **Dr. Kumar G. N.**, and my M.E., guide **Dr. Ramesh D.K.**, UVCE, for their useful motivations to join research.

The present work is carried out under a project sponsored by **Science and Engineering Research Board, Department of Science and Technology, Government of India (SB/FTP/ETA-443/2013)**. The financial support offered by **DST-SERB** is gratefully acknowledged.

I acknowledge my parents, **Rudrappa L.T** and **Gangamma**, for their inspiration and support throughout my studies. Words cannot explain my gratitude to my wife **Rashmi** and son **Chirantan** for supporting me and making my stay pleasant always. My most profound appreciation goes to my elder brother **Karibasavaraja L.R.** Deputy Manager, KMF, Karnataka, for his unconditional support and words of advice. I am grateful to my younger brother **Shivakumar**, sisters **Sarala**, my brother-in-law **Prasanna Kumar** for always encouraging and believing in me. I extend my sincere thanks to my father-in-law **Prabhakar C.V** for his kind support.

My special thanks to my friends Madagonda Biradar, TabishWahidi, Shankar Kodate, Nidhul K, Dr.Venkatesh Lamani, Rudraswamy (Advocate), Pradeep G T, Sangappa, Bhanuprakash, Nuthanprasad, Praveen T. R., Libin, Abdul Buradi, Vasishta, Kalinga, Shashikumar C M, Dr.Harshakumar, Dr.Vignesh, Dr.Shivaprasad K V, Dr.Kotresha, Dr.Vishweshwara, Narendran, PrakashJadhav, Deepak Kolke, Jagadish, Dr.Madhu

Sudhan, Dr.Prashanth, Dr.Gajanan Anne, Mallikarjuna, Dr.Mahanthesh, Rudramoorthy, Jayashish Pandey, Santosh Naik, and list seems to be endless.

I am incredibly grateful to the Mechanical Engineering department, the NITK, the faculty and the non-teaching staff for providing all the facilities for my research work.

I acknowledge with gratitude to all others who have helped directly or indirectly in completing my thesis successfully.

Thippeswamy L. R.

ABSTRACT

The natural circulation loop (NCL) is a highly reliable and noise-free heat transfer device due to the absence of moving components. Working fluid used in the natural circulation loop plays an important role in enhancing the heat transfer capability of the loop. This experimental study investigates the thermo-hydraulic performance of subcritical and supercritical CO₂ based natural circulation loop (NCL). In the subcritical region, different phases of CO₂ such as liquid, vapour and two phase are considered for the study. Operating pressures and temperatures are varied in such a way that the loop fluid should remain in the specified state (subcooled liquid, two phase, superheated vapor, supercritical).

Water and methanol are used as external fluids in cold and hot heat exchangers for temperatures above and below 0 °C respectively, depending on the operating temperature. For loop fluids, the performance of CO₂ is compared with water for above zero and with brine solution for the subzero case. Further, the impact of loop operating pressure (35-90 bar) on the performance of the system is also studied.

Results are obtained for hot heat exchanger inlet temperature ranging from 5 to 70 °C and cold heat exchanger inlet temperature from -18 to 32 °C. It was observed that the maximum heat transfer rates in the case of subcritical vapor, subcritical liquid, two-phase and supercritical CO₂ based systems are 400%, 500%, 900%, and 800% higher than the water/brine-based system respectively.

However, the instability associated with a regular change in fluid flow direction due to an imbalance between friction and buoyant forces is a major disadvantage of NCL. Tilting the entire loop by a certain angle is one of the method to reduce the instability of NCL, with an inherent penalty in heat transfer and pressure drop. Pressure drop and heat transfer performance of CO₂ based NCL with end heat exchangers, operating under subcritical (vapour, liquid and two phase) and supercritical conditions for various tilt angles (0°, 30°, 45°) in XY and YZ planes, have been investigated.

Results are obtained for different operating pressures (35-90 bar) and temperatures (-18 to 70 °C). Results show that the effect of tilting on heat transfer rate, pressure drop and temperature distribution in the case of supercritical, subcritical liquid, subcritical

vapour and two phase CO₂ based system shows a small variation on the performance of the loop. Hence, loop tilting could be a one of the solution to reduce the instability problem associated with NCL without compromising the performance of the loop.

Keywords: Natural circulation loop, Supercritical CO₂, Two phase flow, Heat transfer performance, Pressure drop, and Tilt effect.

TABLE OF CONTENTS

DECLARATION	
CERTIFICATE	
ACKNOWLEDGEMENTS	
ABSTRACT	
TABLE OF CONTENTS	i
LIST OF TABLES	vii
LIST OF FIGURES	ix
NOMENCLATURE	xv
1 INTRODUCTION	1
1.1 TYPES OF REFRIGERATION SYSTEMS	2
1.1.1 Advantages of indirect refrigeration systems	3
1.1.2 Disadvantages of indirect refrigeration systems	3
1.2 NATURAL CIRCULATION LOOPS	4
1.2.1 Different configurations of NCLs	4
1.2.2 Advantages and disadvantages of NCL	6
1.2.3 Applications of NCL	7
1.3 SELECTION OF WORKING FLUIDS FOR NATURAL CIRCULATION LOOPS	7
1.4 COMMONLY USED SECONDARY FLUIDS	7
1.5 SUITABILITY OF CO ₂ AS A SECONDARY FLUID	9
1.6 TWO-PHASE NATURAL CIRCULATION	10
1.7 INSTABILITY IN NCL	11
1.8 STRUCTURE OF THE THESIS	12

2	LITERATURE	13
2.1	SECONDARY COOLANT SYSTEMS	13
2.2	NATURAL CIRCULATION LOOPS	14
2.2.1	Single phase natural circulation loops	15
2.2.2	Two phase natural circulation loops	16
2.3	APPLICATIONS OF NCL IN DIFFERENT ENGINEERING FIELDS	17
2.4	APPLICATION AREAS OF CO ₂ BASED SYSTEMS	18
2.5	COMMERCIAL ASPECTS OF CO ₂ SYSTEMS	20
2.6	CO ₂ BASED SECONDARY LOOP SYSTEMS	21
2.7	HIGH PRESSURE SAFETY ISSUES	22
2.8	INSTABILITY IN NCL	23
2.9	RESEARCH GAP AND OBJECTIVES	24
3	EXPERIMENTAL FABRICATION AND PROCEDURE	27
3.1	INTRODUCTION	27
3.2	THE EXPERIMENTAL TEST FACILITY	27
3.3	THE EXPERIMENTAL TEST FACILITY FOR TILTING	34
3.4	ERROR ANALYSIS	37
3.5	EXPERIMENTAL PROCEDURE	38
4	EXPERIMENTAL INVESTIGATION ON SUPERCRITICAL CO₂ BASED NCL	39
4.1	INTRODUCTION	39
4.2	HEAT TRANSFER RATE AND PRESSURE DROP OF CO ₂ BASED NCL AT DIFFERENT OPERATING PRESSURE AND TEMPERATURES	40
4.3	TEMPERATURE DISTRIBUTION OF CO ₂ BASED NCL AT DIFFERENT OPERATING PRESSURE	42

4.4	TILT ANGLE EFFECT STUDY OF SUPERCRITICAL CO ₂ BASED NCL	43
4.4.1	Effect of tilt angle on heat transfer rate at different operating pressures	46
4.4.2	Effect of tilt angle on pressure drop at different operating pressures	48
4.4.3	Effect of tilt angle on temperature distribution along the loop at different operating pressures	50
4.4.4	Effect of HHX water inlet temperature on heat transfer rate at different tilt angles and different operating pressures	52
4.5	HEAT TRANSFER AND PRESSURE DROP COMPARISON OF SUPERCRITICAL BASED CO ₂ BASED NCL WITH WATER BASED NCL	54
4.6	SUMMARY	56
5	EXPERIMENTAL INVESTIGATION OF SINGLE PHASE (SUBCRITICAL LIQUID/VAPOUR) CO₂ BASED NCL	57
5.1	INTRODUCTION	57
5.2	LOOP FLUID IN SUBCRITICAL VAPOUR CONDITION	58
5.2.1	Heat transfer rate and pressure drop of CO ₂ based NCL at different operating pressure and temperatures	58
5.2.2	Temperature distribution of subcritical vapour CO ₂ based NCL at different operating pressure	60
5.2.3	Effect of tilt angle	61
5.2.3.1	Effect of tilt angle on heat transfer rate at different operating pressures	61
5.2.3.2	Effect of tilt angle on pressure drop at different operating pressures	63
5.2.3.3	Effect of HHX water inlet temperature on heat transfer rate at different tilt angles and different operating pressures	66
5.2.4	Heat transfer and pressure drop comparison of subcritical vapour	

CO ₂ based NCL with water based NCL	67
5.3 LOOP FLUID IN SUBCRITICAL LIQUID CONDITION	70
5.3.1 Heat transfer rate and pressure drop of CO ₂ based NCL at different operating pressure and temperatures	70
5.3.2 Temperature distribution of subcritical liquid CO ₂ based NCL at different operating pressure	72
5.3.3 Effect of tilt angle	73
5.3.3.1 Effect of tilt angle on heat transfer rate at different operating pressures	73
5.3.3.2 Effect of tilt angle on pressure drop at different operating pressures	74
5.3.3.3 Effect of tilt angle on temperature distribution along the loop at different operating pressures	75
5.3.4 Heat transfer and pressure drop comparison of subcritical liquid CO ₂ based NCL with brine based NCL	77
5.4 SUMMARY	80
6 EXPERIMENTAL INVESTIGATION ON TWO PHASE CO₂ BASED NATURAL CIRCULATION LOOP	81
6.1 INTRODUCTION	81
6.2 HEAT TRANSFER RATE AND PRESSURE DROP OF CO ₂ BASED NCL AT DIFFERENT OPERATING PRESSURE AND TEMPERATURES	82
6.3 TEMPERATURE DISTRIBUTION OF TWO PHASE CO ₂ BASED NCL AT DIFFERENT OPERATING PRESSURE	84
6.4 TILT ANGLE EFFECT STUDY ON TWO PHASE GAS CO ₂ BASED NCL	85
6.4.1 Effect of tilt angle on heat transfer rate at different operating pressures	86
6.4.2 Effect of tilt angle on pressure drop at different operating pressures	87

6.4.3	Effect of tilt angle on temperature distribution along the loop at different operating pressures	88
6.4.4	Effect of HHX water inlet temperature on heat transfer rate at different tilt angles and different operating pressures	91
6.5	HEAT TRANSFER AND PRESSURE DROP COMPARISON OF TWO PHASE CO ₂ BASED NCL WITH BRINE BASED NCL	92
6.6	SUMMARY	94
7	CONCLUSIONS	97
7.1	CONCLUSIONS	97
7.1.1	Experimental analysis of supercritical CO ₂ with end heat exchangers	97
7.1.2	Experimental analysis of subcritical CO ₂ (liquid, vapor, and two-phase) with end heat exchangers	98
7.2	SCOPE OF FUTURE WORK	99
	REFERENCES	101
	LIST OF PUBLICATIONS	
	BIODATA	

LIST OF TABLES

Table 1.1	Property comparison of different secondary fluids (CoolPack, 2000; NIST Standard Reference Database, 2006)	8
Table 1.2	CO ₂ Properties – a comparison (Lorentzen et al., 1993; Riffat et al., 1997)	10
Table 3.1	Geometrical parameters of the experimental setup	31
Table 3.2	Range of operating parameters considered during study	32
Table 3.3	Equipment details used for experimentation	33
Table 4.1	Water properties variation with pressure	54
Table 4.2	Comparison of the properties of supercritical CO ₂ at different pressures with water at atmospheric pressure for different operating temperatures	56
Table 5.1	Comparison of the properties of subcritical vapour CO ₂ at different pressures with water at atmospheric pressure for different operating temperatures	69
Table 5.2	Brine properties variation with pressure	78
Table 5.3	Comparison of the properties of subcritical liquid CO ₂ at different pressures with brine at atmospheric pressure for different operating temperatures	79
Table 6.1	Operating parameters for two phase CO ₂	83
Table 6.2	Brine properties variation with pressure	93

LIST OF FIGURES

Figure 1.1	Indirect refrigeration system with forced circulation type secondary loop	3
Figure 1.2	Evacuated tube solar water heaters	4
Figure 1.3	Classification of Natural Circulation Loops (Vijayan 2007)	5
Figure 1.4	Different NCL models	6
Figure 1.5	Phase diagram of CO ₂ (Kim <i>et al.</i> , 2004)	9
Figure 1.6	Thermo-hydraulic behavior of NCL: (a) Stable case, and (b) Unstable case (Welander 1967)	11
Figure 3.1	Schematic of the NCL with end heat exchangers	28
Figure 3.2	Cross section view of the heat exchanger	28
Figure 3.3	Experimental setup photographic view:(a) Without insulation, (b) With one layer of asbestos rope insulation	29
Figure 3.4	Experimental setup photographic view:(a) Differential pressure transducer, (b) CO ₂ charging line and thermocouple arrangement	29
Figure 3.5	Equipments used for test facility:(a) Safety valve, (b) Pressure gauge, (c) Loop base	30
Figure 3.6	Equipments used for test facility (a) Thermostatic bath, (b) Vacuum pump (c) DAQ	31
Figure 3.7	Experimental setup	32
Figure 3.8	Schematic representation of experimental setup at XY-30° position	34
Figure 3.9	Schematic representation of experimental setup at XY-45° position	35
Figure 3.10	Schematic of the NCL:(a) YZ 30° position (a)YZ 45° position	36
Figure 3.11	Photographic view of tilting arrangement:(a) XY plane, (b) YZ plane	36
Figure 4.1	Variation of heat transfer rate of CO ₂ at different operating pressures and at different HHX inlet temperatures	41

Figure 4.2	Variation of heat transfer rate of CO ₂ at different operating pressures and at different HHX inlet temperatures	41
Figure 4.3	Variation of temperature along the loop at different operating pressures and different HHX inlet temperatures at (a) 75 bar, (b) 80 bar and (c) 90 bar	43
Figure 4.4	Experimental setup at XY-30° position	44
Figure 4.5	Experimental setup at YZ-30° position	45
Figure 4.6	Variation of heat transfer rate of CO ₂ at different pressures and $T_H = 50$ °C in (a) XY-plane and (b) YZ-plane	46
Figure 4.7	Variation of heat transfer rate of CO ₂ at different pressures and $T_H = 60$ °C in (a) XY-plane and (b) YZ-plane	47
Figure 4.8	Variation of heat transfer rate of CO ₂ at different pressures and $T_H = 70$ °C in (a) XY-plane and (b) YZ-plane	47
Figure 4.9	Pressure drop comparison of CO ₂ at different pressures and $T_H = 40$ °C in (a) XY-plane and (b) YZ-plane	48
Figure 4.10	Pressure drop comparison of CO ₂ at different pressures and $T_H = 50$ °C in (a) XY-plane and (b) YZ-plane	49
Figure 4.11	Pressure drop comparison of CO ₂ at different pressures and $T_H = 60$ °C in (a) XY-plane and (b) YZ-plane	49
Figure 4.12	Pressure drop comparison of CO ₂ at different pressures and $T_H = 70$ °C in (a) XY-plane and (b) YZ-plane	50
Figure 4.13	Variation of temperature along the loop at 90 bar in (a) XY-plane and (b) YZ-plane	51
Figure 4.14	Variation of temperature along the loop at 80 bar in (a) XY-plane and (b) YZ-plane	51
Figure 4.15	Variation of temperature along the loop at 75 bar in (a) XY-plane and (b) YZ-plane	52
Figure 4.16	Effect of HHX inlet temperature on heat transfer at different operating pressure (a) 90 bar, (b) 80 bar, and (c) 75 bar	53
Figure 4.17	Variation of heat transfer rate for water and supercritical CO ₂ at different pressure	54

Figure 4.18	Variation of pressure drop for water and supercritical CO ₂ at different pressure	55
Figure 5.1	Variation of heat transfer rate of CO ₂ at different operating pressures and at different HHX inlet temperatures	59
Figure 5.2	Variation of pressure drop of CO ₂ at different operating pressures and at different HHX inlet temperatures	59
Figure 5.3	Variation of temperature along the loop at different HHX inlet temperatures and different operating pressures (a) 40 bar, (b) 50 bar, (c) 60 bar and (d) 70 bar	60
Figure 5.4	Variation of heat transfer rate of CO ₂ at different pressures and $T_H = 42$ °C in (a) XY-plane and (b) YZ-plane	62
Figure 5.5	Variation of heat transfer rate of CO ₂ at different pressures and $T_H = 50$ °C in (a) XY-plane and (b) YZ-plane	62
Figure 5.6	Variation of heat transfer rate of CO ₂ at different pressures and $T_H = 60$ °C in (a) XY-plane and (b) YZ-plane	63
Figure 5.7	Variation of heat transfer rate of CO ₂ at different pressures and $T_H = 70$ °C in (a) XY-plane and (b) YZ-plane	63
Figure 5.8	Pressure drop comparison of CO ₂ at different pressures and $T_H = 40$ °C in (a) XY-plane and (b) YZ-plane	64
Figure 5.9	Pressure drop comparison of CO ₂ at different pressures and $T_H = 50$ °C in (a) XY-plane and (b) YZ-plane	64
Figure 5.10	Pressure drop comparison of CO ₂ at different pressures and $T_H = 60$ °C in (a) XY-plane and (b) YZ-plane	65
Figure 5.11	Pressure drop comparison of CO ₂ at different pressures and $T_H = 70$ °C in (a) XY-plane and (b) YZ-plane	66
Figure 5.12	Effect of HHX inlet temperature on heat transfer at different operating pressure (a) 40 bar, (b) 50 bar, (c) 60 bar and (d) 70 bar	67
Figure 5.13	Variation of heat transfer rate for water and subcritical vapour CO ₂ at different pressure	68

Figure 5.14	Variation of pressure drop for water and subcritical vapor CO ₂ at different pressure	69
Figure 5.15	Variation of heat transfer rate of CO ₂ at different operating pressures and at different HHX inlet temperatures	71
Figure 5.16	Variation of pressure drop of CO ₂ at different operating pressures and at different HHX inlet temperatures	71
Figure 5.17	Variation of temperature along the loop at different HHX inlet temperatures and different operating pressures (a) 35 bar, (b) 40 bar, and (c) 45 bar.	73
Figure 5.18	Variation of heat transfer rate of CO ₂ at different pressures and $T_H - T_C = 25$ °C in (a) XY-plane and (b) YZ-plane	74
Figure 5.19	Pressure drop comparison of CO ₂ at different pressures and $T_H - T_C = 25$ °C in (a) XY-plane and (b) YZ-plane	75
Figure 5.20	Variation of temperature along the loop at 35 bar in (a) XY-plane and (b) YZ-plane	76
Figure 5.21	Variation of temperature along the loop at 40 bar in (a) XY-plane and (b) YZ-plane	76
Figure 5.22	Variation of temperature along the loop at 45 bar in (a) XY-plane and (b) YZ-plane	77
Figure 5.23	Variation of heat transfer rate for brine and subcritical liquid CO ₂ at different pressure	78
Figure 5.24	Variation of pressure drop for water and subcritical liquid CO ₂ at different pressure	79
Figure 6.1	Variation of heat transfer rate of CO ₂ at different operating pressures and at different HHX inlet temperatures	82
Figure 6.2	Variation of heat transfer rate of CO ₂ at different operating pressures and at different HHX inlet temperatures	84
Figure 6.3	Variation of temperature along the loop at different HHX inlet temperatures and different operating pressures (a) 50 bar, (b) 55 bar, (c) 60 bar and (d) 65 bar	85

Figure 6.4	Variation of heat transfer rate of CO ₂ at different pressures and $T_H - T_C = 42$ °C in (a) XY-plane and (b) YZ-plane	86
Figure 6.5	Variation of heat transfer rate of CO ₂ at different pressures and $T_H - T_C = 46$ °C in (a) XY-plane and (b) YZ-plane	87
Figure 6.6	Pressure drop comparison of CO ₂ at different pressures and $T_H - T_C = 42$ °C in (a) XY-plane and (b) YZ-plane	88
Figure 6.7	Pressure drop comparison of CO ₂ at different pressures and $T_H - T_C = 46$ °C in (a) XY-plane and (b) YZ-plane	88
Figure 6.8	Variation of temperature along the loop at 50 bar in (a) XY-plane and (b) YZ-plane	89
Figure 6.9	Variation of temperature along the loop at 55 bar in (a) XY-plane and (b) YZ-plane	90
Figure 6.10	Variation of temperature along the loop at 60 bar in (a) XY-plane and (b) YZ-plane	90
Figure 6.11	Variation of temperature along the loop at 65 bar in (a) XY-plane and (b) YZ-plane	91
Figure 6.12	Effect of HHX inlet temperature on heat transfer at different operating pressure (a) 50 bar, (b) 55 bar, and (c) 60 bar	92
Figure 6.13	Variation of heat transfer rate for brine and two phase CO ₂ at different pressure	93
Figure 6.14	Variation of pressure drop for water and supercritical CO ₂ at different pressure	94

NOMENCLATURE

c_{p-xf}	Specific heat of external fluid (kJ/kgK)
c_p	Specific heat (kJ/kgK)
D_i	Internal diameter of external pipe (m)
m	Maximum mass flow rate (kg/sec)
Δm	Minimum mass flow rate (kg/sec)
Q	Heat transfer rate (W)
Q_{CHX}	Heat transfer rate of CHX (W)
Q_{HHX}	Heat transfer rate of HHX (W)
T	Maximum temperature ($^{\circ}\text{C}$)
T_C	CHX inlet temperature ($^{\circ}\text{C}$)
T_H	HHX inlet temperature ($^{\circ}\text{C}$)
ΔT	Minimum temperature
ΔT_{CHX}	External fluid temperature difference in CHX
ΔT_{HHX}	External fluid temperature difference in HHX
T_{sat}	Saturation temperature ($^{\circ}\text{C}$)
Greek symbols	
ρ	Density (kg/m^3)
λ	Thermal conductivity (W/mK)
μ	Viscosity (Pa-s)
β	Volumetric expansion coefficient (K^{-1} or $^{\circ}\text{C}^{-1}$)
Abbreviations	
CHX	Cold heat exchanger
HHX	Hot heat exchanger
NCL	Natural circulation loop

Chapter 1

INTRODUCTION

Globally, synthetic coolants are being phased out to combat the twin threat of depletion of the ozone layer and global warming. The goal of achieving holistic environmental safety has facilitated the emergence of natural refrigerants as the most beneficial working fluids in cooling and heating systems. Several natural refrigerants are regaining their significance and are on a revival path. Many of these natural refrigerants, however, are either toxic or flammable, or both. In such situations, the amount of refrigerant used in the device should be low, and the refrigerant should be limited to the plant space. Such two goals are achieved by introducing a secondary fluid loop to transfer heat between the refrigeration plant and the cooled room. Reducing the quantity of refrigerant also used results in faster cooling and defrosting. Secondary fluid loops are widely used in different applications for cooling, air conditioning, and heating. There has been a recent spurt in the universal interest of studying alternatives to conventional direct cooling systems and the use of natural refrigerants as secondary fluids. Secondary fluids that are traditionally used are water, brines, glycols, alcohols, etc. Recent studies indicate that carbon dioxide can also be used as an alternative secondary fluid.

Carbon dioxide is an environmentally friendly natural working fluid with no potential for ozone depletion and minimal potential for global warming ($GWP \approx 1$). It is also inexpensive, non-explosive, non-flammable, and plentiful. In addition to these benefits, the carbon dioxide-based secondary loops offer many advantages compared to other secondary fluids due to certain favorable thermophysical properties and near critical point operation. Unlike other conventional secondary fluids, however, secondary loops based on carbon dioxide operate at very high pressures, requiring components that can withstand such high pressures. Therefore, it may be essential to evaluate the size and weight of carbon dioxide based systems when compared with such as mobile cooling and air conditioning. Recent studies have demonstrated that carbon dioxide is an ideal secondary solvent for a wide variety of applications, including cooling, air conditioning, and heating (Wang et al. 2010, Milanovic et al.

2004, Palm 2007, Aittomiiki and Lahti 1997). In recent years, both forced and natural circulation loops have witnessed the growing popularity of carbon dioxide as a secondary fluid. Natural circulation loops (NCLs), however, offer certain benefits over forced circulation systems, especially in small to medium capacity systems. NCLs are also favored where safety, for example, in nuclear power plants, is the primary concern.

1.1 TYPES OF REFRIGERATION SYSTEMS

Refrigeration systems can be broadly classified into direct and indirect systems. The indirect systems, also known as secondary loop systems, lies in the physical separation between the primary loop, where the cooling effect is produced, and the secondary loop, where cooling takes place. An indirect cooling system incorporates two different refrigerants (primary and secondary) to provide cooling. In all these systems, the primary loop is a conventional refrigeration system that uses a phase changing fluid as the primary refrigerant, which is restricted to the plant room. A separate fluid (secondary refrigerant) circulates in the secondary loop and transports thermal energy between the refrigerated space and the refrigeration plant. An additional heat exchanger is required to transfer heat between the conditioned space and plant room via the secondary loop. The fluid used in the secondary loop is normally a safe and environmentally benign fluid that does not undergo any phase change during the process of heat transfer. However, it is possible to build indirect systems in which the secondary fluid may also undergo phase change.

A secondary loop integrated with a conventional refrigeration system is shown in Figure 1.1. As mentioned before, the indirect systems require an additional heat exchanger (HX) and a secondary refrigerant pump. This may result in increased initial cost and energy requirements compared to equivalent direct systems (Kruse 2004, Richard and Donal 2008). However, employing an NCL with suitable secondary fluid can eliminate the use of a secondary fluid pump.

Faramarzi and Walker (2004) investigated secondary loop supermarket refrigeration systems for California, USA, and concluded with the following statements:

- On average, a conventional direct refrigeration system can be expected to lose 30 – 50% of the total refrigerant charge annually, whereas, for a secondary loop refrigeration system, the loss of primary refrigerant is less than 15%.
- The secondary loop refrigeration system has a refrigerant charge that is almost ten times less than the conventional direct refrigeration system.
- Secondary loop refrigeration systems consumed approximately 14% less electricity than a conventional direct refrigeration system because of the lower viscosity of the secondary fluid.

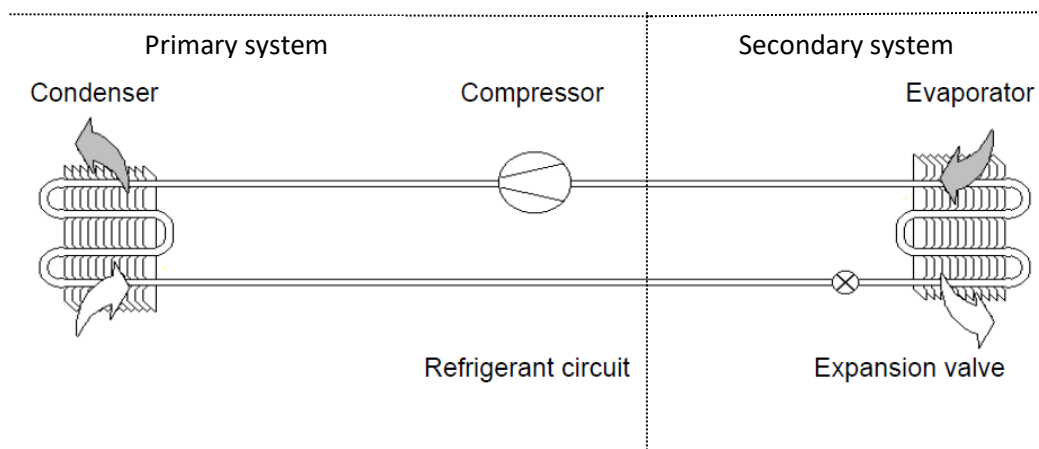


Figure 1.1 Indirect refrigeration system with forced circulation type secondary loop

1.1.1 Advantages of indirect refrigeration systems

- Since primary refrigerant is confined to the plant room, a flammable and/or toxic but eco-friendly fluid can be used as the primary refrigerant.
- Less refrigerant charge in the primary loop: reduces capital cost and refrigerant leakage.
- Faster pump-down and defrost.
- Smaller primary cooling loops further benefit in maintenance and checking operations.
- A secondary loop system is also simpler to modify.

1.1.2 Disadvantages of indirect refrigeration systems

- Additional heat exchanger and circulating pump increase initial cost.
- An added temperature difference may result in lower efficiency.

- The selection of a suitable secondary fluid requires additional investigation.

1.2 NATURAL CIRCULATION LOOPS

Heat transfer loops (secondary loops) are classified into two groups: a forced circulation loop (FCL) in which an external pump is used to drive the flow, and a natural circulation loop (NCL). In NCLs, circulation of fluid is maintained due to the buoyancy effect caused by thermally generated density gradient, so that a pump is not required. In an NCL, the heat sink is located at a higher elevation than the heat source that establishes a gradient of unstable density in the system, and therefore, under the influence of gravity, lighter (warmer) fluid rises, and heavier (cooler) fluid falls. NCL is also sometimes referred to as a thermosyphon or natural convection loop. Japikse (1973) made a clear distinction between NCL, where the flow is usually in one direction around the loop, and thermosyphon, where the flow can be upward along the heated wall and downward along the cooler wall with the corresponding return flow. Figure 1.2 shows evacuated tube solar water heaters that utilize the principle of a thermosyphon.

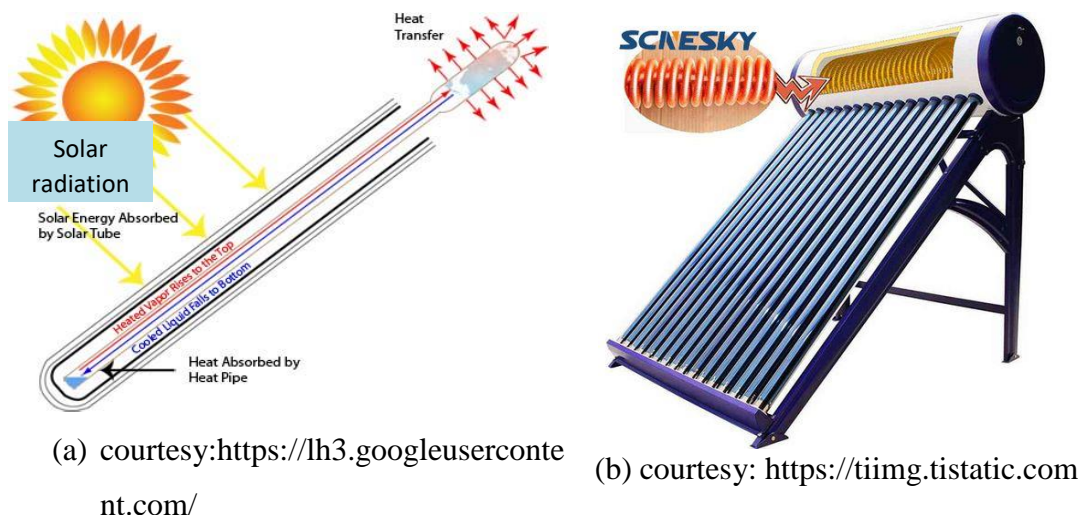


Figure 1.2 Evacuated tube solar water heaters

1.2.1 Different configurations of NCLs

Natural Circulation loops may have different configurations based on the working fluid, surrounding interaction, shapes, inventory, number of channels, and body force. A detailed description of NCL is shown in Figure 1.3 (Vijayan 2007).

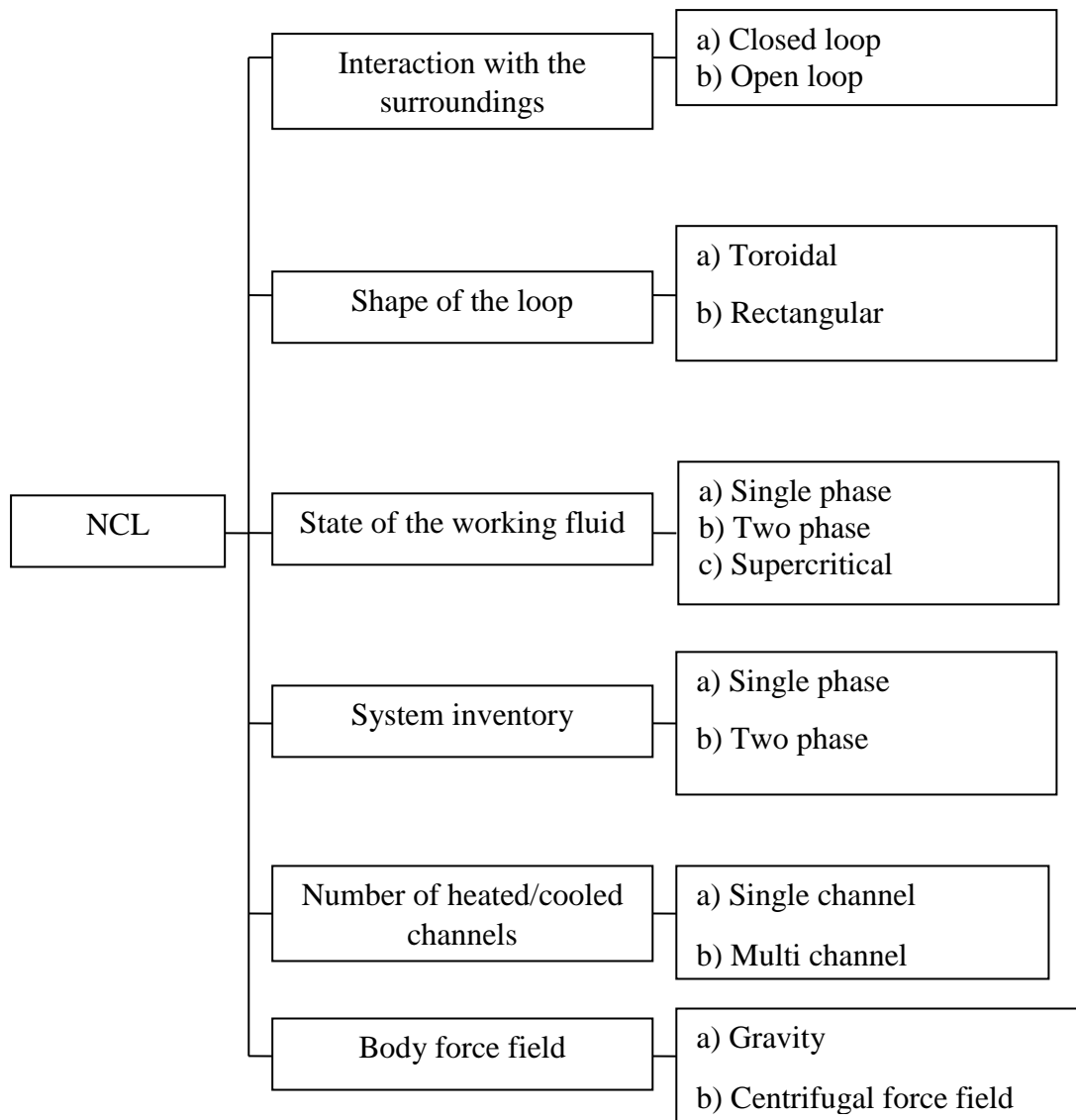


Figure 1.3 Classification of Natural Circulation Loops (Vijayan 2007)

Apart from this classification, it can be further classified based on heat transfer mode at heat source and heat sink. Depending on the application in various engineering fields, heat can be transferred as constant heat flux, radiative heat exchange, or at a constant temperature. Figure 1.4 shows the commonly used NCL configurations for theoretical studies.

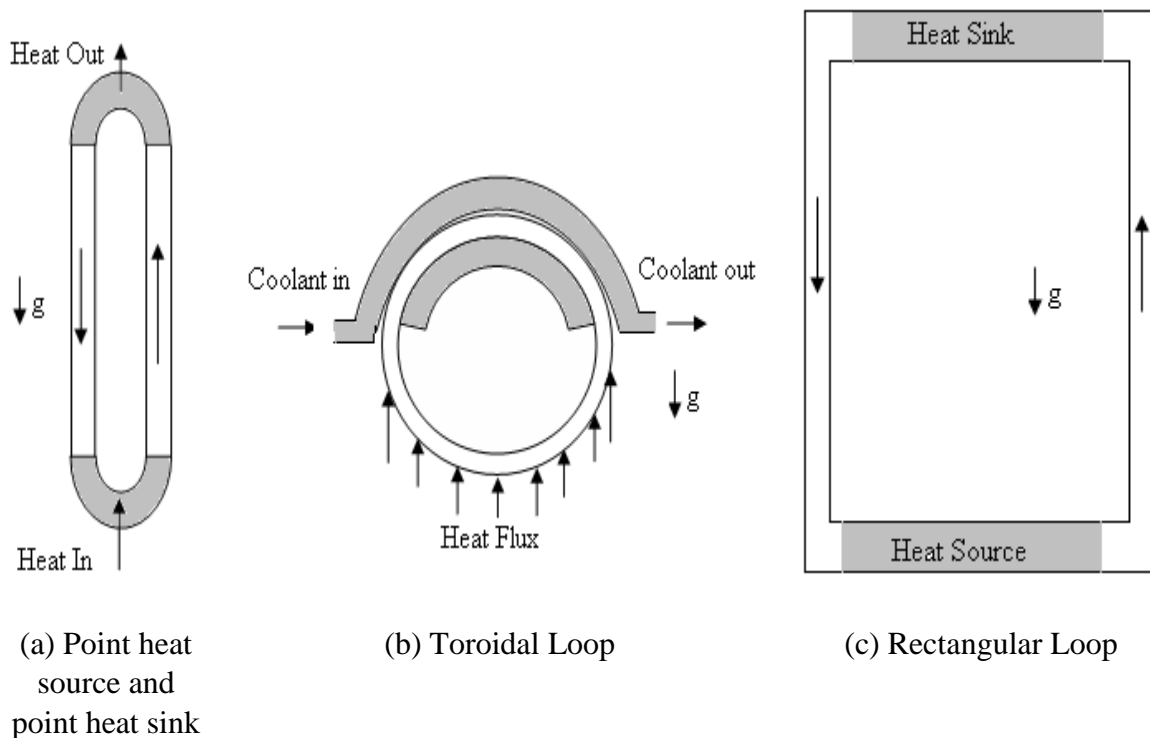


Figure 1.4 Different NCL models

1.2.2 Advantages and disadvantages of NCL

The various advantages and disadvantages of an NCL could be considered while choosing NCL as a possible design choice for a specified application.

Advantages of NCL

- Simplicity and low cost
- Pumps are not required; operation is safe
- Possibility of better distribution of flow
- Better two phase characteristics
- Large thermal inertia

Disadvantages of NCL

- Low driving head
- Lower maximum power per channel
- Possible instabilities in the flow
- Low critical heat flux
- Specific start-up procedures are required

1.2.3 Applications of NCL

As stated in the literature, the NCLs have a wide range of industrial and engineering applications. These include solar heaters (Close 1962, Huang 1980, Mertol et al. 1981, Ong 1974, Shitzer et al. 1977, Zvirin et al. 1977), thermosyphon reboilers (McKee 1970, Sarma et al. 1973), electronic chip cooling (Tuma and Mortazavi 2006), turbine blade cooling (Cohen and Bayley 1955), chemical process industries (Joshi 2001, Nottenkamper et al. 1983), geothermal energy extraction processes (Kreitlow et al. 1978, Torrance 1979), closed loop pulsating heat pipe (Khandekar and Gupta 2007, Tong et al. 2001), refrigeration (Kaga et al. 2008), and nuclear power generation (Agrawal et al. 1980, Zvirin 1981).

1.3 SELECTION OF WORKING FLUIDS FOR NATURAL CIRCULATION LOOPS

Selection of working fluid (secondary fluid) for NCLs are typically carried out based on the following properties:

- Low freezing point
- Low viscosity
- High specific heat
- High volumetric expansion coefficient
- High thermal conductivity
- Chemically stable, non-toxic, non-corrosive nature
- Environment friendliness
- High density
- Cost, availability, etc.

The first criterion for choosing a secondary fluid for refrigeration applications is the low freezing point and should be well below the system's operating temperature. It is important to find the right balance between viscosity, heat flux, and thermal conductivity for the optimal design of the secondary cooling system.

1.4 COMMONLY USED SECONDARY FLUIDS

Commonly used secondary fluids can be divided into an aqueous and non-aqueous category. Aqueous solutions are generally either salt-based or alcohol-based products.

These are having one or more non-favorable effects like corrosiveness, toxicity, high pH value, etc. Non-aqueous solutions are commercially available chemicals. Table 1.1 shows a comparison between conventional secondary fluids in terms of relevant properties.

Table 1.1: Property comparison of different secondary fluids (NIST Standard Reference Database REFPROP, 2013, Version 9.1)

Secondary fluids	ρ (kg/m ³)	c_p (kJ/kgK)	λ (W/mK)	μ ($\times 10^{-5}$) (Pa-s)	β (K ⁻¹)	T_{freezing} (°C)
Calcium chloride # (29.4%)	1293.2	2.718	0.529	596.6	0.000114	-55
Ethanol # (90%)	839.2	2.417	0.213	218.1	0.000247	-80
Ethylene glycol @ (90%)	1131.4	2.312	0.272	3374.1	0.000293	-29.17
Magnesium chloride # (20.6%)	1187.6	3.016	0.512	550.4	0.000714	-33.6
Methanol# (90%)	816.8	2.597	0.243	137.2	0.000557	-80
Potassium carbonate # (38.4%)	1418.7	2.65	0.508	901	0.000098	-35.5
Sodium chloride# (23.1%)	1181.8	3.314	0.543	304.7	0.00009	-21.2
Syltherm XLT	862.6	1.598	0.107	186.2	0.000963	-93
Freezium# (50%)	1387.5	2.646	0.475	461.8	0.000597	-58.61
Propylene glycol @ (90%)	1069.7	2.479	0.235	12201	0.00089	-51.1
Tyfoxit@ (98%)	1252.7	2.854	0.423	828	0.00047	-55
Dowtherm Q	986.26	1.59	0.127	836.2	-	-40
HYCOOL 20	1202.2	2.955	0.517	289.1	-	-20
Aspen Temper -20	1157.72	3.291	0.475	395.4	-	-23
Water*	1000	4.227	0.548	178.6	-0.000078	0
Carbon dioxide*	927.6	2.541	0.109	10.46	0.007385	-56.6 ^{\$}
<p>* Water properties: At 0.1 °C, 1atm, CO₂: 0 °C, 35 bar (subcooled) # Composition % by mass @ Composition % by volume \$ Triple point temperature Note: all properties are at specified composition and 0 °C</p>						

All the properties are at 0 °C and atmospheric pressure except water and CO₂. From Table 1.1, it is observed that the viscosity of the aqueous solutions is very high compared to CO₂. Moreover, the thermal expansion coefficient, which is a key property in natural circulation systems, is very low for aqueous solutions.

1.5 SUITABILITY OF CO₂ AS A SECONDARY FLUID

Table 1.1 exhibits that CO₂ offers very low viscosity and a very high coefficient of thermal expansion. Due to these favorable properties, CO₂ is expected to perform well as a secondary fluid. The suitability of CO₂ as a secondary fluid has been studied by Kiran Kumar and Ramgopal (2009) for NCL and by Yadav et al. (2012) for forced circulation loop (FCL).

The phase diagram of CO₂ is shown in Figure 1.5 on the P-T plane. Studies show that any fluid that operates near its critical point offers very good thermophysical properties that favor natural circulation in a loop. Most engineering applications (operating temperatures) lie around the critical temperature CO₂ (about 31 °C, Table 1.2), which makes CO₂ one of the best secondary fluids for NCLs. Due to this reason, in recent years, there is a growing interest in the operation of supercritical secondary loops using carbon dioxide as the working fluid for applications such as solar heaters, solar thermal power generation systems, etc. However, due to abrupt changes in many thermophysical properties near the critical region, studies on supercritical loops require suitable models to account for the property variations with high precision.

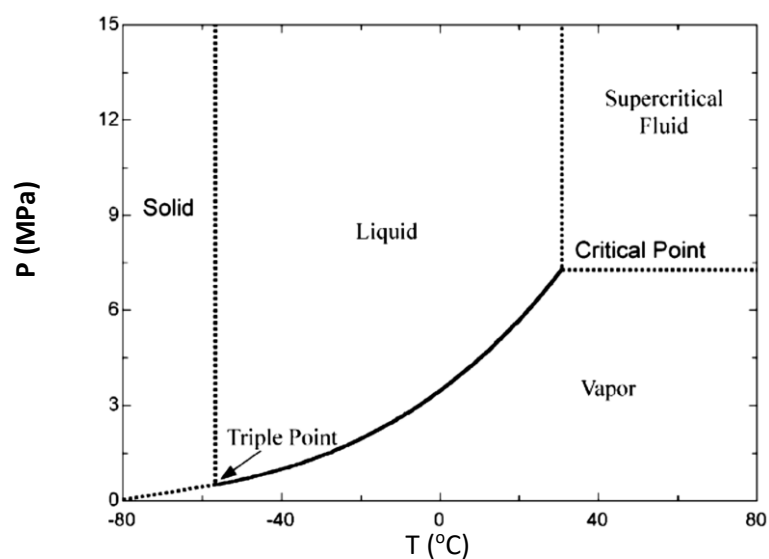


Figure 1.5 Phase diagram of CO₂ (Kim et al. 2004)

Table 1.2: CO₂ Properties – a comparison (Lorentzen et al. 1993, Riffat et al. 1997)

<i>Refrigerant</i>	<i>R12</i>	<i>R22</i>	<i>R134a</i>	<i>R600a</i>	<i>R717</i>	<i>R744</i>
ODP	0.82	0.055	0.0	0.0	0.0	0.0
GWP _{IPCC value} (100 yrs)	8100	1700	1300	0.0	0.0	1
Flammable	No	No	No	Yes	Yes	No
Toxic	No	No	No	No	Yes	No
Molecular weight	120.9	86.5	102.03	58.0	17.03	44.01
Normal boiling point (° C)	-29.8	-40.8	-26.2	-11.6	-33.3	-78.4
Critical pressure (bar)	41.1	49.7	40.7	36.4	114.27	73.8
Critical temperature (° C)	112.0	96.0	101.1	134.7	133.0	31.2
Saturation pressure at 0 °C	3.09	4.98	2.93	1.56	4.29	34.8

1.6 TWO-PHASE NATURAL CIRCULATION

Natural circulation in two phases is capable of generating greater forces of buoyancy and hence greater flows. Two-phase natural circulation finds its application in nuclear steam generators, thermosyphon boilers, boilers for fossil-fueled power plants, and core cooling of reactors, etc. The ability of natural circulation loops to carry heat depends on the rate of flow circulation that it can produce. For two-phase natural circulation loops, explicit parallels for the steady-state flow are not available. This makes it difficult to compare the performance of the various natural two-phase circulation loops.

Though in recent times, there is a growing interest in CO₂ based NCLs, it is observed that very few studies are available on CO₂ based systems. Most of the studies which are available in the open literature are for single phase (subcritical) or supercritical carbon dioxide based NCLs. Studies on two phases carbon dioxide based NCLs are not available in the open literature. Two phase natural circulation can generate large

buoyancy forces (due to high density gradients along the loop) and hence large flow rates, which will make a system smaller in size. Experimental studies on carbon dioxide based NCLs are scant in the open literature.

1.7 INSTABILITY IN NCL

It is said that natural circulation loops are in a stable state when the buoyancy and the frictional impacts create a vibrant balance between them. Otherwise, NCL may experience flow fluctuations instability. Instability is undesirable since continued flow oscillations can lead to mechanical component compelled vibration and can decrease the efficiency of the system. Natural circulation systems excited by various mechanisms show different types of instability. Keller (1966) did a theoretical study on a rectangular natural circulation loop and predicted that the flow oscillation is the interaction of friction forces with buoyancy forces but is unaffected by inertia. Welander (1967) first explored NCL's dynamic behavior and characterized instability mechanism based on the growth of amplitude oscillations. Figure 1.6 (a) and (b) show the thermo-hydraulic behavior of NCL at stable and unstable conditions. Chen et al. (1985a) assessed the influence of the orientation of heater and cooler on supercritical CO₂ based NCL. They discovered that when the heater and cooler were kept horizontal, the loop had the highest instability but also gave the highest flow rate among all other combinations. However, when both were kept vertical system was highly stable but with the least flow rate.

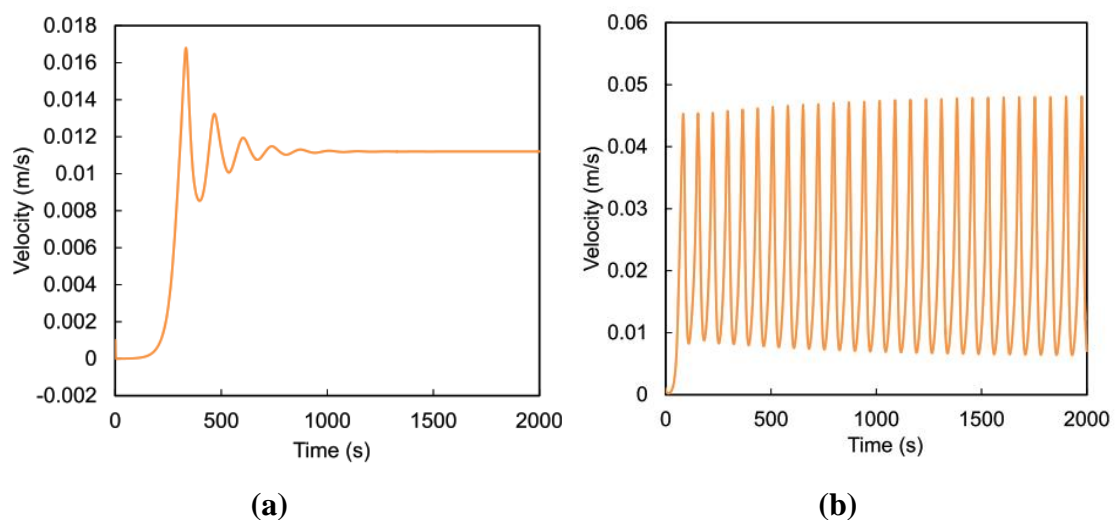


Figure 1.6 Thermo-hydraulic behavior of NCL: (a) Stable case, and (b) Unstable case (Welander 1967)

Chen et al. (1985b) explored the impact of diameter on the flow stability and found that due to the developed flow field and greater heat transfer of supercritical CO₂, higher stability exists in larger diameter loops. Therefore, NCLs require precise design assessment that focuses on the interaction of all the transient response of buoyancy and friction forces, which ensures a stable zone of operation.

1.8 STRUCTURE OF THE THESIS

Chapter 1 presents a brief introduction to types of refrigeration systems, NCL, and suitability of single/two phase CO₂ in NCL.

Chapter 2 presents a complete review of the relevant literature. It contains the study on heat transfer loops, NCLs, subcritical and supercritical CO₂ based NCLs, several applications of NCL, a summary of the literature, research gap, and objective of the present study.

Chapter 3 presents the complete information of the fabrication of the experimental setup and details of the equipment used to carry out the study.

Chapter 4 presents an experimental study on steady-state analysis of a supercritical CO₂ based NCL with end heat exchangers for different operating pressures and temperatures with and without tilting effect.

Chapter 5 presents an experimental study on steady-state analysis of a subcritical vapor and subcritical liquid CO₂ based NCL with end heat exchangers for different operating pressures and temperatures with and without tilting effect.

Chapter 6 presents an experimental study on steady-state analysis of a two phase CO₂ based NCL with end heat exchangers for different operating pressures and temperatures with and without tilting effect.

Major conclusions and recommendations for future work are presented in **Chapter 7**.

Chapter 2

LITERATURE REVIEW

A literature review on various aspects of natural circulation loops is discussed in this chapter, which covers secondary loop systems, single phase NCL, applications of NCL in different engineering fields, application areas of CO₂ based systems, CO₂ based systems secondary systems, and high-pressure safety issues.

2.1 SECONDARY LOOP SYSTEMS

A comprehensive review of secondary loop cooling systems is provided by Wang et al. (2010). Increasing concern over the environmental effects of traditional primary refrigerants and safety leads researchers to work on secondary loops. A critical review on properties of commonly used secondary coolants presented by Melinder (1998). Horton et al. (2003) compared a direct system to an indirect system with an equivalent cooling capacity. The charge of primary refrigerant required for the indirect system was only 10% of the refrigerant charge required for the direct system (Richard et al. 2008). Mao et al. (2003) proposed an energy storage device that can be easily integrated into the structure of the buildings. This stores heat supplied to the storage tank by solar energy via the two-phase closed loop thermosyphon and releases stored heat in energy storage to the heat exchanger via the transport fluid flow. Georgi et al. (2006) have presented detailed operational and design characteristics of a secondary coolant system. Energy analysis was performed, showing that secondary coolant systems achieve energy parity or better compared with direct expansion systems. Melinder (2007) compared different secondary coolants for supermarket cooling applications. He concluded that aqueous solutions are better than non-aqueous solutions in terms of heat transfer performance. The use of carbon dioxide as a secondary fluid in forced convection loops has been shown by Winkler et al. (2007), which leads to very compact systems suitable for miniaturization. Minea (2007, 2008) reported a supermarket refrigeration system with secondary loops in Canada. These papers show that the usage of CO₂ as a coolant and/or refrigerant reduces the piping lengths and diameters and achieves low-charge refrigeration systems in supermarkets. He claims that the entire secondary loop supermarket refrigeration systems did not

degrade the overall energy performances and/or the thermal parameters for safe food storage and may reduce the synthetic refrigerant inventory up to 80%. Moreover, this kind of system allows energy recovery with heat pumps and/or direct waste heat recovery coils and efficient defrosting with warm secondary fluids. Importantly, refrigerant confinement areas allow low refrigerant annual leakage rates equivalent to more than a 79% reduction in CO₂ emission compared to baseline multiplex systems. Hinde et al. (2008) reported that the use of CO₂ in supermarket refrigeration is increasing in the USA. They reported significant installation savings for CO₂ systems in terms of the amount of required copper piping, and an energy analysis indicated that both low-temperature CO₂ secondary and direct expansion systems could be better implemented with energy consumption than traditional HFC direct expansion systems by 3 to 12 percent depending on the type and configuration of the system. Finn et al. (2008) examined defrost performance issues associated with a finned-tube air chiller, utilized as a heat exchanger in an indirect multi-temperature transport refrigeration system, where a glycol antifreeze mixture is deployed as a secondary working fluid. Direct electric heat input defrosting mode and secondary loop defrosting mode were compared. No general conclusions were drawn but, in some cases, secondary loop defrosting was found to be faster.

Christensen (1999), Pearson (2005), Verhoef et al. (2004), and Van Riessen (2004) have also carried out studies on forced circulation type CO₂ secondary loops.

2.2 NATURAL CIRCULATION LOOPS

Due to the coupled nature of momentum and energy equations, theoretical analysis of the natural circulation loop is relatively complex. So many studies available in literature deal with simple cases like rectangular and toroidal loops with point heat source and sink, etc. Most of the studies are idealized by considering either known heat flux conditions or convective heat transfer with the known coefficient of heat transfer and wall temperature. Even though some studies are carried out on two, and three-dimensional variations of flow parameters along the loop, the majority of the studies are one-dimensional. Zvirin (1981) and Grief (1988) give an insight on a categorization of loops and a basic understanding of the phenomena. Zvirin (1981) has done a survey on the theoretical and experimental work in single phase NCLs, which includes available methods (analytical and numerical) to describe steady-state

flows, transient and stability characteristics of the various loops. have general analyses of the NCL.

2.2.1 Single phase natural circulation loops

Misale et al. (2001) experimentally studied the effect of pressure drop on the stabilization of the loop. For this study, they made a provision for introducing localized pressure drops by using orifices with different diameters. A small diameter orifice stabilized the loop faster than larger diameter orifices. Vijayan (2002) developed a correlation based on experimental results for flow rate in terms of Reynolds number, Grashof number, and a dimensionless loop parameter. Testing these correlations with experimental data showed reasonable agreement. The above equation suggests that simulation of the steady-state flow in single phase NCL's can be achieved by simulating the non-dimensional parameter (Gr_m/N_G). Tahsin et al. (2007) compared experimental results with their theoretical two dimensional results. Misale (2007) experimentally investigated the effect of the orientation angle of a rectangular natural circulation loop and found that the quiescent state (steady temperature difference across the heat sinks) duration increases as power decreases and the loop inclination increases. Vijayan et al. (2007) demonstrated the effect of the heater and cooler orientations on the single-phase natural circulation loop and concluded that the maximum flow occurs in a horizontal position for orientation with both the heater and the cooler. Nevertheless, this orientation is found to be less stable, with both warmer and cooler vertical.

Nayak et al. (2008) studied the circulation behavior in a rectangular loop with water and different concentration of Al_2O_3 nanofluids. From this study, it was shown that by using nanofluids, not only the flow instabilities are suppressed but also the normal circulation flow rates are increased. The increase in the flow rate of natural circulation and the suppression of instabilities were found to be dependent on the concentration of nanoparticles in water. Garibaldi et al. (2008) experimentally studied the effect of geometric parameters and fluid properties on the thermal efficiency of rectangular single-phase natural circulation mini loops, which could be used for electronic device cooling. Water and FC43 (a commercial secondary fluid) were chosen for comparison. Results show that the FC43 velocity is nearly twice that of water at the

same power, but the thermal performance is worst due to the low specific heat characterizing FC43.

2.2.2 Two phase natural circulation loops

In a low pressure natural circulation loop, Chexal et al. (1973) studied two phase flow instabilities, and several different types of instabilities were identified with a brief description of the flow pattern in some of those regions. For example, a region with very low heat fluxes and a wide range of inlet subcooling was defined for periodic large bubble formation at the exit. Lee et al. (1990) carried out experimental studies on two phase Freon-113 loop and showed that flow behavior strongly depends on phase change and coupling between hydrodynamic and heat transfer phenomena. Non-equilibrium phase-change phenomena such as flashing create unstable hydrodynamic conditions, which lead to cyclic or oscillatory flow behaviors. Experimentally Chen et al. (1991) showed that fluid temperature and pressure increase at each position in the system, with increased input power at a fixed percentage charge point. Higher fluid temperatures are observed at low percentage charge rates, and the loop's average heat transfer coefficient decreases at a fixed input power with a rise in percentage charge. With a view to obtaining a relation between two-phase flow patterns and thermal-hydraulics in an NCL. Hsieh et al. (1997) developed an image processing technique and showed the different flow patterns at different flow rates. Jong et al. (2000) experimentally studied the function of the expansion tank line and observed that when the frictional resistance on the expansion tank line becomes greater, the circulation becomes stable, particularly under high heat-flow and high inlet-subcooling conditions, and as a whole, the stable operating area becomes larger in the instability map. Similarly, the mechanism is balanced by the longer expansion-tank line. Samuel et al. (2004) constructed a test rig to demonstrate the effect of liquid fill ratio and evaporator length and found that the thermal resistance decreases for the lowest fill ratio, changing the evaporator length also changes the power input, but the lowest thermal resistances were achieved for the shortest evaporator.

Jain et al. (1966), Delmastr et al. (1991), Wu et al. (1996), Kyung (1994), Soo et al. (1994), and Juei-Tsuen et al. (1998) also carried out experimental studies on two phase NCL.

2.3 APPLICATIONS OF NCL IN DIFFERENT ENGINEERING FIELDS

Natural circulation loops have been used in different engineering applications such as nuclear reactors, solar heaters, electronic cooling, refrigeration, air conditioning, and geothermal energy, etc.

Elias (2000) presented theoretical and experimental verification on the behavior of a passive cooling system for electronic components. Pin (2001) investigated the parameters affecting the capillary pumped loops used to transfer heat from chips. He found that for his system, which is designed for 40 W, there should be a minimum relative height between the evaporator and condenser to initiate the flow. Pal et al. (2002) experimentally studied the effect of inclination of a two phase closed thermosyphon designed for cooling of a microprocessor. Haider et al. (2002) presented a study on a closed loop two phase thermosyphon for electronic cooling. Rahmatollah (2005) designed a thermosyphon for the cooling of three parallel high heat flux electronic components. Iso butane was used as a loop fluid. He developed a correlation for the prediction of pressure drop based on the homogeneous model. Tuma et al. (2006) studied a two-phase natural circulation system for electronic device cooling. They used this technique of heat transfer to remove a 200 W dissipated power from a silicon chip. Vladimir et al. (2007) proposed a low noise cooling system for a personal computer using a natural circulation loop. They designed a system that can sustain temperatures of 72-78 °C and interacts with 100 W thermal dissipation at a heat source. Water was used as a working fluid, and the radiator was cooled by air naturally.

Due to its simplicity, reliability, and low cost, natural circulation mode is being used in solar heat extraction systems for many years. Solar based systems can be operated in forced circulation mode or in natural circulation mode. Jabbar (1998) compared the efficiency of the forced circulation system with the natural circulation system and found that the former system is 30% to 80% more efficient than later. But, one has to consider the extra cost and complexity in using a forced circulation loop. Morrison (1980) compared theoretical predictions of flow rate in thermosyphon solar collectors with experimental measurements using a laser Doppler anemometer. In another paper, Morrison et al. (1980) carried out a transient analysis of thermosyphon solar collector and concluded that although there were long time delays associated with the

development of the thermosyphon flow, the energy collection capability is not affected by thermosyphon time delays. Close (1962) proposed a simple mathematical model for a solar hot water device with natural circulation between the collector and the storage tank, assuming solar radiation as a function of time; no provision for the removal of hot water from the tank was made. Gupta et al. (1968) studied the device on the basis of Close's study, adding a plate efficiency factor and describing the solar intensity and ambient temperatures as a Fourier time series. Zvirin et al. (1977) analytically predicted the performance by assuming a linear and nonlinear distribution of temperature. Zerrouki et al. (2002) assumed linear temperature distribution and compared the theoretical model with experimental results.

Some other works related to solar closed loop thermosyphon can be found in Shitzer et al. (1979), Norton et al. (1983), Thomas et al. (1987), Lawrence et al. (1990), Altamush Siddiqui (1997), Hussein (2002, 2003) and Kang et al. (2003). Da Silva et al. (2004) carried out studies on thermal applicability of two phase thermosyphons in ovens/furnaces.

2.4 APPLICATION AREAS OF CO₂ BASED SYSTEMS

In recent times there is a growing interest in the use of carbon dioxide in various cooling, heating, and power applications. A revival of CO₂ as a refrigerant in the recent past can be found in Pearson (2005).

Lorentzen et al. (1993, 1995) studied the efficiency of a carbon dioxide-based automotive air conditioning system and showed that the environmentally friendly CO₂ system had comparable performance to the R12. Yin et al. (1998) and Mathur (2000) compared the cooling performance of the CO₂ system and R134a system. The COP of the CO₂ system is found to be lower than that of R134a the system at high outdoor temperatures and is higher at low outdoor ambient temperatures. Neksa (2002) addressed the important characteristics of the transcritical CO₂ system applied to heat pumps and demonstrated that CO₂ is an attractive alternative to synthetic fluids. Tomoichiro et al. (2005) concentrated on a solution using a CO₂-based heat pump in which waste heat from the heat pump process is recovered during incoming air dehumidification (referred to as the dehumidifying condition) and used as an auxiliary heat source instead of an electric heater. Based on this concept, they aimed at

developing an effective automotive cooling and heating air conditioning system using CO₂ as a refrigerant by establishing an intermediate pressure control method for adjusting the optimum refrigerant amount. This has resulted in the successful development of a prototype CO₂ based cooling and heating air conditioning system for medium-sized vehicles. With this system, it has obtained superior performance to that of the existing HFC134a system. Sung et al. (2009) theoretically and experimentally studied the effect of different operating parameters on the performance of CO₂ based automobile air conditioning systems and found optimum pressure for higher COP and also developed a high pressure control algorithm for the transcritical CO₂ cycle to achieve the maximum COP. Bhatti (1997), Hafner (2002), Preissner et al. (2002), Hirao (2002), and Brown et al. (2002) are some of the other studies on CO₂ based automobile air conditioning systems.

Aarlien et al. (1998) compared CO₂ based residential air conditioning systems with that of R 22. Adriansyah (2004) developed a prototype model using CO₂ as a refrigerant for integrated air conditioning and tap water heating plants. He concluded that the combined system offers promising potential as an energy recovery method in which the water heating system's energy consumption can be significantly reduced or completely eliminated when all of the rejected heat is used to generate hot water. Studies on CO₂ based supermarket refrigeration system located in north Italy concludes that the total annual energy consumption is estimated to be about 10% higher than the direct expansion R404A solution (Giroto et al. 2004).

Different kinds of heat pumps using CO₂ as working fluid have been investigated theoretically and experimentally by many researchers. Neksa (2002) theoretically and experimentally showed that CO₂ could be successfully used as working fluid in heat pumps with very competitive performance. Energetic and energetic analyses, as well as optimization studies of a transcritical carbon dioxide heat pump system, were done by Sarkar et al. (2004), and also useful correlations and guidelines for optimum system configuration have been proposed. In the heating process. Richter et al. (2003) experimentally compared a commercially available R410A heat pump and an R744 prototype (carbon dioxide) system. Even though the cooling power of the two systems matches and the slightly smaller size of the R744 heat exchangers has a negative effect on performance, the system efficiency of R744 is equal or slightly better than

R410A on an annual basis, including the effect of low-quality supplementary heating. Luca et al. (2005) made a comparison between a system working with CO₂ and a similar one working with HFC R134a. Some other studies on the comparison of CO₂ with different refrigerants are done by Hafner (2002), Cho (2005), etc.

2.5 COMMERCIAL ASPECTS OF CO₂ SYSTEMS

After years of research, commercial usage of CO₂ is growing rapidly in recent times. Installation of CO₂ systems is based on the transcritical cycle, secondary fluid, or as a bottoming (subcritical) cycle refrigerant in cascade systems with other natural refrigerants. For example, Loblaw, Canada's leading retailer, has opened the country's first superstore using a secondary CO₂ system for low temperature refrigeration and space heating (www.R744.com). Use CO₂ for frozen food; the refrigeration system reduces the amount of chemical refrigerant R507 by 90%-from 3,600 pounds in a regular supermarket to just 350 pounds in the Scarborough Superstore. In fact, the synthetic refrigerant does not spread throughout the store but stays in the plant space. The cold storage is handled by two secondary loops with either propylene glycol for medium temperature or CO₂ for application at low temperature. Canada-based firm CSC Group has launched its CO₂ refrigeration system. Greek ice-cold merchandisers producer Frigoglass recently launched a new range of R744 beer coolers. The Ecocool coolers use as much as 50% less energy than comparable units produced ten years ago, according to the manufacturer. Leading beverage companies PepsiCo and Coca-Cola installed 30 and 4 CO₂ vending machines, respectively, in Washington DC.

Ms. Greco B.V., a Netherlands based company, introduced NH₃-CO₂ based cascade system for freezing applications. Stellar Group of USA commissioned the world's largest CO₂/NH₃ plant in the year 2002. In a joint venture, Kansai Electric Power Co. and Mayekawa Mfg. Co. has successfully tested an 80 kW CO₂/NH₃ ultra low temperature cascade system using CO₂ as a bottoming cycle refrigerant. Several other fluid combinations are already in operation in the Nordic countries employing CO₂ as a volatile secondary refrigerant (Neeraj 2008). Denso of Japan is the leading manufacturer of CO₂ heat pump water heater. By using the patented Shecco technology, they developed a CO₂ heat pump hot water supply unit named EcoCute. A Norway company, Larvik, installed a 25 kW pilot plant in a food-processing

factory by using waste heat from an industrial NH₃ refrigeration system. Several car manufactures are switching to CO₂ based automobile air conditioning. German carmaker BMW has confirmed to a leading automotive news source that they will use CO₂ as the refrigerant for their next-generation air conditioning systems.

2.6 CO₂ BASED SECONDARY LOOP SYSTEMS

In recent times CO₂ is being considered as a secondary fluid. This may be attributed to many favorable properties of CO₂, which make it an excellent secondary fluid.

Yanagisawa et al. (2004) performed experimental studies on a natural system of circulation using carbon dioxide as a secondary fluid. The primary vapor compression cooling system uses ammonia in its system, while the secondary fluid, i.e., carbon dioxide, changes phase as it flows through the tube. He has experimentally proved that CO₂ based natural circulation secondary loop system is feasible. Frobese et al. (2004) saved power by using liquid CO₂ as a volatile secondary refrigerant instead of conventional water-based solutions such as glycol. Rieberer et al. (2004) studied the efficiency of the CO₂ based two-phase thermosyphon was tested experimentally and theoretically. He used the thermosyphon as a heat source to the heat pump and found that overall efficiency is improved due to the absence of an external mechanical pump. Following the above research, Rieberer (2005) carried out theoretical and experimental studies on ground-coupled heat pumps using thermosyphons based on carbon dioxide to extract geothermal energy. His paper discusses that after trying different working fluids like R 22, R 134a, propane, and CO₂, an Austrian company selected CO₂ as the most appropriate thermosyphon working fluid. It is also claimed that there are already about 100 such units in service in the market. Yoshikawa (2005) presented a paper on the efficiency of using supercritical CO₂ in a natural circulation system. Experiments are conducted to measure the flow rates using the acetone tracer technique. He found that circulation rate is a function of density difference between heating and cooling systems. He compared the theoretical results with experimental results, and a correlation was suggested for velocity in terms of effective density difference, Grashof number and Prandtl number. Melinder (2004) compared different aqueous and non-aqueous solutions (including liquid CO₂) as secondary fluids for applications under low temperature conditions. He has found that, due to its very low viscosity, CO₂ offers the lowest pressure drop among the several working fluids

examined. Pruess (2006) used CO₂ instead of water in geothermal systems. He found that CO₂ in its capacity to extract the heat from a hot molten rock is superior to water. Carbon dioxide also provides some advantages with regard to well bore hydraulics, since its greater compressibility and expansiveness compared to water, it increases the buoyancy forces and reduces the parasitic power consumption of the fluid circulation system. Zhang and Yamaguchi (2007) conducted experimental studies on evacuated solar collectors using supercritical CO₂ as the working fluid under various weather conditions. They noted that replacing water with supercritical CO₂ as working fluid will significantly improve the efficiency of the annually averaged solar collector. Yet, their system uses a hydraulic pump to disperse the supercritical carbon dioxide through the network of solar collectors. Kaga et al. (2008) developed a small cooling system that uses the flammable hydrocarbon (R600a) as a coolant. The flammable refrigerant is held outside the refrigerated space and carbon dioxide is used to transfer heat from the refrigerated space to the evaporator of a R600a refrigeration system as secondary fluid. Their studies show that with the correct optimization, the same level of performance could be achieved with the secondary system as that of a standard R600a system, although the introduction of a secondary loop adds an additional heat exchanger. This is due to the excellent CO₂ properties and optimized system design. Zimmermann and Melo (2008) have carried out theoretical and experimental studies on a Stirling cooler that uses CO₂ based two phase thermosyphon loop between the cold end of the cooler and the refrigerated space. Rasmussen (2008) replaced a traditional glycol based chiller system with a CO₂ cooling system and claimed that energy has been saved by CO₂ system.

2.7 HIGH PRESSURE SAFETY ISSUES

Owing to the thermodynamic properties of CO₂, operating pressures are quite high even though NCL operates at moderate temperatures for different refrigeration and air conditioning applications. For example, in air conditioning applications, if one wants to operate at 10 °C, then the system pressure is around 45 bar. High pressure is always a concern that influences the component design as well as cost. However, at high pressures, the allowable pressure drop increases, which leads to more compact heat exchangers even with extruded multiport tubing and parallel flow of refrigerant in several tubes and flow channels. Pettersen et al. (1998) built and tested a CO₂

microchannel type heat exchanger and compared it with baseline units in terms of physical dimensions, mass and performance. Transcritical operation and high pressure is expected to considerably increase the convective heat transfer. The higher vapour density and low velocity of CO₂ typically reduce the low side tubing inner diameter by 60-70% compared to HFC systems (Kim et al. 2004). Due to reduction in tube diameter, even at high pressure, pipe thickness is more or less the same as in HFC systems, which leads to size and weight reduction of the CO₂ system (Neeraj 2008).

CO₂ system can be associated with two types of hazards, one with physical and chemical characteristics and the other due to pressure and temperature. Being a natural substance, CO₂ is not hazardous. It is non-flammable and non-toxic and is present in the atmospheric air within the safety limit. Nevertheless, the toxicological effects in humans vary from headaches, elevated respiratory and heart rates, dizziness, muscle twitching, confusion, unconsciousness, coma and death depending on the concentration of CO₂ inhaled and exposure period. Due to the toxicological consequences, breathing air with a CO₂ concentration above 5% will pose a significant risk to people. It would be lethal to inhale 30% of CO₂ in minutes. It is a myth that with CO₂ systems, high pressure is a serious safety concern since the equipment will be equipped for this. Nevertheless, the explosion energy (stored energy) characterizes the degree of possible damage in case of a system breakup. Similar results are also observed with baseline R134a systems; explosion energy of the baseline system is smaller at normal temperature but becomes higher at elevated temperature (Kim et al. 2004). New safety requirements are proposed for the CO₂ mobile air conditioning and heat pump (Neeraj, 2008).

2.8 INSTABILITY IN NCL

A natural circulation loop is commonly used where there is a need for a quick and safe heat transfer device, but it has a significant instability problem caused by changes in regular fluid flow directions. One of the best ways to solve such a problem is to tilt the entire loop by some angle, which can affect the heat transfer and pressure drop of the loop. Yadav et al. (2016) carried out a numerical study on the instability of NCL, suggested that loop tilting is one of the elegant solutions for instability in NCL. The present experimental study is conducted to quantify the tilting effect on the heat transfer rate and pressure drop as well.

However, natural circulation loops have an inherent problem of instability, which causes a frequent change in fluid flow direction and magnitude. Various researchers have studied the different configurations of NCL and reported instability problems (Welander1967, Vijayan 2002, Cammarata et al. 2003, Mousavian et al. 2004, Jain and Rizwan-uddin 2008). The study on the instability of the loop carried out by Welander (1967) employed direct numerical time integration of the model equations and observed the pulsative type of motions in convection experiments. The experimental observations made on non-uniform diameter single-phase NCLs reported that the stability depends on a large number of geometric parameters (Vijayan 2002). Considering the effect of geometrical loop configurations and parameters like vertical/horizontal length of the tube and inner tube diameters, stability analysis is carried out employing a nonlinear mathematical model describing the dynamic behavior of the non-dimensional flow velocity and temperature inside the loop (Cammarata et al. 2003). One-dimensional linear stability analysis was carried out for single-phase NCL employing RELAP5 and numerical perturbation technique. The results of the same were compared with experimental data available in the literature (Mousavian et al. 2004). Using a one-dimensional model, the steady-state and dynamic behavior of the loop for supercritical conditions reveals similar instability characteristics in two-phase flow (Jain and Rizwan-uddin 2008). The instability problem was noticeable when the loop was geometrically and thermally symmetrical. As a solution for this, few studies demonstrated that the tilting of an entire loop in XY/YZ planes could offer a key solution to the instability problems in a single phase NCL (Misale et al. 2007, Yadav et al. 2016, Yadav et al. 2017). Tilting the loop also deteriorates the performance of the loop in terms of heat transfer and pressure drop. Detailed measurement of the heat transfers and pressure drop is required to understand these effects.

2.9 RESEARCH GAP AND OBJECTIVES

The above discussion gives a broad overview of research work carried out so far on secondary loops, CO₂ based systems, etc. Based on the literature survey, the following observations are made:

- The majority of studies have been conducted on forced circulation loops.
- Although there is growing interest in CO₂-based secondary loops in recent times, it is observed that limited studies are available on these systems.
- Eventhough natural circulation loops have been used in some engineering fields like nuclear power plants, solar water heating, electronic cooling, and geothermal systems, their application to refrigeration systems is very limited.
- Eventhough some experimental investigations have been carried out on natural circulation loops, those are mostly related to constant heat flux heat addition. Experimental works with end heat exchangers are relatively scarce.

Because systematic research on natural circulation loops with CO₂ as the working fluid is less for refrigeration and air conditioning applications, the following aspects are discussed in depth in the present thesis.

1. Design and fabrication of an experimental facility for high pressure (150 bar) CO₂ based NCL with tilting arrangement.
2. Experimental study on widely accepted working fluid i.e., water and brine based NCL for different operating temperatures and tilt angles.
3. Study the effect of operating pressure, temperature and tilt angle in supercritical CO₂ based NCL.
4. Experimental study on single phase (subcritical vapor and liquid) CO₂ based NCL for different operating pressures, temperatures and tilt angles.
5. Experimental investigation on two phase CO₂ based NCL considering the parameters like operating pressure, temperatures and tilt angles.
6. Comparative study between CO₂ based NCL with a widely used water/brine based system.

Chapter 3

EXPERIMENTAL FABRICATION AND PROCEDURE

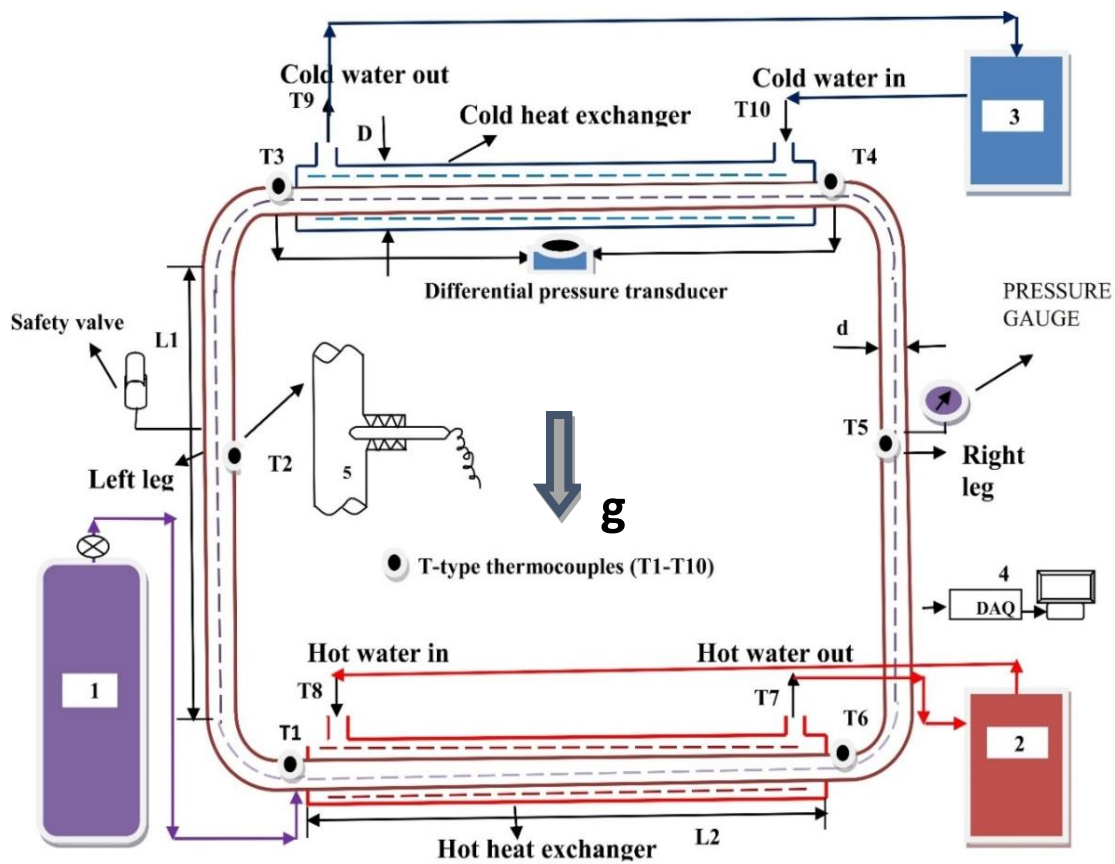
3.1 INTRODUCTION

This chapter describes the methodology involved in developing the experimental and the instruments used to perform the experiments. Loop tilting arrangement, testing procedure, and the uncertainty analysis are also presented in this chapter.

3.2 THE EXPERIMENTAL TEST FACILITY

A detailed schematic representation of the experimental facility used in this study is shown in Figure 3.1. The experimental facility has two tube-in-tube heat exchangers (hot heat exchanger and cold heat exchanger) and two insulated legs (left and right leg). In addition to these main components, a CO₂ reservoir is also employed in the experimental setup.

A natural circulation loop of 2 m×2 m is made up of stainless steel (SS-316) of outer diameter 32 mm, inner diameter 26 mm, having thickness 3 mm, and it has a capacity to withstand pressure up to 250 bar. To reduce heat transfer from loop to ambient, the entire loop is insulated with asbestos rope and foam tape types insulating material of thickness 3mm each. Stainless steel 316 includes the addition of molybdenum that enhances corrosion resistance, and when exposed to corrosive conditions, it has outstanding corrosion resistance. Stainless steel 316 has good oxidation resistance to up to 870 °C. The heat exchangers are having a length of 1600 mm, an outer diameter of 51 mm, and a thickness of 3 mm. Figure 3.2 (a) and (b) show the photographic view of the setup without insulation and with one-layer asbestos rope insulation, respectively. Six T-type thermocouples are used to monitor the temperature of CO₂ at various locations along the loop.



1: CO₂ reservoir cylinder, 2: Thermostatic bath for HHX, 3: Thermostatic bath for CHX 4: Data acquisition system, 5: An enlarged portion of inside thermocouple arrangement (Nut and ferrule)

Figure 3.1 Schematic of the NCL with end heat exchangers

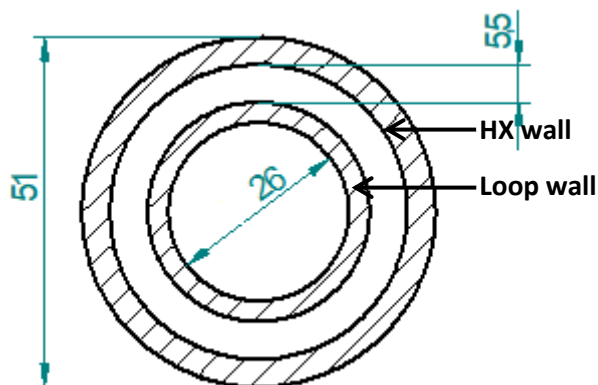


Figure 3.2 Cross section view of the heat exchanger (Dimensions in mm)

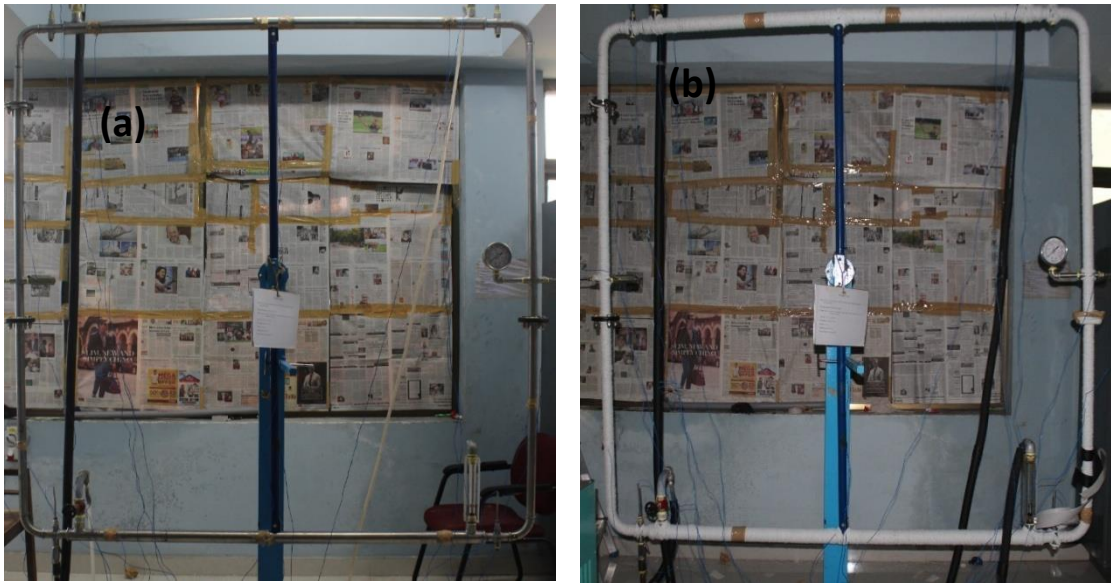


Figure 3.3 Experimental setup photographic view (a) Without insulation, (b) With one layer of asbestos rope insulation

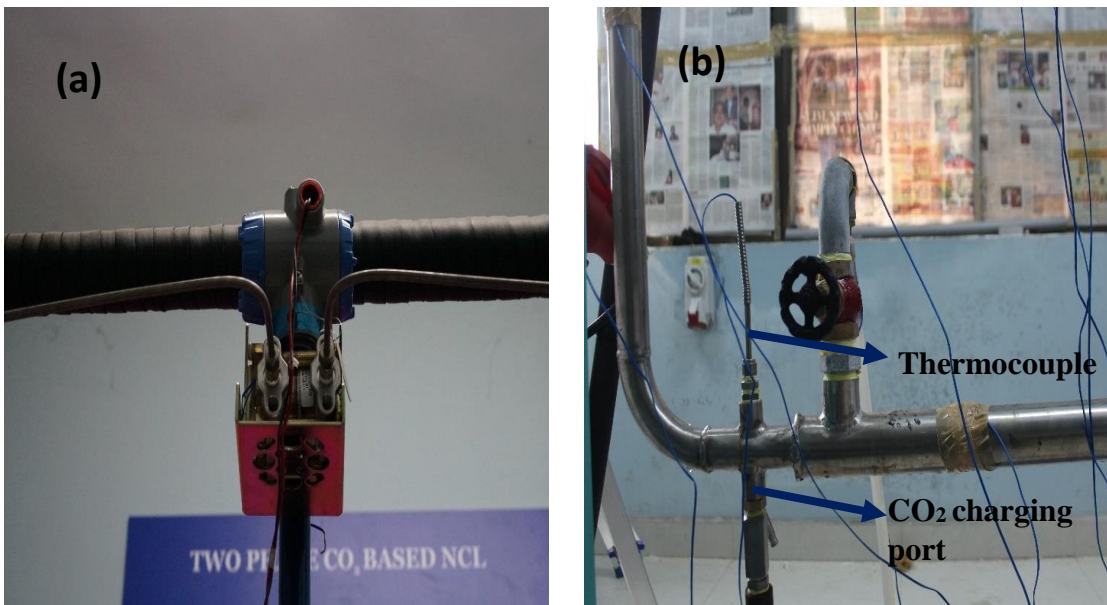


Figure 3.4 Experimental setup photographic view (a) Differential pressure transducer, (b) CO₂ charging line and thermocouple arrangement

Thermocouples are connected directly with the internal loop fluid CO₂, as shown in Figure 3.3 (b) of an enlarged portion of nut and ferrule arrangement. Locations of thermocouples for loop temperature are shown in Figure 3.1 (T1-T6).

Two thermostatic baths (Thermo scientific PC200) having a heating/cooling capacity of 2 kW supplies external fluid (water/methanol) at a fixed temperature to the heat exchangers. The mass flow rate of external fluids is measured using two calibrated

rotameters (0-20 LPM range) with valve arrangement, connected separately to HHX and CHX. A differential pressure transducer made by Honeywell (range 0-1000 mbar) is connected to either end of the cold heat exchanger. At the middle of the right leg, a bourdon pressure gauge (0-150 bar range) is attached. A safety valve is connected at the center of the left leg, and its set is for 120 bar for the entire experiment. A computer-integrated data acquisition system (KEITHLY-2700, Kickstart Software) is used to collect and store various loop temperatures. Table 3.1 shows the geometric description of the experimental setup. The operating variables and their operating range is presented in Table 3.2 for the entire experiment. Depending on the operating conditions, CO₂ can exist as vapor, liquid, or in two phase liquid-vapor mixture inside the loop. Figures 3.3 and 3.4 show the equipment's details used for experimentation. The photographic view of the assembled test facility is shown in Figure 3.5. Table 3.3 shows the equipment details, operating range, and accuracy.

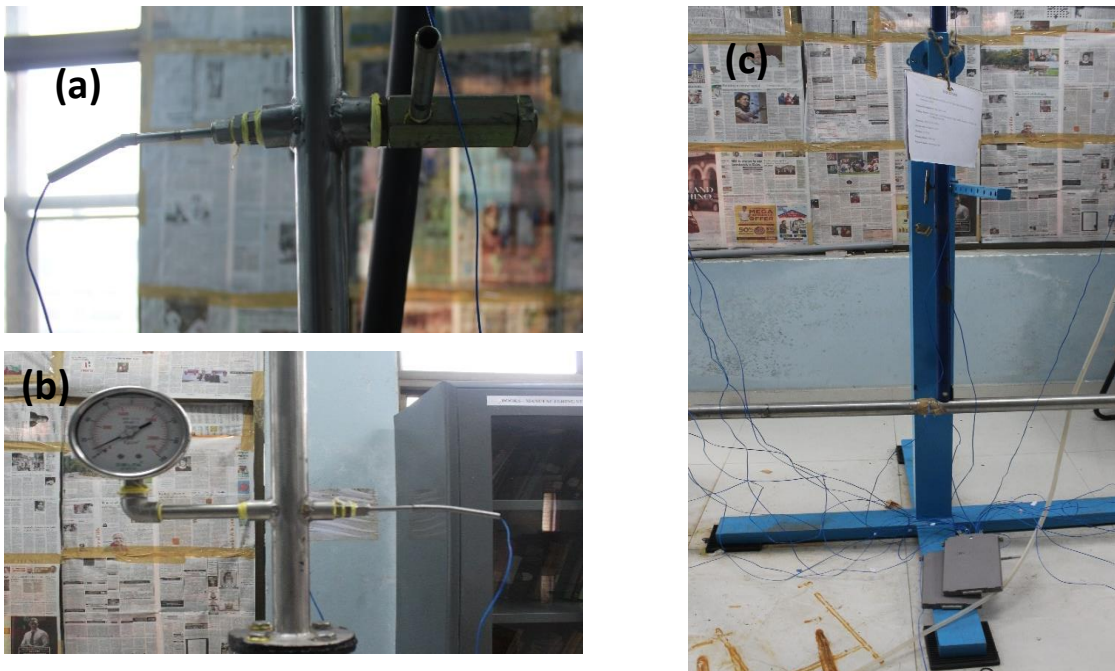


Figure 3.5 Equipments used for test facility (a) Safety valve, (b) Pressure gauge, (c) Loop base

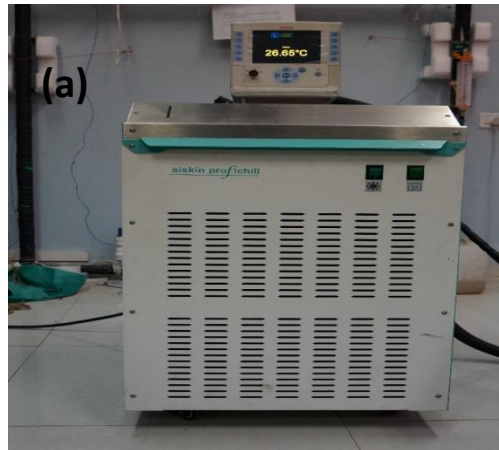


Figure 3.6 Equipments used for test facility (a) Thermostatic bath, (b) Vacuum pump
(c) DAQ

Table 3.1: Geometrical parameters of the experimental setup

Loop details	Size (mm)
Outer diameter of the loop pipe (d)	32
Internal diameter of the loop pipe	26
Thickness of the loop pipe	3
Length of left leg or right leg loop (L1)	1800
Length of the bend of the loop (outer)	157
Length of the bend of the loop (inner)	122.5
Distance from heat exchanger up to the bend of the loop	100
Heat exchanger details	
Outer Diameter of the heat exchanger (D)	51
Thickness of the heat exchanger wall	4
Length of heat exchanger (L2)	1600
Annulus distance (radial)	5.5



1: Thermostatic bath- 1(HHX), 2: DAQ, 3: Computer to read DAQ Data, 4: Thermostatic bath -2(CHX), 5: Pressure Gauge, 6: Rotameter, 7: Differential Pressure Transducer, 8: Safety Valve, 9: CO₂ cylinder, 10:Vaccum pump.

Figure 3.7 Experimental setup

Table 3.2: Range of operating parameters considered during the study

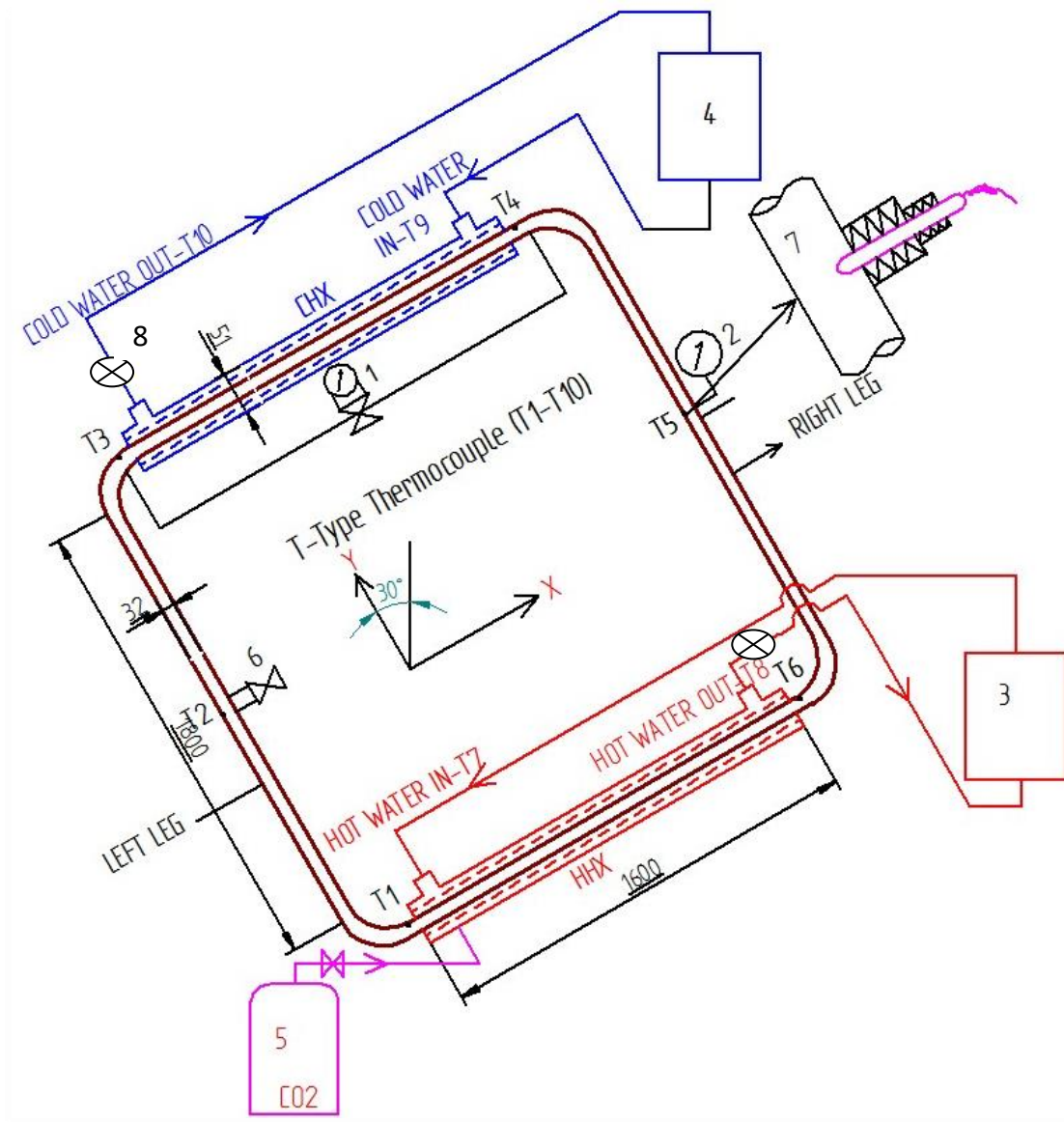
Parameters	Range	Error range (%)
Hot water/brine inlet temperature (T_H)	-10–70 °C	±0.05
Cold water/brine inlet temperature (T_C)	-18–32 °C	±0.05
System pressure	35–90 bar	±2.5
External fluid mass flow rate (m_{ex})	5 LPM	±5.0

Table 3.3: Equipment details used for experimentation

Equipment	Make/Type	Range	Accuracy
Thermostatic bath with inbuilt pump and heat exchanger	Thermo scientific PC200	-60 to 150 °C Heating/cooling capacity 2 kW	±0.01 °C
Thermocouple	T-type	-270-370 °C	±0.25 °C
Data Acquisition System	KEITHLY-2700	-	±0.01 °C
Differential Pressure transducer	Honeywell	0-1000 mbar	±0.1 mbar
Rotameter	-	0-20 LPM	±0.2 LPM
Pressure Gauge	Delta/Bourdon tube	0-150 bar	±1 bar

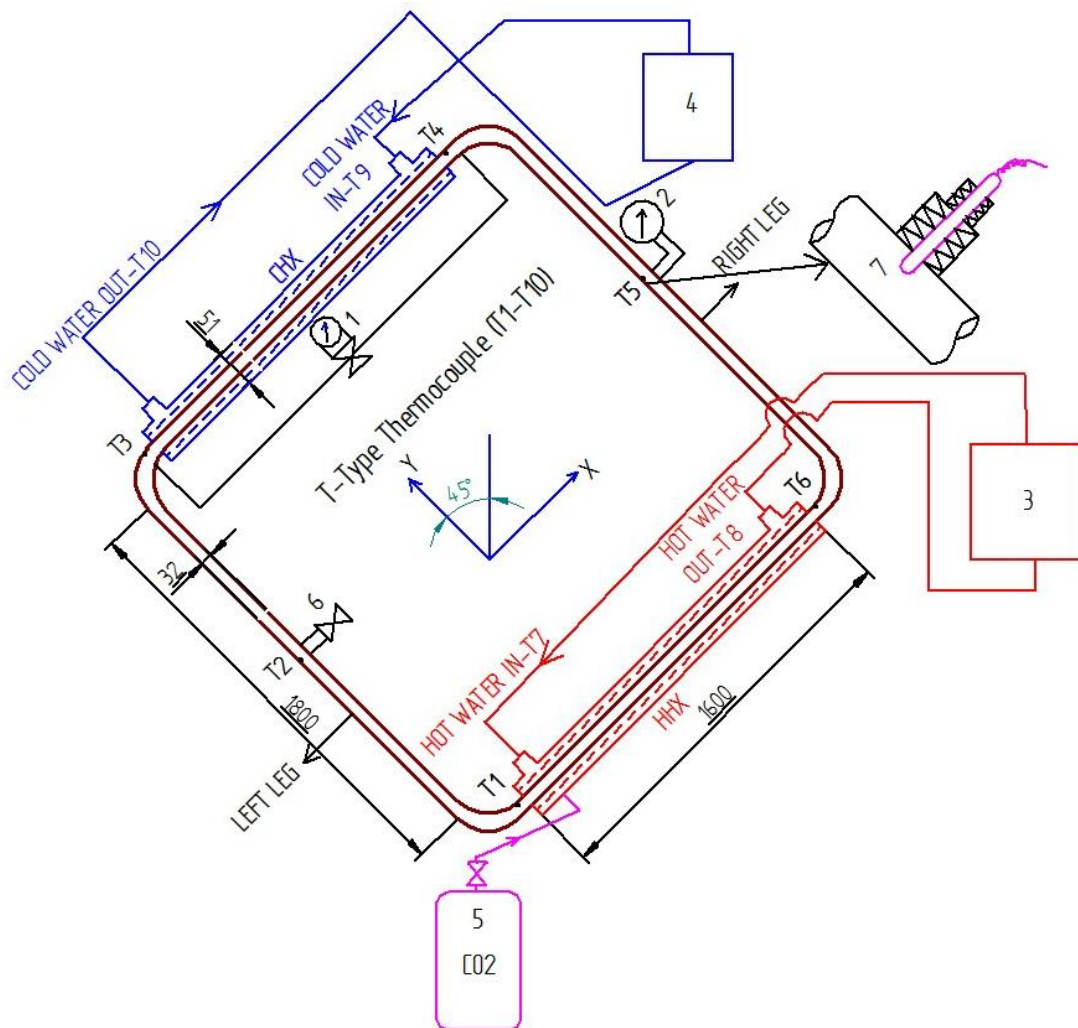
3.3 THE EXPERIMENTAL TEST FACILITY FOR TILTING

The experimental setup is designed so that the entire loop can be tilted at any specified angle in XY and YZ planes (as shown in Figures 3.6, 3.7, and 3.8).



1: Differential pressure transducer, 2: Pressure gauge, 3: Thermostatic bath for HHE, 4: Thermostatic bath for CHE, 5: CO₂ reservoir cylinder, 6: Safety valve, 7: Enlarge portion of inside thermocouple arrangement (Nut and ferrule), 8: Rotameter.

Figure 3.8 Schematic representation of experimental setup at XY-30° position



1: Differential pressure transducer, 2: Pressure gauge, 3: Thermostatic bath for HHE, 4: Thermostatic bath for CHE, 5: CO₂ reservoir cylinder, 6: Safety valve, 7: Enlarge portion of inside thermocouple arrangement (Nut and ferrule)

Figure 3.9 Schematic representation of experimental setup at XY-45° position

The base structure is fabricated to tilt the loop in the XY plane and arrest the loop moment in the YZ plane and vice versa, as shown in Figure 3.9.

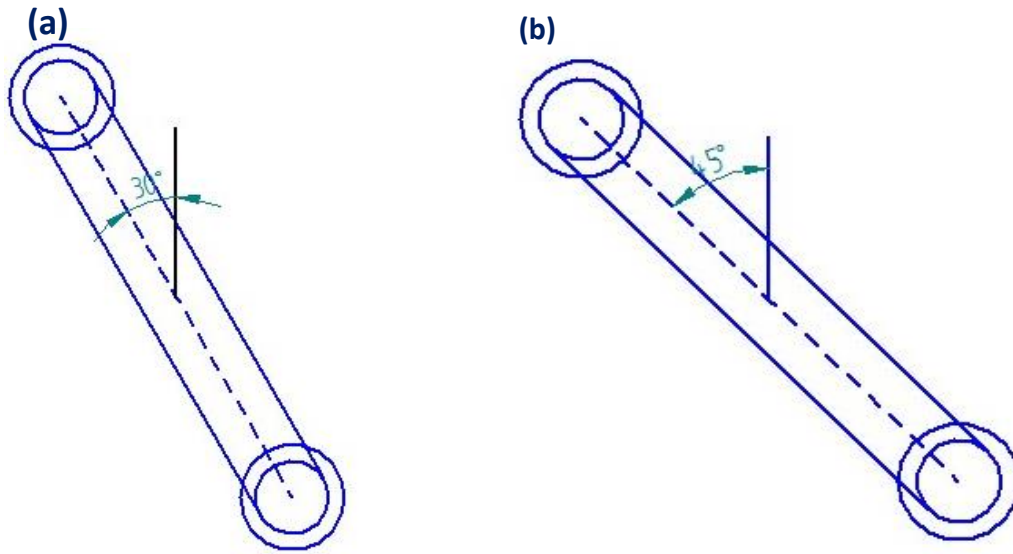


Figure 3.10 Schematic of the NCL (a) YZ 30° position (a)YZ 45° position

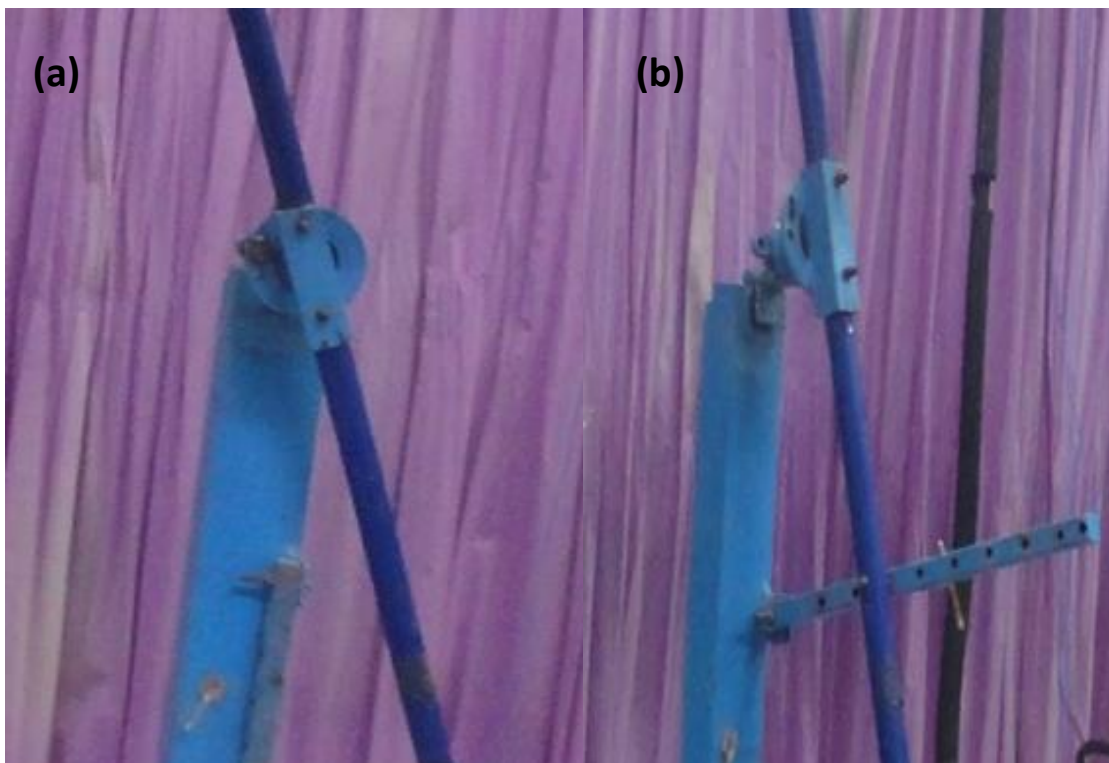


Figure. 3.11 Photographic view of tilting arrangement (a) XY plane, (b) YZ plane

3.4 ERROR ANALYSIS

Error analysis is carried out to find measurement errors that occurred during experiments in various parameters. In this study, the heat transfer rate is an important parameter that depends on the mass flow rate (m), temperature difference (ΔT), and specific heat of the external fluid. Since specific heat (density) of external fluid is considered to be constant, the relation formula is given as:

$$Q_{HHX} = f(m, \Delta T_{HHX}) \quad (3.1)$$

$$Q_{CHX} = f(m, \Delta T_{CHX}) \quad (3.2)$$

Uncertainty in heat transfer rate:

The minimum operating mass flow rate measured is 5 LPM, and the least count of the rotameter is 0.2 LPM.

Therefore, the maximum uncertainty in mass flow rate measurement is

$$\frac{\Delta m}{m} = \frac{0.2}{5} = \pm 0.04 = \pm 4.0\% \quad (3.3)$$

The minimum operating temperature recorded is -18°C , and the accuracy for the T-type thermocouple is $\pm 0.25^\circ\text{C}$.

Maximum uncertainty in temperature measurement is

$$\frac{\Delta T}{T} = \frac{0.25}{18} = \pm 0.0138 = \pm 1.38\% \quad (3.4)$$

Uncertainty in the heat transfer rate is calculated by

$$\begin{aligned} \frac{\Delta Q}{Q} &= \left[\left(\frac{\Delta m}{m} \right)^2 + 2 \left(\frac{\Delta T}{T} \right)^2 \right]^{1/2} \quad (3.5) \\ \frac{\Delta Q}{Q} &= [(0.04)^2 + 2(0.0138)^2]^{1/2} = \pm 4.45\% \end{aligned}$$

Overall uncertainty including all devices and parameters (from Table 3.3)

$$\begin{aligned} &= \left[\left(\frac{\Delta m}{m} \right)^2 + 2 \left(\frac{\Delta T_1}{T_1} \right)^2 + \left(\frac{\Delta T_2}{T_2} \right)^2 + \left(\frac{\Delta T_3}{T_3} \right)^2 + \left(\frac{\Delta p_1}{p_1} \right)^2 + \left(\frac{\Delta p_2}{p_2} \right)^2 \right]^{1/2} \quad (3.6) \\ &= \left[\left(\frac{0.2}{5} \right)^2 + 2 \left(\frac{0.25}{18} \right)^2 + \left(\frac{0.01}{18} \right)^2 + \left(\frac{0.01}{18} \right)^2 + \left(\frac{0.1}{1} \right)^2 + \left(\frac{1}{50} \right)^2 \right]^{1/2} = \pm 5.3\% \end{aligned}$$

3.5 EXPERIMENTAL PROCEDURE

After fabrication of setup, the annulus parts of the heat exchangers are tested for leakages at 2 bar pressure, and the loop is tested at 150 bar. The entire loop is monitored for the leakages for 24 hours at testing pressure; no leakages are observed as the pressure drop during the testing is zero. Later, the loop is evacuated, and a required amount of CO₂ is charged into the loop from the CO₂ cylinder. Charging of CO₂ is stopped once the loop fluid pressure reaches the required operating condition. External fluid is made to flow inside both heat exchangers' annular tube at a specified mass flow rate and temperatures. When external fluid starts flowing, loop temperature starts varying with a small variation in loop pressure. To maintain specified operating pressure, CO₂ is transferred to/from the cylinder, which is kept at operating pressure. This practice continues until the loop reaches a steady state. The loop is said to be reached a steady state if the transient variation in all temperatures and pressures are less than 0.5%. All experiments are repeated twice to reduce experimental errors.

The supercritical condition inside the loop is achieved by a continuous supply of external fluid (HHX and CHX) at low temperature. Because of the low temperature, the loop fluid pressure is reduced. Once the loop pressure is reduced, the charging of CO₂ is done, and the same procedure is continued to build the required pressure of loop fluid inside the loop (even though cylinder pressure is low below 60 bar).

Chapter 4

EXPERIMENTAL INVESTIGATION ON SUPERCRITICAL CO₂ BASED NCL

4.1 INTRODUCTION

This experimental study covers the operating conditions ranging from 32 °C to 70 °C temperatures and operating pressure from 75 to 90 bar in the supercritical region of CO₂. The heat transfer rate and pressure drop of supercritical CO₂ based natural circulation loop (NCL) is compared with water based system at the same operating temperatures. The temperature distribution of CO₂ along the loop at different operating temperatures and pressure is studied to ensure the condition/state of the inside the loop fluid.

As loop tilting is one of the elegant solution for instability in mini loop NCL suggested by Yadav et al. (2016, 2017) numerically as well as experimentally, the present experimental study is conducted to quantify the tilting effect on the heat transfer rate and pressure drop as well. To get the effect at a various tilt angle, the entire loop is tilted in XY plane (30°, 45°) as well as in YZ plane (30°, 45°). Results on supercritical CO₂ with and without tilting are presented.

To ensure turbulent flow conditions in heat exchanges (CHX and HHX), external fluid (water) at a mass flow rate of 0.083 kg/s (5 liters/min) is circulated in the annulus. Calculation of the heat transfer rate is done by the heat carried away or supplied by external fluid in the heat exchangers.

Heat transfer rate (Q),

$$Q = m \times c_{p-HHX} \times \Delta T_{HHX} = m \times c_{p-CHX} \times \Delta T_{CHX} \quad (4.1)$$

Where m = mass flow rate of external fluid in kg/s

c_{p-HHX} = specific heat of HHX in J/kg-K

c_{p-CHX} = specific heat of CHX in J/kg-K

ΔT_{HHX} = HHX temperature difference between inlet and outlet

ΔT_{CHX} = CHX temperature difference between inlet and outlet

Average temperature is calculated by

$$T_{avg} = \frac{T_C + T_H}{2} \quad (4.2)$$

Where, T_C = CHX inlet temperature in °C

T_H = HHX inlet temperature in °C.

4.2 HEAT TRANSFER RATE AND PRESSURE DROP OF CO₂ BASED NCL AT DIFFERENT OPERATING PRESSURES AND TEMPERATURES

In this study, water is considered as the external fluid in both heat exchangers (HHX and CHX). CHX water inlet temperature is kept constant at 32 °C (just above the CO₂ critical temperature of ~31 °C), whereas water temperature at HHX inlet is varied from 40 °C to 70 °C in steps of 10 °C and operating pressure is varied from 75 to 90 bar (above critical pressure ~73.7 bar). The effect of operating pressure on the heat transfer rate at different HHX inlet temperatures (T_H) for a fixed T_C is depicted in Figure 4.1.

Figure 4.1 shows that as the water inlet temperature of HHX increases, the heat transfer rate increases due to the increase in buoyancy effect caused by an increase in temperature difference between CHX and HHX. Even though there is a decrease in density at a higher temperature at a given pressure, which may cause a drop in mass flow rate, but the heat transfer rate does not decrease. It shows the dominancy of the buoyancy force. The heat transfer rate is found to be maximum for the operating pressure of 90 bar.

Average operating temperature (~loop fluid temperature) of 41 °C (obtained in this case) is near to the pseudo critical point (40.2 °C) of CO₂ at 90 bar, which leads to a maximum heat transfer rate at this pressure because of a very high volumetric expansion coefficient of CO₂. Experiments are also carried out for average operating temperatures of 46 °C and 51 °C and similar trends are observed.

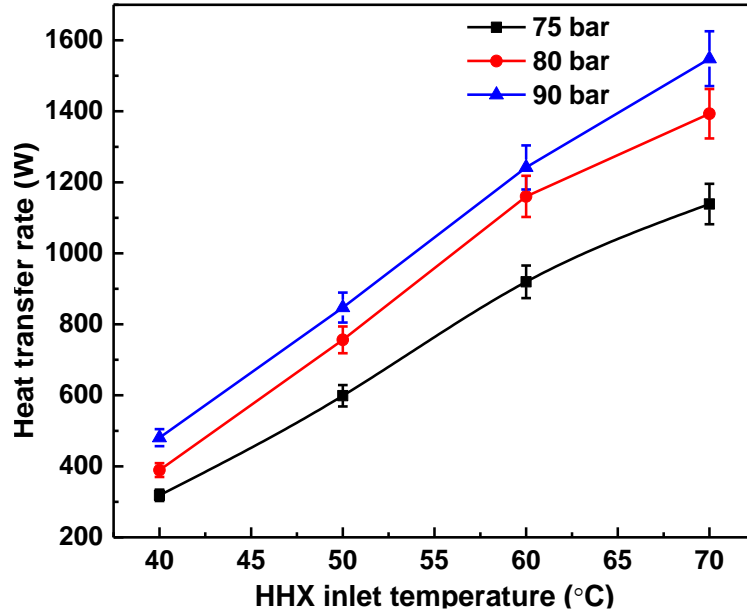


Figure 4.1 Variation of the heat transfer rate of CO₂ at different operating pressures and at different HHX inlet temperatures

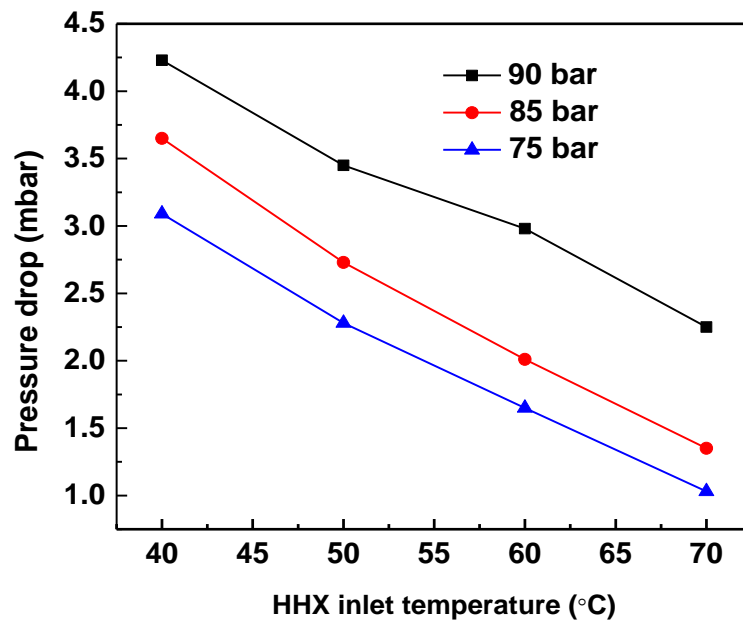


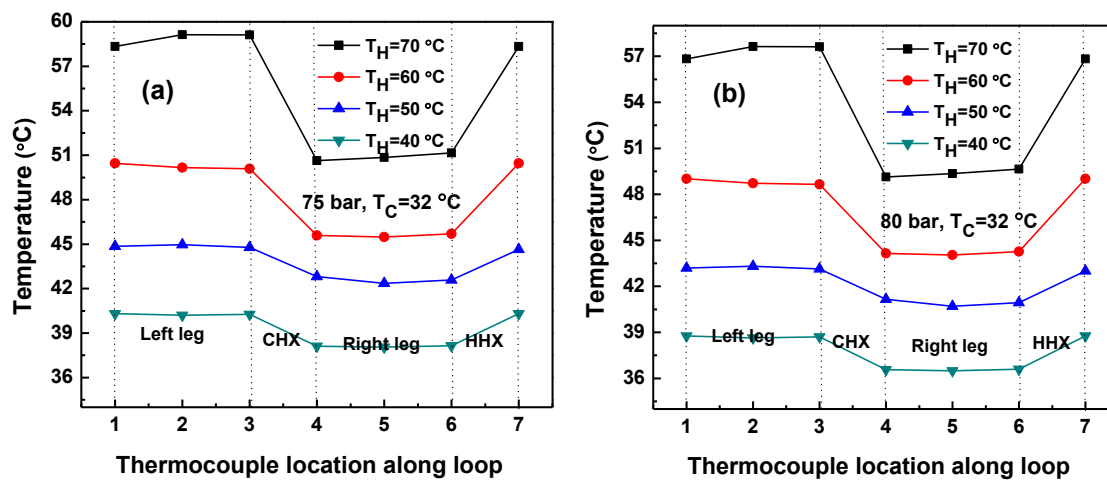
Figure 4.2 Variation of pressure drop of CO₂ at different operating pressures and different HHX inlet temperatures

The effect of operating pressure on the pressure drop at different HHX inlet temperatures (T_H) for a fixed T_C is depicted in Figure 4.2. The result shows that if an increase in operating pressure, there is an increase in pressure drop. With an increase in HHX inlet temperature there is a decrease in pressure drop. At higher temperatures, the decrease in viscosity leads to a lower pressure drop in the loop (shown in Table 4.2).

4.3 TEMPERATURE DISTRIBUTION OF CO₂ BASED NCL AT DIFFERENT OPERATING PRESSURES

Figures 4.3 (a) to (c) show the temperature variation throughout the loop at different operating pressures (75, 80 and 90 bar) and different HHX inlet temperature. The temperature variation is also recorded for all operating pressures to make sure the loop fluid (CO₂) is in the supercritical state throughout the loop.

Figure 4.3(a) shows with an increase in the HHX inlet temperature, the loop fluid temperature increases and the loop fluid temperature difference between the left leg center and right leg center also increases. Similar trends are also observed in Figure 4.3 (b) and (c) for 80 and 90 bar. Figure 4.3 (a-c) shows the effect of pressure on the loop fluid temperature difference between the left leg center and right leg center. Results clearly show that as pressure increases, temperature difference decreases, which occurs due to an increase in specific heat (shown in Table 4.2) at higher pressure at a particular average operating temperature ($T_{avg} = 46 \text{ }^\circ\text{C}$, $T_H = 60 \text{ }^\circ\text{C}$).



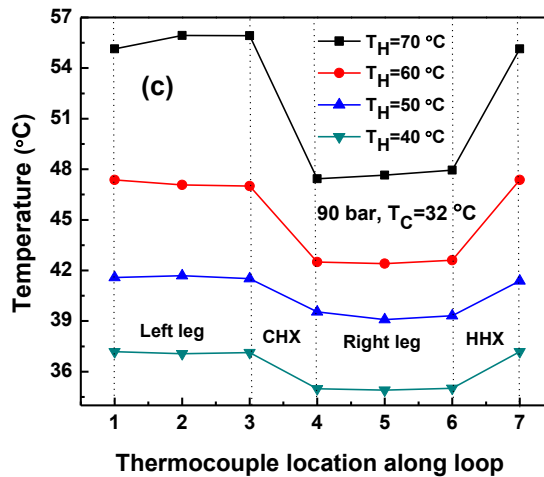


Figure 4.3 Variation of temperature along the loop at different operating pressures and different HHX inlet temperatures at (a) 75 bar, (b) 80 bar and (c) 90 bar

4.4 EFFECT OF TILT ANGLE ON THE PERFORMANCE OF SUPERCRITICAL CO₂ BASED NCL

The heat transfer performance and pressure drop of CO₂ based NCL with end heat exchangers operating under supercritical conditions for various tilt angles (30°, 45°) in XY and YZ planes have been investigated.

The Experimental setup is designed in such a way that, the entire loop can be tilted at any specified angle in XY and YZ planes as shown in Figures 4.4 and 4.5. The operating conditions are maintained the same as explained in the above section.



1:Thermostatic bath- 1(HHX), 2: Computer to read DAQ data, 3: DAQ (Data acquisition system), 4: Thermostatic bath -2(CHX), 5: Rotameter, 6: Pressure Gauge, 7: T-Type thermocouple, 8: Differential Pressure Transducer, 9: Safety Valve, 10: CO₂ cylinder.

Figure 4.4 Experimental setup at XY-30° position



1:Thermostatic bath- 1(HHX), 2: Computer to read DAQ data, 3: DAQ (Data acquisition system), 4: Thermostatic bath -2(CHX), 5: Rotameter, 6: Pressure Gauge, 7: T-Type thermocouple, 8: Differential Pressure Transducer, 9: Safety Valve, 10: CO₂ cylinder.

Figure 4.5 Experimental setup at YZ-30° position

4.4.1 Effect of tilt angle on the heat transfer rate at different operating pressures

Figure 4.6 (a) and (b) shows the effect of tilt angle on heat transfer rate for 50 °C HHX water inlet temperature at different operating pressures in XY/YZ (0°, 30°, 45°) planes and fixed CHX water inlet temperature (32 °C). Results show that there is a marginal drop in heat transfer rate after tilting the loop in XY (30°, 45°) as well as in YZ (30°, 45°) planes, which occurs due to lower buoyancy on account of reduction in effective height of the loop between CHX and HHX.

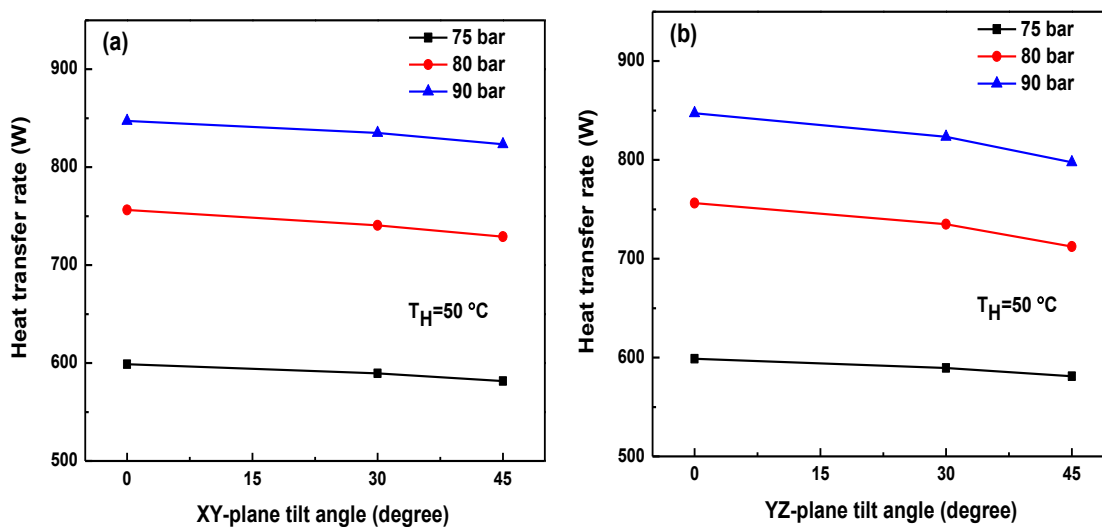


Figure 4.6 Variation of heat transfer rate of CO₂ at different pressures and $T_H = 50$ °C in (a) XY-plane and (b) YZ-plane

Figure 4.7 (a) and (b) show the effect of tilt angle on heat transfer rate for 60 °C HHX water inlet temperature at different operating pressures in XY/YZ (0°, 30°, 45°) planes and fixed CHX water inlet temperature (32 °C). Results show that there is a small marginal drop in heat transfer rate after tilting in XY (30°, 45°) as well as in YZ (30°, 45°) planes, maximum drop in heat transfer rate found in YZ planes.

Figure 4.8 (a) and (b) show the effect of tilt angle on heat transfer rate for 70 °C HHX water inlet temperature at different operating pressures in XY/YZ (0°, 30°, 45°) planes and fixed CHX water inlet temperature (32 °C). Results show that similar trends observed in 70 °C HHX water inlet temperature, there is a small marginal drop

in heat transfer rate after tilting in XY (30°, 45°) as well as in YZ (30°, 45°) planes, maximum drop in heat transfer rate found in YZ planes.

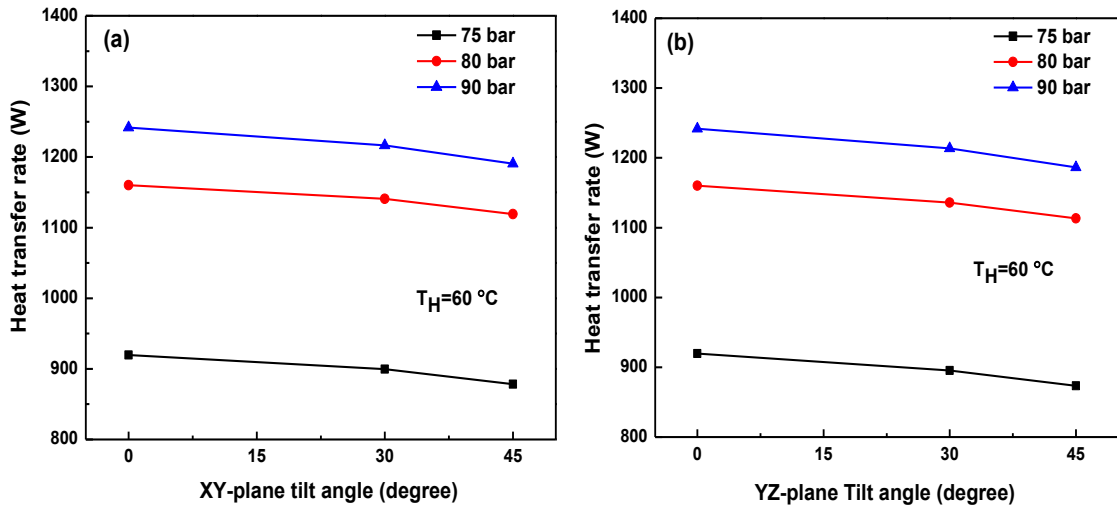


Figure 4.7 Variation of heat transfer rate of CO₂ at different pressures and $T_H = 60^\circ\text{C}$ in (a) XY-plane and (b) YZ-plane

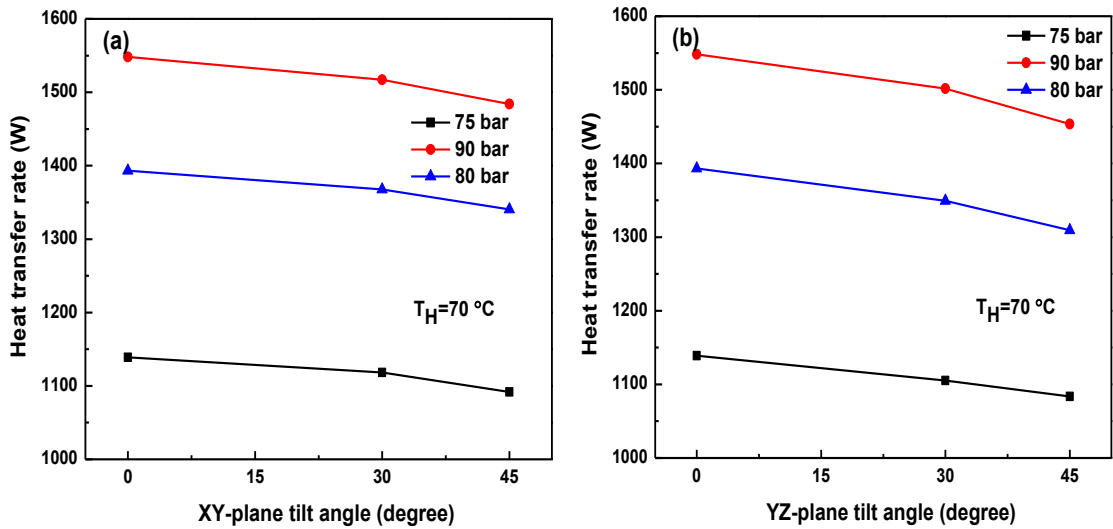


Figure 4.8 Variation of heat transfer rate of CO₂ at different pressures and $T_H = 70^\circ\text{C}$ in (a) XY-plane and (b) YZ-plane

It is also observed that the drop in heat transfer rate due to tilting the loop in YZ plane is slightly higher than the tilting in XY plane (6.2% in YZ plane and 4.3% in XY plane at 45° tilt angle). This occurs due to an additional drop in effective height by tilting loop in YZ plane compared to XY plane. Heat transfer rate in YZ plane

becomes zero if a loop is tilted by 90° as both the heat exchangers are at a horizontal position, which is not the case in XY plane. Hence, tilting of the loop could be a solution for instability with a small reduction of heat transfer rate.

As HHX inlet temperature increases, the heat transfer rate increases due to an increase in buoyancy effect caused by the increase in temperature difference between CHX and HHX. Even though there is a decrease in density at a higher temperature at a given pressure, which may cause in a drop in mass flow rate, but heat transfer rate does not decrease.

4.4.2 Effect of tilt angle on pressure drop at different operating pressures

Figure 4.9 (a) and (b) shows the effect of tilt angle on pressure drop for 40°C HHX water inlet temperature at different operating pressures in XY/YZ (0° , 30° , 45°) planes and fixed CHX water inlet temperature (32°C). Results show that, as pressure increases, pressure drop also increases in both cases due to an increase in viscosity at higher pressure. Maximum pressure found in 90 bar and minimum pressure drop found in 75 bar. A differential pressure transducer is connected across the CHX to measure the pressure drop, as shown in Figure 3.5. The marginal pressure drop increases in XY plane tilting and maximum pressure drop found in XY 45° angle. The pressure drop decreases in YZ plane tilting and minimum pressure drop is found in YZ 45° angle.

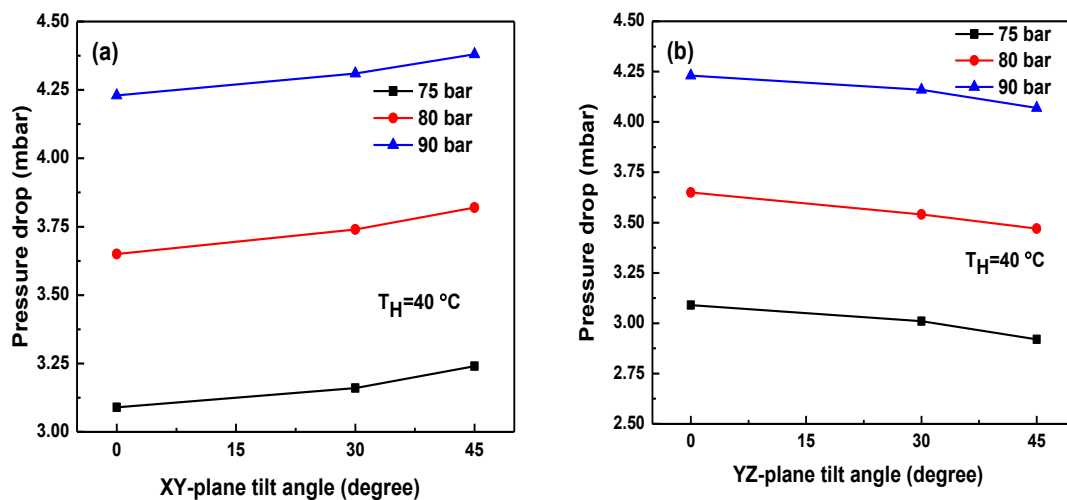


Figure 4.9 Pressure drop comparison of CO₂ at different pressures and $T_H = 40^\circ\text{C}$ in (a) XY-plane and (b) YZ-plane

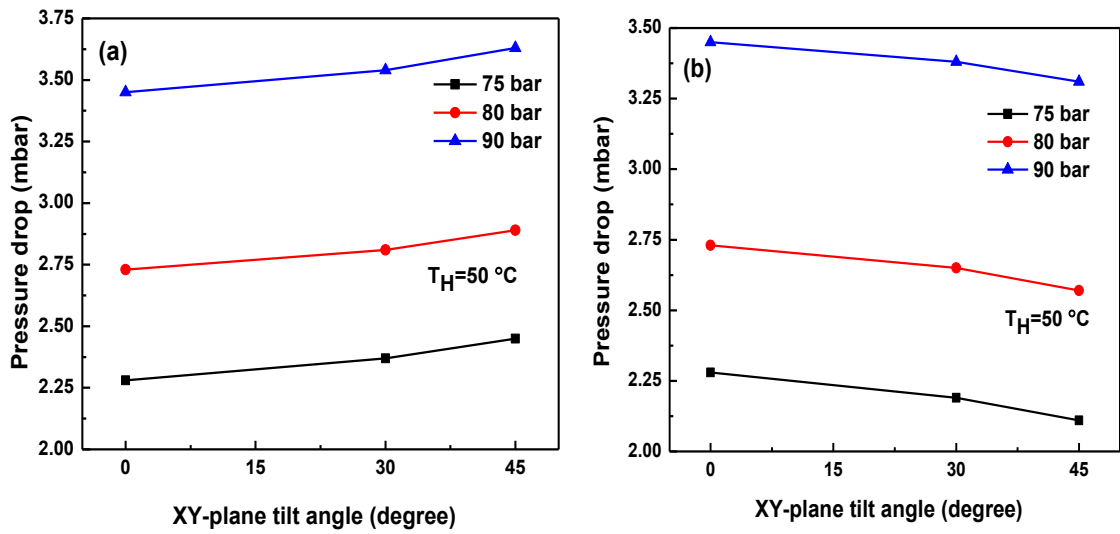


Figure 4.10 Pressure drop comparison of CO₂ at different pressures and $T_H = 50\text{ }^\circ\text{C}$ in (a) XY-plane and (b) YZ-plane

Figure 4.10 (a) and (b) show the effect of tilt angle on pressure drop for $50\text{ }^\circ\text{C}$ HHX water inlet temperature at different operating pressures in XY/YZ (0°, 30°, 45°) planes and fixed CHX water inlet temperature ($32\text{ }^\circ\text{C}$). Similar trends were observed at $50\text{ }^\circ\text{C}$, the pressure drop decreases in YZ plane tilting and minimum pressure drop was found in YZ 45° angle.

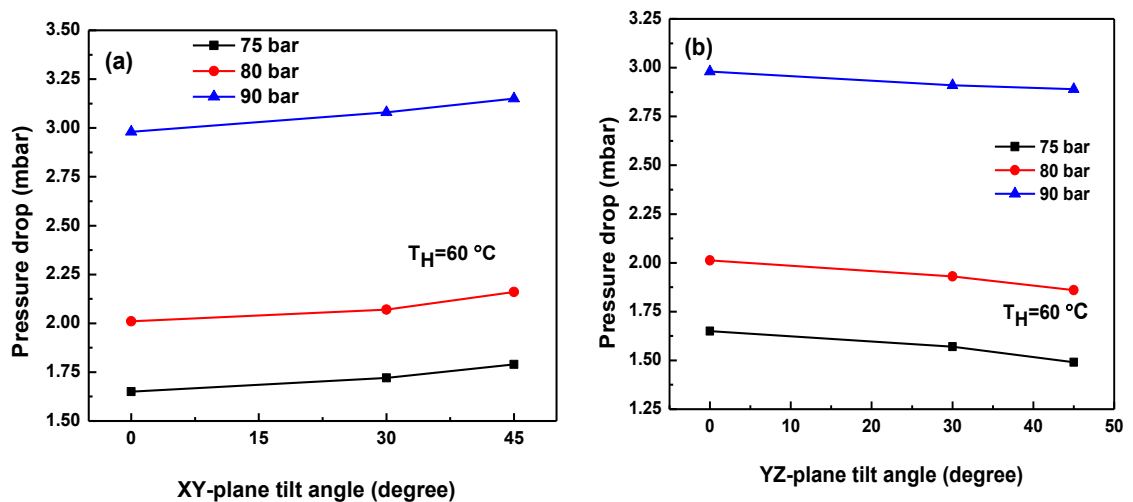


Figure 4.11 Pressure drop comparison of CO₂ at different pressures and $T_H = 60\text{ }^\circ\text{C}$ in (a) XY-plane and (b) YZ-plane

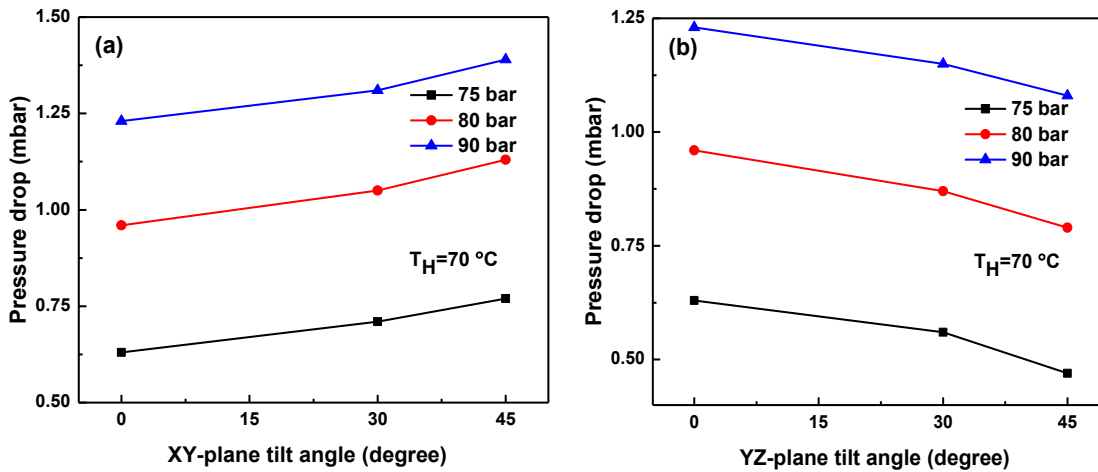


Figure 4.12 Pressure drop comparison of CO₂ at different pressures and $T_H = 70\text{ }^\circ\text{C}$ in (a) XY-plane and (b) YZ-plane

Figures 4.11 and 4.12 show the effect of tilt angle on pressure drop for HHX water inlet temperature of 60 °C and 70 °C respectively, at different operating pressures in XY/YZ (0°, 30°, 45°) planes and fixed CHX water inlet temperature(32 °C). Similar trends were observed in both cases (60 °C and 70 °C), the pressure drop decreases in YZ plane tilting and minimum pressure drop found in YZ 45° angle.

From the above figures, it is observed that there is an increase in height between the connecting ends of a differential pressure transducer with an increase in tilt angle in XY plane, which causes a rise in the additional pressure head. In YZ plane tilting, the connecting ends of differential pressure transducer remain horizontal, but the mass flow rate decreases due to a decrease in buoyancy effect, and causes a lower pressure drop.

4.4.3 Effect of tilt angle on temperature distribution along the loop at different operating pressures

Figures 4.13 (a) and (b) show the temperature variation throughout the entire loop at 75 bar for loop tilting in XY (0°, 30°, 45°) and YZ (0°, 30°, 45°) planes, respectively for different HHX water inlet temperatures and fixed CHX inlet temperature. Results show that the temperature at left leg and right leg temperature is above the critical temperature of (~31 °C) confirming the supercritical condition of the CO₂ inside the loop and as HHX temperature increases, the loop fluid temperature increases. Tilting

the loop in XY and YZ plane, there is a marginal decrease in loop fluid temperature, the maximum decrease in temperature is observed in YZ plane.

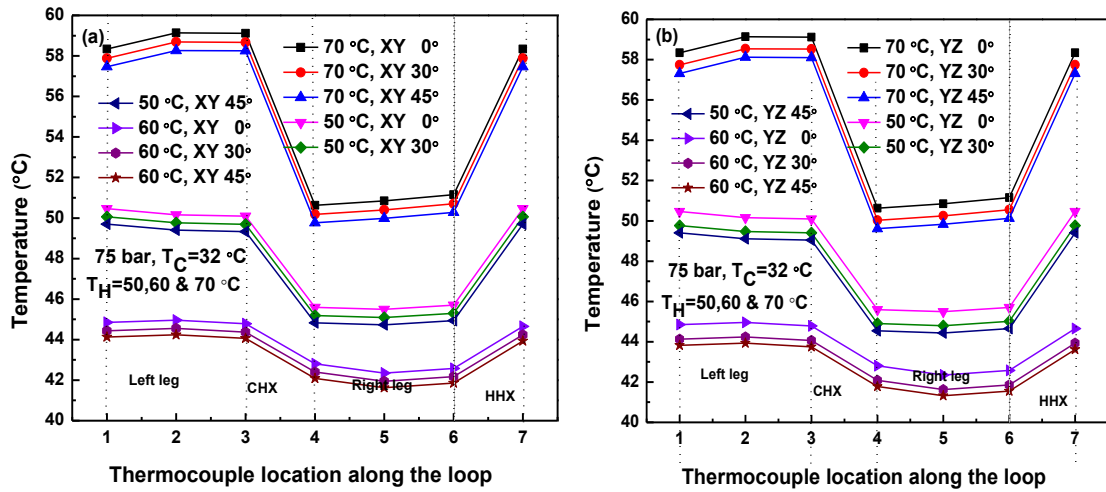


Figure 4.13 Variation of temperature along the loop at 75 bar in (a) XY-plane and (b) YZ-plane

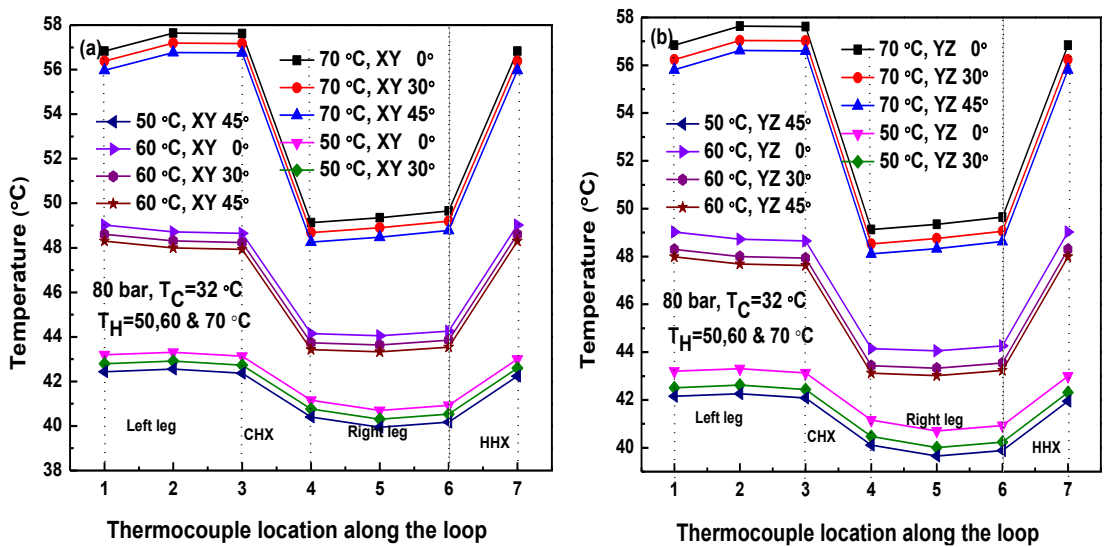


Figure 4.14 Variation of temperature along the loop at 80 bar in (a) XY-plane and (b) YZ-plane

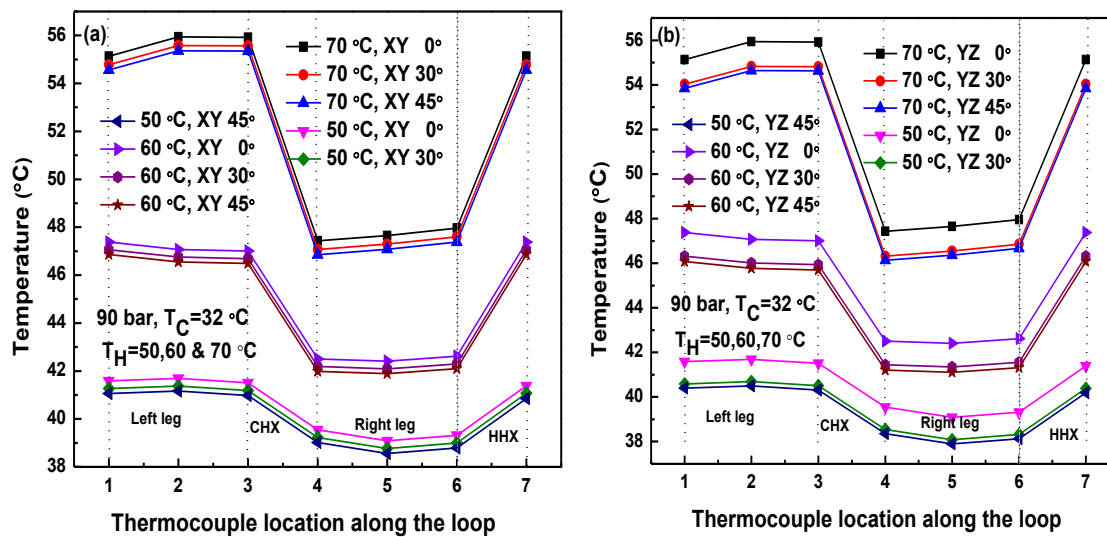


Figure 4.15 Variation of temperature along the loop at 90 bar in (a) XY-plane and (b) YZ-plane

Figures 4.14 (a) and (b) shows the temperature variation throughout the entire loop at 80 bar for loop tilting in XY (0°, 30°, 45°) and YZ (0°, 30°, 45°) planes, respectively for different HHX water inlet temperatures and fixed CHX inlet temperature. Tilting the loop in XY and YZ plane, there is a marginal decrease in loop fluid temperature, the maximum decrease in temperature is observed in YZ plane compared to XY plane.

Figures 4.15 (a) and (b) show the temperature variation throughout the entire loop at 90 bar for loop tilting in XY (0°, 30°, 45°) and YZ (0°, 30°, 45°) planes, respectively for different HHX water inlet temperatures and fixed CHX inlet temperature. A similar trend is observed in 90 bar case also.

From the above Figures 4.13 to 4.15, it is observed that as HHX inlet temperature increases, the overall loop temperature increases, which is obvious, but as tilt angle increases, the drop in temperature in YZ plane case is slightly higher compared to XY plane case.

4.4.4 Effect of HHX water inlet temperature on heat transfer rate at different tilt angles and different operating pressures

Figures 4.16 (a) to (c) show the effect of HHX water inlet temperature and operating pressure on heat transfer rate at different tilt angles at 75, 80 and 90 bar respectively.

Results show that as HHX inlet temperature increases, the heat transfer rate increases due to the higher buoyancy effect caused by, the higher temperature difference between CHX and HHX (explained in section 4.2).

Results show that there is a marginal decrease in the heat transfer rate after tilting the loop in XY/YZ (30°, 45°) planes. A maximum drop in heat transfer rate is observed in YZ plane. This occurs due to an additional drop in effective height by tilting loop in YZ plane compared to XY plane. Heat transfer rate in YZ plane becomes zero if a loop is tilted by 90° as both the heat exchangers are at a horizontal position, which is not the case in XY plane.

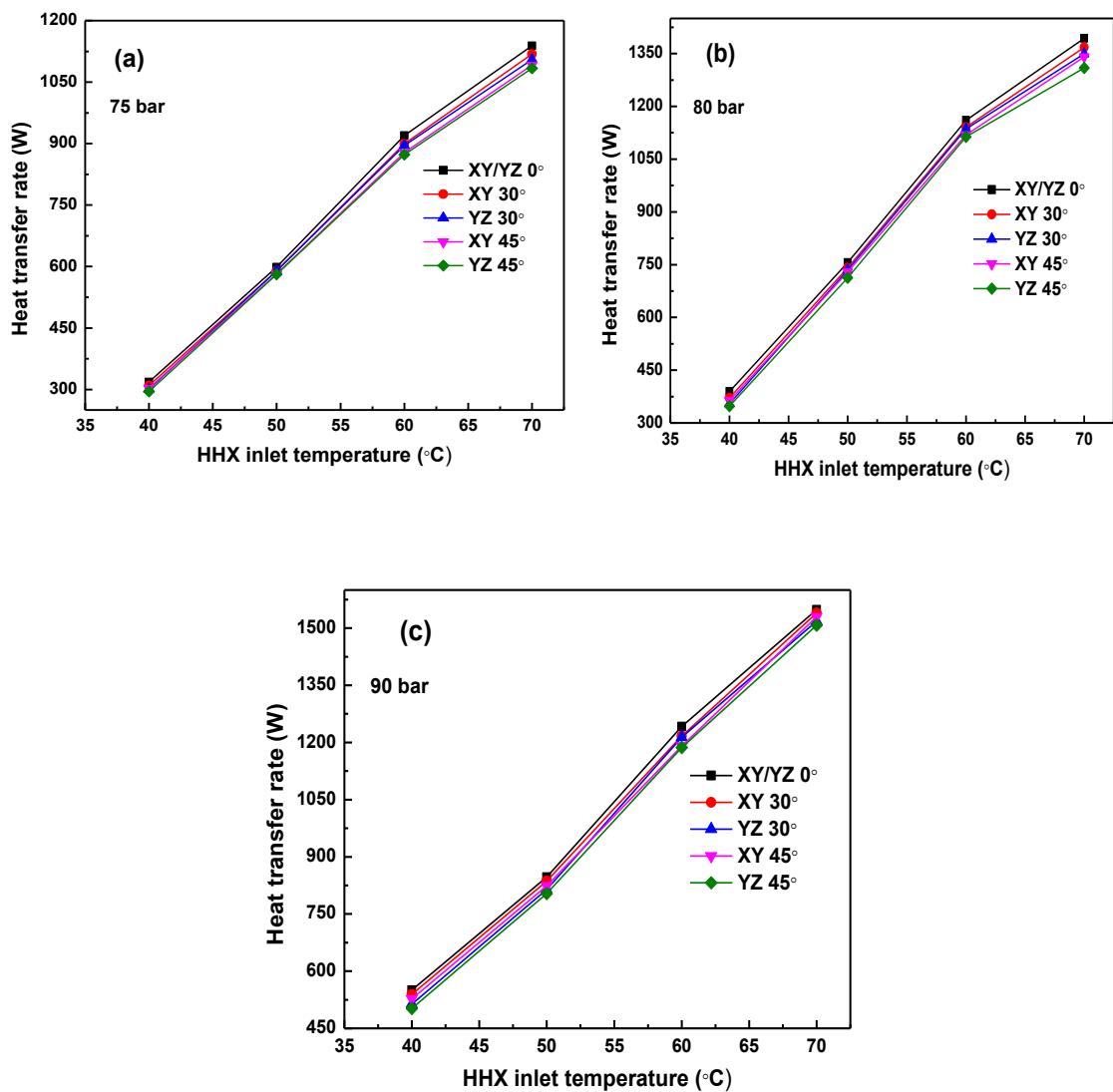


Figure 4.16 Effect of HHX inlet temperature on heat transfer at different operating pressure (a) 75 bar, (b) 80 bar, and (c) 90 bar

4.5 HEAT TRANSFER AND PRESSURE DROP COMPARISON OF SUPERCRITICAL CO₂ NCL WITH WATER BASED NCL

The heat transfer rate and pressure drop of supercritical CO₂ based NCL is compared with widely used water based natural circulation loop at the same CHX and HHX temperatures as explained in section 4.1. The operating pressure for water as loop fluid is kept at 1 atm pressure as the variation of thermophysical properties of water with operating pressure is insignificant (less than 1%), which in turn does not affect the heat transfer rate significantly Table 4.1.

Table 4.1: Water properties variation with pressure

Temperature (K)	Pressure (bar)	Density (kg/m ³)	C_p (kJ/kg-K)	Viscosity (μPa-s)	Volumetric expansion coefficient 1/K
311	1	993.02	4.1793	680.00	0.00036878
311	75	996.25	4.1611	680.80	0.00037165

Figure 4.17 shows the variation of heat transfer at different operating temperatures and different operating pressures. Results show that an increase in temperatures increases the heat transfer rate of water as well as CO₂ based NCL, the heat transfer rate is found to be maximum for the operating pressure of 90 bar.

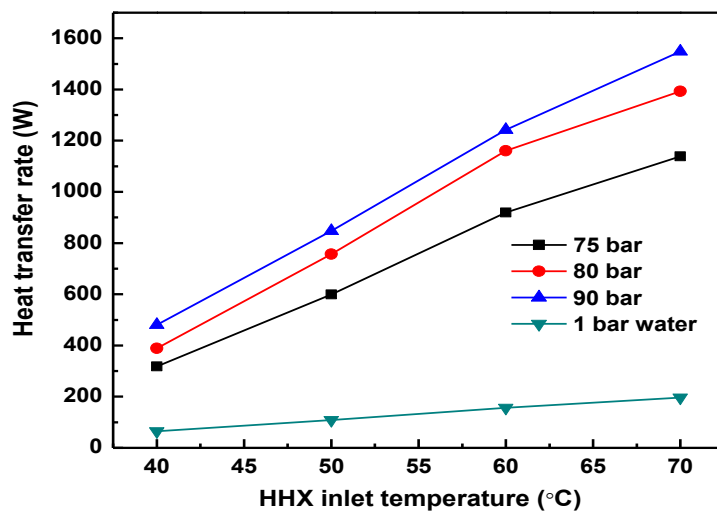


Figure 4.17 Variation of heat transfer rate for water and supercritical CO₂ at different pressure

Average operating temperature (~loop fluid temperature) of 41 °C (obtained in this case) is near to the pseudo critical point (40.2 °C) of CO₂ at 90 bar, which leads to a maximum heat transfer rate at this pressure because of a very high volumetric expansion coefficient of CO₂ compared to water (~240 times) as shown in Table 4.2.

In this case, the maximum heat transfer rate of CO₂ based NCL yields ~8 times (800%) higher than water-based NCL as shown in Figure 4.15. At higher HHX inlet temperature, the buoyancy effect predominates increasing the heat transfer rate.

Figure 4.18 shows the variation of pressure drop at different operating temperatures and different operating pressures. The result shows that with an increase in operating pressure there is increase in pressure drop and if an increase in HHX inlet temperature there is a decrease in pressure drop. At higher temperatures, there is a decrease in viscosity leads to a lower pressure drop in the loop. From the results, it is clear that maximum pressure is found in water based NCL compare to CO₂ based NCL because of the higher viscosity of water.

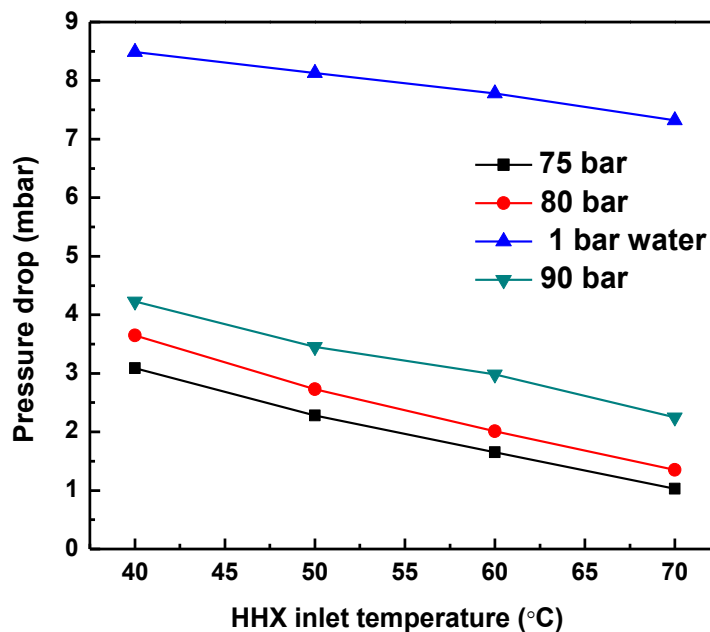


Figure 4.18 Variation of pressure drop for water and supercritical CO₂ at different pressure

Table 4.2: Comparison of the properties of supercritical CO₂ at different pressures with water at atmospheric pressure for different operating temperatures

Pressure of CO ₂ (bar)	Avg. Temperature, T_{avg} (°C)	Density ratio, ρ_{CO_2}/ρ_{Water}	Specific heat ratio, $C_{p_CO_2}/C_{p_Water}$	Thermal conductivity ratio, k_{CO_2}/k_{Water}	Viscosity ratio, μ_{CO_2}/μ_{Water}	Ratio of volumetric coefficient, $\beta_{CO_2}/\beta_{Water}$
75	41	0.23	0.75	0.05	0.03	56.68
	46	0.21	0.59	0.05	0.03	37.89
	51	0.19	0.50	0.05	0.04	28.21
80	41	0.27	1.05	0.06	0.03	83.50
	46	0.24	0.72	0.05	0.04	48.29
	51	0.22	0.58	0.05	0.04	33.70
90	41	0.44	2.89	0.11	0.05	240.54
	46	0.33	1.27	0.07	0.04	91.65
	51	0.28	0.83	0.06	0.04	51.69

4.6 SUMMARY

Steady state analysis is carried out on the loop with end heat exchangers. The supercritical phase of CO₂ is considered with operating pressures of 75, 80 and 90 bar and operating temperatures in the range of 40 °C to 70 °C. Studies are undertaken for various loop tilt angles 0°, 30°, 45° in XY and YZ plane conditions. The following conclusions are drawn from this study:

- In the case of supercritical CO₂ as loop fluid, an 800% higher heat transfer rate is obtained compared to water as loop fluid.
- After tilting the loop in XY (0°, 30°, 45°) and YZ (0°, 30°, 45°) planes, there is a decrease in heat transfer rate 4.3% for XY plane and 6.2% in YZ plane.
- After tilting the loop in XY (0°, 30°, 45°) and YZ (0°, 30°, 45°) planes, there is an increase in pressure drop for XY plane and a decrease pressure drop in YZ plane.

Chapter 5

EXPERIMENTAL INVESTIGATION ON SINGLE PHASE (SUBCRITICAL LIQUID/VAPOUR) CO₂ BASED NCL

5.1 INTRODUCTION

This experimental study covers the operating conditions ranging from -18 °C to 70 °C temperatures and operating pressure from 50 to 65 bar in subcritical vapour and subcritical liquid region of CO₂. The heat transfer rate and pressure drop of subcritical vapour /subcritical liquid CO₂ based natural circulation loop (NCL) is compared with water/brine based system at the same operating temperatures. The temperature distribution of CO₂ along the loop at different operating temperatures and pressure is studied to ensure the condition/state of the fluid inside the loop.

Yadav et al. (2016) carried out a numerical study on the instability of NCL and suggested that loop tilting is one of the elegant solution for instability in NCL. The present experimental study is conducted to quantify the tilting effect on the heat transfer rate and pressure drop. To get the result at a various tilt angle, the entire loop is tilted in XY plane (30°, 45°) as well as in YZ plane (30°, 45°). Results on subcritical vapour and subcritical liquid CO₂ with and without tilting are presented.

To ensure turbulent flow condition in heat exchangers (CHX and HHX), external fluid (water/methanol) at a mass flow rate of 0.083 kg/s (5 liters/min) is circulated in the annulus. Calculation of heat transfer rate is done by the heat carried away or supplied by external fluid in the heat exchangers.

Heat transfer rate (Q),

$$Q = m \times c_{p-HHX} \times \Delta T_{HHX} = m \times c_{p-CHX} \times \Delta T_{CHX} \quad (1)$$

Where, m = mass flow rate of external fluid in kg/s

c_{p-HHX} = specific heat of HHX in J/kg-K

c_{p-CHX} = specific heat of CHX in J/kg-K

ΔT_{HHX} = HHX temperature difference between inlet and outlet, and

ΔT_{CHX} = CHX temperature difference between inlet and outlet.

Average temperature is calculated by

$$T_{avg} = \frac{T_C + T_H}{2} \quad (2)$$

Where, T_C = CHX inlet temperature in °C

T_H = HHX inlet temperature in °C.

5.2 LOOP FLUID IN SUBCRITICAL VAPOUR CONDITION

In this study, water is employed as the external fluid in both CHX and HHX, for a fixed inlet temperature in CHX (32 °C), and the inlet temperature in HHX is varied from 40°C to 70 °C for incremental values of 10 °C. Results are obtained for different operating pressures of CO₂ ranging from 40 to 70 bar.

5.2.1 Heat transfer rate and pressure drop of CO₂ based NCL at different operating pressure and temperatures

Figure 5.1 shows the variation of the heat transfer rate of CO₂ at different operating pressures 40, 50, 60, and 70 bar at different HHX water inlet temperatures 40 °C to 70°C. It is observed that with an increase in hot fluid inlet temperature, the heat transfer rate increases due to an increase in the temperature gradient between CO₂ and water in HHX. With the rise in system pressure, the heat transfer rate also increases. As the water inlet temperature of HHX increases, the heat transfer rate increases due to the increase in buoyancy effect. The heat transfer rate is found to be maximum for the operating pressure of 70 bar.

Figure 5.2 shows the effect of HHX water inlet temperature on pressure drop at different operating pressures 40, 50, 60, and 70 bar. Results show that as HHX inlet temperature increases, pressure drop increases owing to the higher buoyancy effect caused by a higher temperature difference between CHX and HHX, and an increase in viscosity of carbon dioxide at a higher temperature at fixed operating pressures.

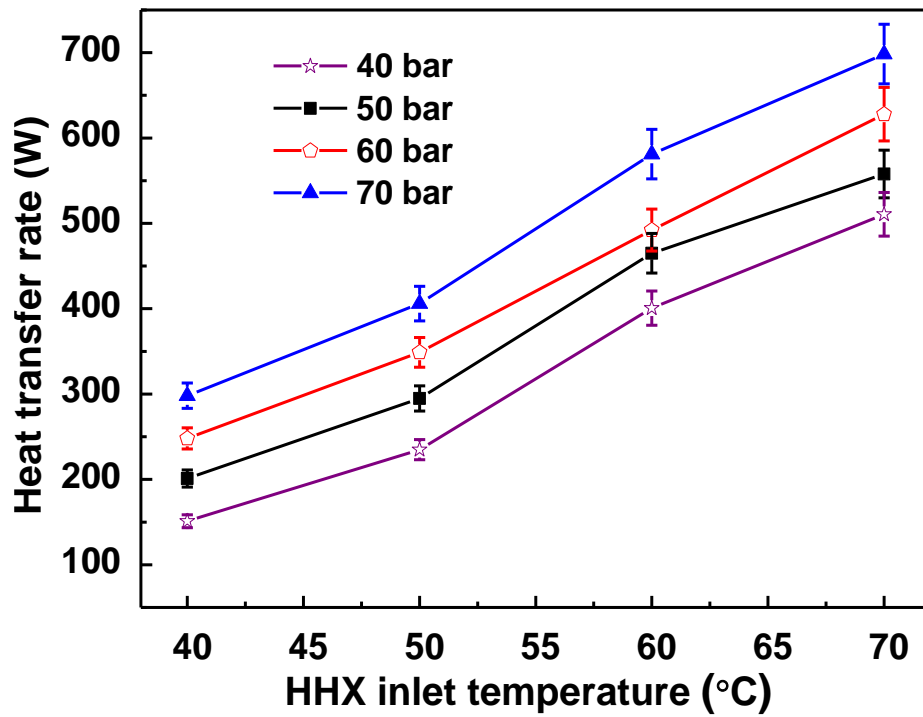


Figure 5.1 Variation of heat transfer rate of CO₂ at different operating pressures and at different HHX inlet temperatures.

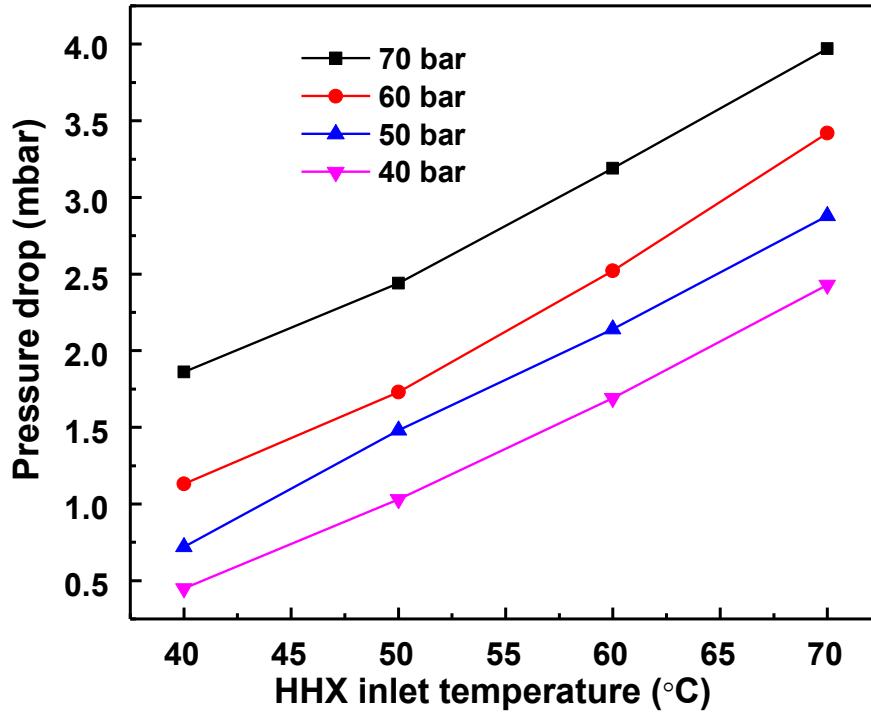


Figure 5.2 Variation of pressure drop of CO₂ at different operating pressures and different HHX inlet temperatures.

5.2.2 Temperature distribution of subcritical vapour CO₂ based NCL at different operating pressure

Figures 5.3 (a) to (d) show the temperature variation throughout the loop at different operating pressures (40, 50, 60 and 70 bar) and different HHX inlet temperatures. The temperature variation is also recorded for all operating pressures to make sure that the loop fluid (CO₂) is in the subcritical liquid state throughout the loop.

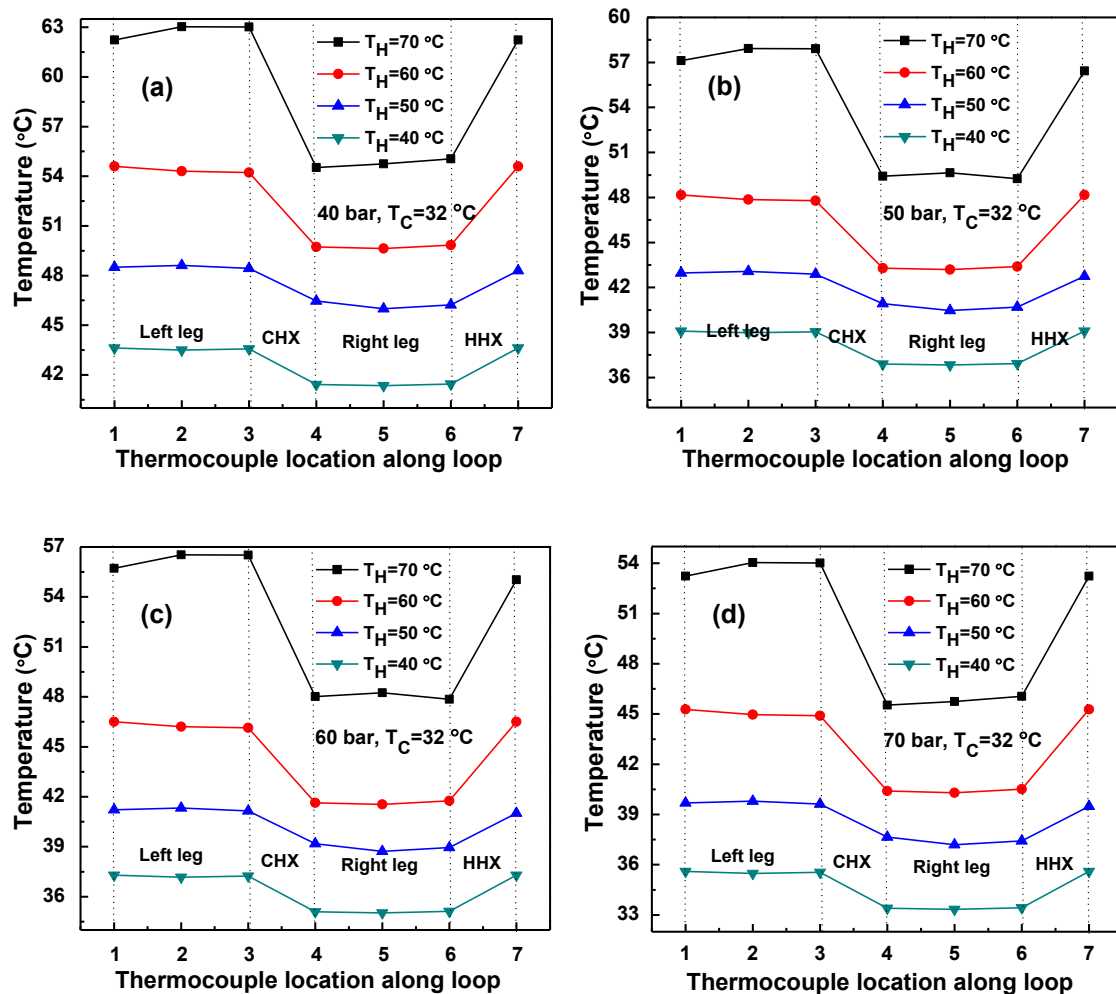


Figure 5.3 Variation of temperature along the loop at different HHX inlet temperatures and different operating pressures (a) 40 bar, (b) 50 bar, (c) 60 bar and (d) 70 bar

Figures 5.3 (a-d) show the effect of pressure on the loop fluid temperature difference between the left leg center and right leg center. Results show that with an increase in the HHX inlet temperature, the loop fluid temperature increases and the loop fluid

temperature difference between the left leg center and right leg center increases. This occurs due to an increase in specific heat (shown in Table 5.2) at higher pressure at a particular average operating temperature.

5.2.3 Effect of tilt angle

A natural circulation loop is commonly used where there is a need for a quick and safe heat transfer device, but it has a significant instability problem caused by changes in regular fluid flow directions. One of the best ways to solve such a problem is to tilt the entire loop by some angle, which can affect the heat transfer and pressure drop of the loop. Pressure drop and heat transfer performance of CO₂ based NCL with end heat exchangers, operating under subcritical conditions for various tilt angles (30°, 45°) in XY and YZ planes are investigated.

The Experimental setup is designed in such a way that, the entire loop can be tilted at any specified angle in XY and YZ planes as shown in Figures 4.4 and 4.5. The operating conditions are maintained the same as explained in the above section.

5.2.3.1 Effect of tilt angle on heat transfer rate at different operating pressures

Figures 5.4 (a) and (b) show the effect of tilt angle on heat transfer rate at different operating pressures in XY/YZ (0°, 30°, 45°) planes for fixed water inlet temperature of 40 °C and 32 °C at HHX and CHX respectively. Results show that there is a marginal drop in heat transfer rate after tilting the loop in XY (30°, 45°) as well as in YZ (30°,45°) planes, which occurs due to lower buoyancy on account of reduction in effective height of the loop between CHX and HHX.

Experiments are also conducted for HHX water inlet temperatures of 50 °C, 60 °C, and 70 °C, and the effect of water inlet temperature of HHX on the heat transfer rate is studied. Figures 5.5, 5.6 and 5.7 show the impact of tilt angle on heat transfer rate for HHX water inlet temperature of 50 °C, 60 °C, and 70 °C respectively at different operating pressures in XY/YZ (0°, 30°, 45°) planes and fixed CHX water inlet temperature (32 °C). Results show that there is a marginal drop in heat transfer rate after tilting in XY (30°, 45°) as well as in YZ (30°, 45°) planes, maximum drop in heat transfer rate found in YZ planes. With the increase in HHX water inlet

temperature, there is no significant effect on the heat transfer rate observed, and the same trend is obtained in all the cases.

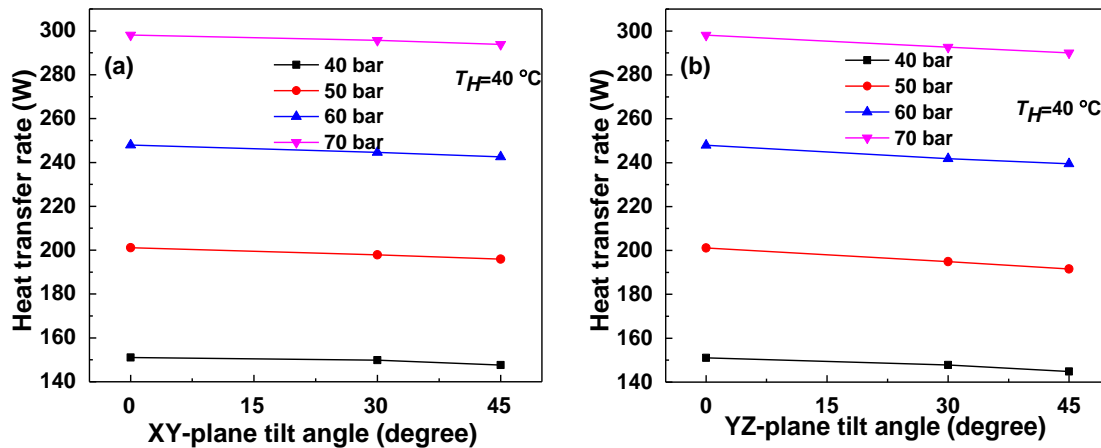


Figure 5.4 Variation of heat transfer rate of CO₂ at different pressures and $T_H = 40^\circ\text{C}$ in (a) XY-plane and (b) YZ-plane.

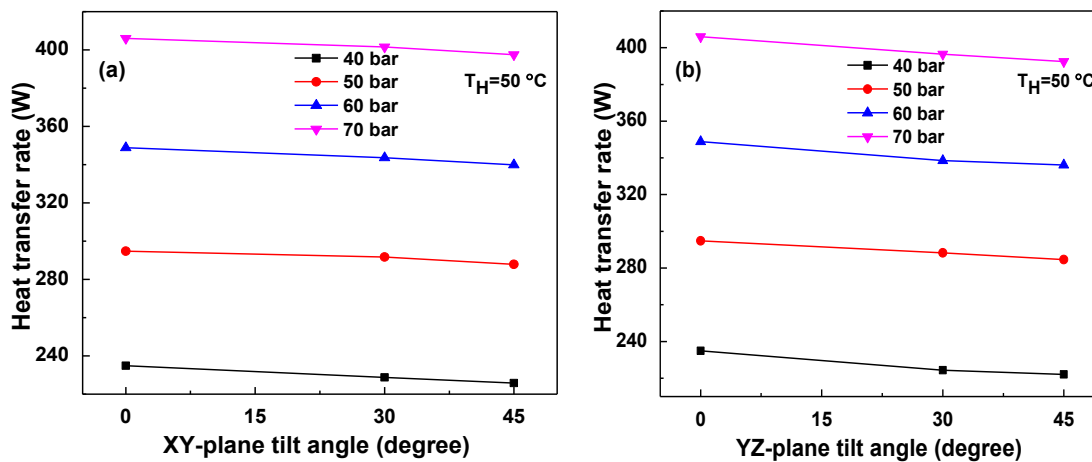


Figure 5.5 Variation of heat transfer rate of CO₂ at different pressures and $T_H = 50^\circ\text{C}$ in (a) XY-plane and (b) YZ-plane.

It is also observed that the drop in heat transfer rate due to tilting the loop in YZ plane is slightly higher than the tilting in XY plane (6% in YZ plane and 3.8% in XY plane at 45° tilt angle). This occurs due to an additional drop in effective height by tilting loop in YZ plane compared to XY plane. Heat transfer rate in YZ plane becomes zero if a loop is tilted by 90° as both the heat exchangers are at a horizontal position, which

is not the case in XY plane. Hence, tilting of the loop could be a solution for instability with a small reduction of heat transfer rate.

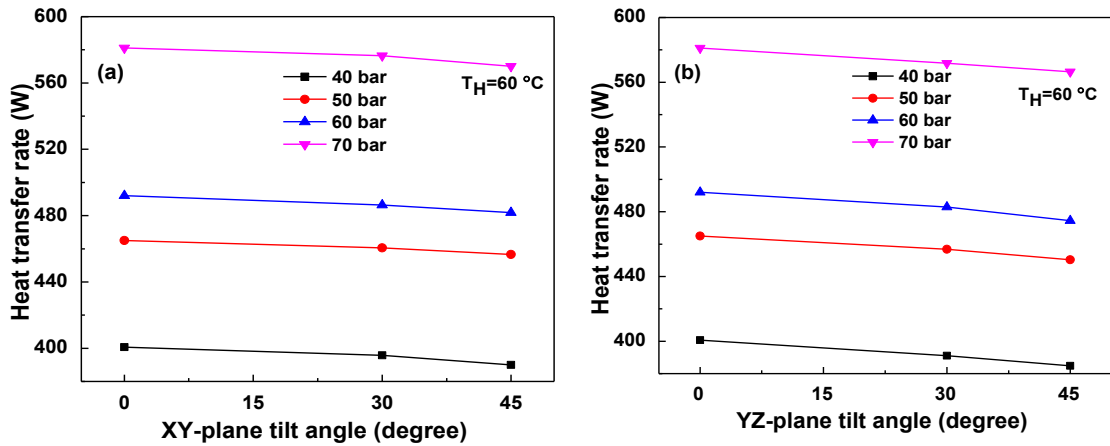


Figure 5.6 Variation of heat transfer rate of CO₂ at different pressures and $T_H = 60\text{ }^\circ\text{C}$ in (a) XY-plane and (b) YZ-plane.

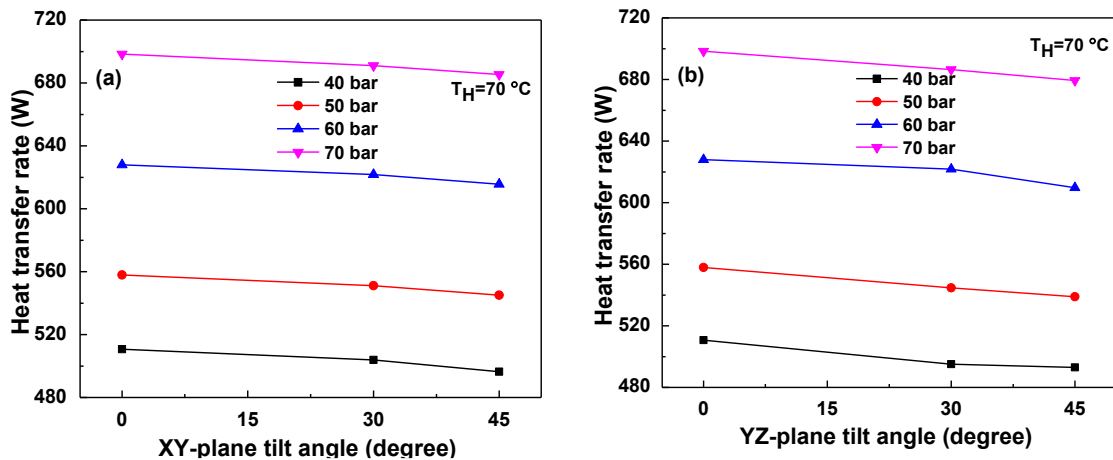


Figure 5.7 Variation of heat transfer rate of CO₂ at different pressures and $T_H = 70\text{ }^\circ\text{C}$ in (a) XY-plane and (b) YZ-plane.

5.2.3.2 Effect of tilt angle on pressure drop at different operating pressures

Figures 5.8 (a) and (b) show the effect of tilt angle on pressure drop for $40\text{ }^\circ\text{C}$ HHX water inlet temperature at different operating pressures in XY/YZ (0° , 30° , 45°) planes and fixed CHX water inlet temperature ($32\text{ }^\circ\text{C}$). Results show that, as pressure increases, pressure drop also increases in both cases due to an increase in viscosity at higher pressure. Maximum pressure found in 70 bar and minimum pressure drop

found in 40 bar. A differential pressure transducer is connected across the CHX to measure the pressure drop shown in Figure 3.6. The marginal increase in pressure drop is observed while tilting the loop in XY plane, and a maximum pressure drop is found at a 45° angle. However, a reverse trend, i.e., decreasing pressure drop, is observed while tilting the loop in YZ plane, and minimum pressure drop was found at a 45° angle.

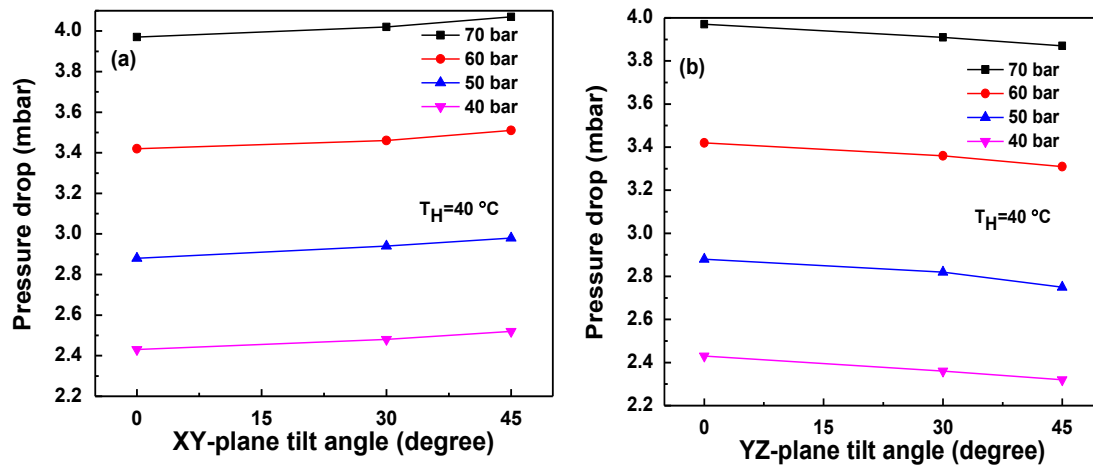


Figure 5.8 Pressure drop comparison of CO₂ at different pressures and $T_H = 40\text{ }^\circ\text{C}$ in (a) XY-plane and (b) YZ-plane

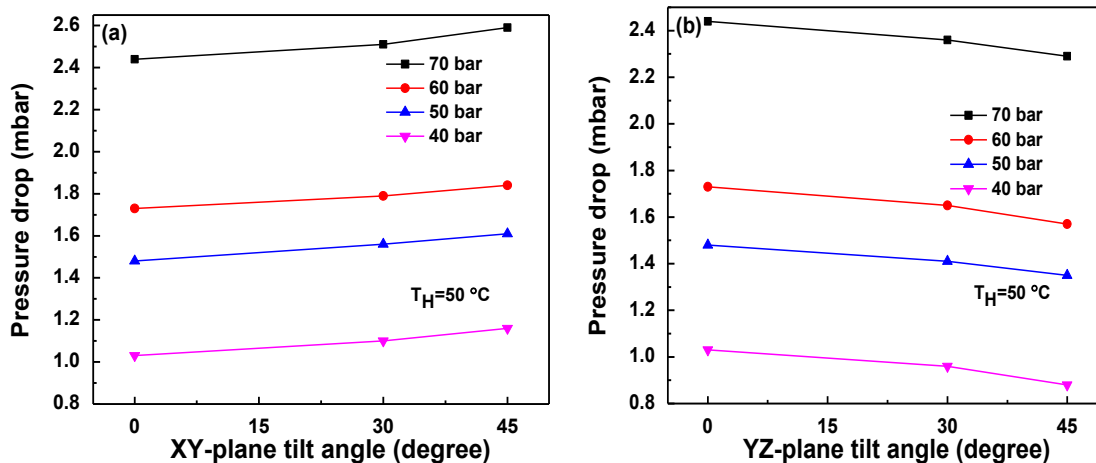


Figure 5.9 Pressure drop comparison of CO₂ at different pressures and $T_H = 50\text{ }^\circ\text{C}$ in (a) XY-plane and (b) YZ-plane

Experiments are also conducted for HHX water inlet temperatures of 50 °C, 60 °C, and 70 °C, and the effect of water inlet temperature of HHX on the pressure drop is studied. Figures 5.9, 5.10 and 5.11 show the effect of tilt angle on pressure drop for

HHX water inlet temperature of 50 °C, 60 °C, and 70 °C respectively at different operating pressures in XY/YZ (0°, 30°, 45°) planes and fixed CHX water inlet temperature (32 °C). Results show that there is a marginal drop in heat transfer rate after tilting in XY (30°, 45°) as well as in YZ (30°, 45°) planes, maximum drop in heat transfer rate found in YZ planes. With the increase in HHX water inlet temperature, there is no significant effect on the heat transfer rate observed, and the same trend is obtained in all the cases.

From the above figures, it is observed that there is an increase in height between the connecting ends of a differential pressure transducer with an increase in tilt angle in XY plane, which causes a rise in the additional pressure head. In YZ plane tilting, the connecting ends of differential pressure transducer remain horizontal, but the mass flow rate decreases due to a decrease in buoyancy effect, and causes a lower pressure drop.

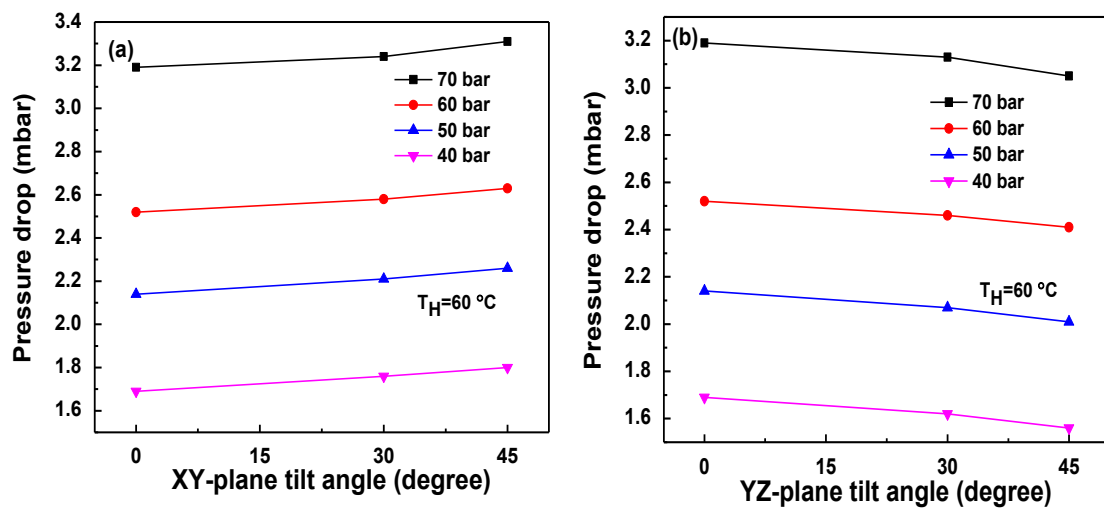


Figure 5.10 Pressure drop comparison of CO₂ at different pressures and $T_H = 60\text{ }^\circ\text{C}$ in (a) XY-plane and (b) YZ-plane

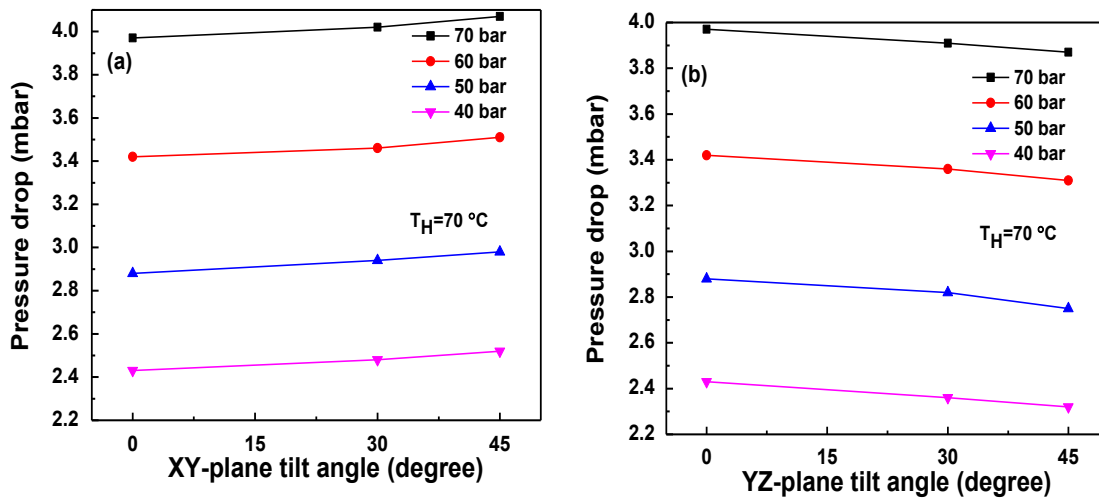
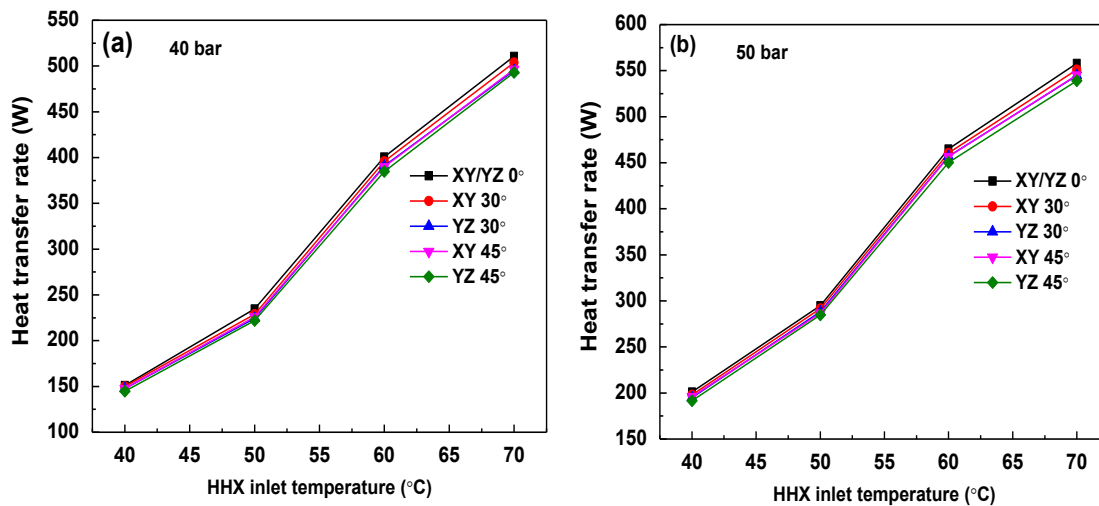


Figure 5.11 Pressure drop comparison of CO₂ at different pressures and $T_H = 70\text{ }^\circ\text{C}$ in (a) XY-plane and (b) YZ-plane

5.2.3.3 Effect of HHX water inlet temperature on heat transfer rate at different tilt angles and different operating pressures

Figures 5.12 (a) to (d) show the effect of temperature difference between inlet HHX and inlet CHX on heat transfer rate at different tilt angles. Results show that as HHX inlet temperature increases, heat transfer rate increases due to higher buoyancy effect caused by a higher temperature difference between CHX and HHX,



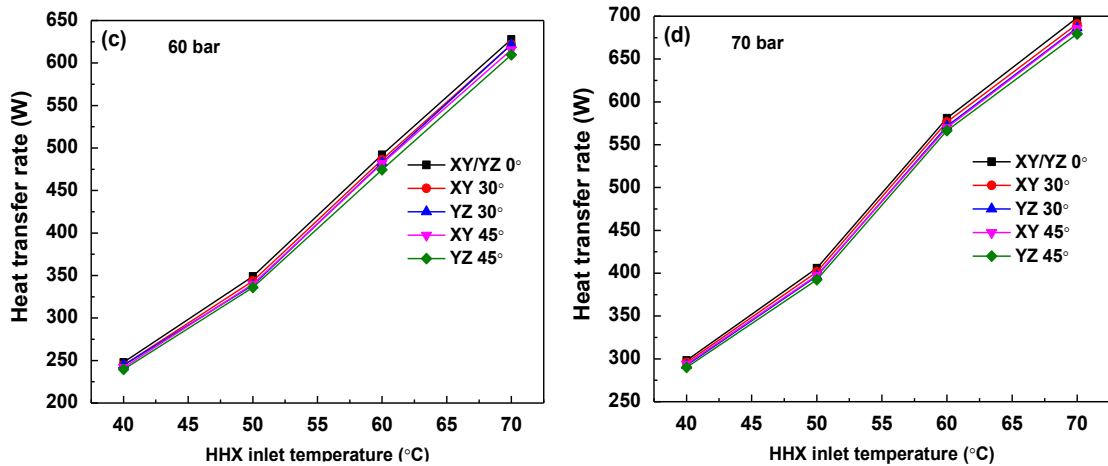


Figure 5.12 Effect of HHX inlet temperature on heat transfer at different operating pressure (a) 40 bar, (b) 50 bar, (c) 60 bar and (d) 70 bar

Figure 4.16 (a) to (d) show the effect of HHX water inlet temperature and operating pressure on heat transfer rate at different tilt angles at 40, 50, 60 and 70 bar respectively. Results show that as HHX inlet temperature increases, the heat transfer rate increases due to the higher buoyancy effect caused by a higher temperature difference between CHX and HHX (explained in section 5.2).

Results show that there is a marginal decrease in the heat transfer rate after tilting the loop in XY/YZ (30°, 45°) planes. A maximum drop in heat transfer rate is observed in YZ plane. This occurs due to an additional reduction in effective height by tilting loop in YZ plane compared to XY plane. Heat transfer rate in YZ plane becomes zero if a loop is tilted by 90° as both the heat exchangers are at a horizontal position, which is not the case in XY plane.

5.2.4 Heat transfer and pressure drop comparison of subcritical vapour CO₂ based NCL with water based NCL

The heat transfer rate and pressure drop of subcritical vapour CO₂ based NCL is compared with widely used water based natural circulation loop at the same CHX and HHX temperatures as explained in section 5.1. The operating pressure for water as loop fluid is kept at 1 atm pressure as the variation of thermophysical properties of water with operating pressure is insignificant (less than 1%), which in turn does not affect the heat transfer rate significantly (explained in chapter 4, section 4.5).

Figure 5.13 shows the variation of heat transfer at different operating temperatures and different operating pressures. Results show that the increase in temperatures increases the heat transfer rate of water as well as CO₂ based NCL, the heat transfer rate is found to be maximum for the operating pressure of 70 bar.

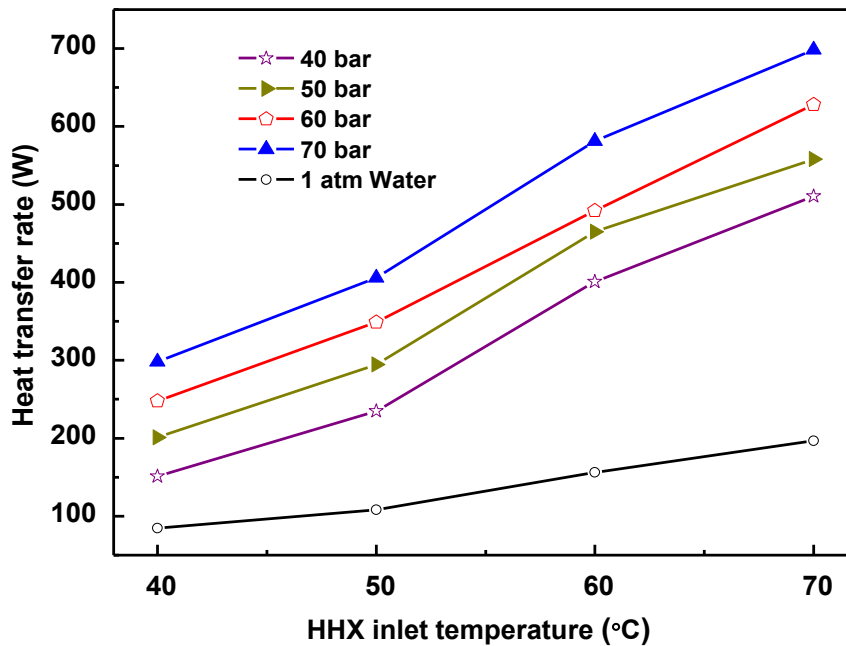


Figure 5.13 Variation of heat transfer rate for water and subcritical vapour CO₂ at different pressures

It is observed that with increase in hot fluid inlet temperature heat transfer rate increases due to an increase in the temperature gradient between CO₂ and water in HHX. With the increase in system pressure, the heat transfer rate also increases. In this case, the heat transfer rate of CO₂ based NCL yields ~4 times (400%) higher than water-based NCL (1 atm) for the same operating temperatures.

Figure 5.14 shows the variation of pressure drop at different operating temperatures and pressures. Results show that as HHX water inlet temperature increases pressure drop of CO₂ increases which occurs due to an increase in viscosity of carbon dioxide at higher temperature at fixed operating pressures. From the results it is clear that maximum pressure drop is found in water based NCL compared to CO₂ based NCL, because of the higher viscosity of water.

Table 5.1: Comparison of the properties of subcritical vapour CO₂ at different pressures with water at atmospheric pressure for different operating temperatures

Pressure of CO ₂ (bar)	Avg. Temperature, T_{avg} (°C)	Density ratio, ρ_{CO_2}/ρ_{Water}	Specific heat ratio, $C_{p_CO_2}/C_{p_Water}$	Thermal conductivity ratio, k_{CO_2}/k_{Water}	Viscosity ratio, μ_{CO_2}/μ_{Water}	Ratio of volumetric coefficient $\beta_{CO_2}/\beta_{Water}$
40	41	0.08	0.30	0.03	0.03	16.11
	46	0.08	0.29	0.03	0.03	13.83
	51	0.07	0.28	0.03	0.03	12.08
50	41	0.11	0.35	0.04	0.03	20.56
	46	0.11	0.33	0.04	0.03	17.17
	51	0.11	0.32	0.04	0.03	14.67
60	41	0.15	0.43	0.04	0.03	27.92
	46	0.14	0.40	0.04	0.03	22.27
	51	0.14	0.37	0.04	0.03	18.39
70	41	0.20	0.59	0.05	0.03	42.45
	46	0.18	0.50	0.05	0.03	30.91
	51	0.17	0.45	0.04	0.03	24.09

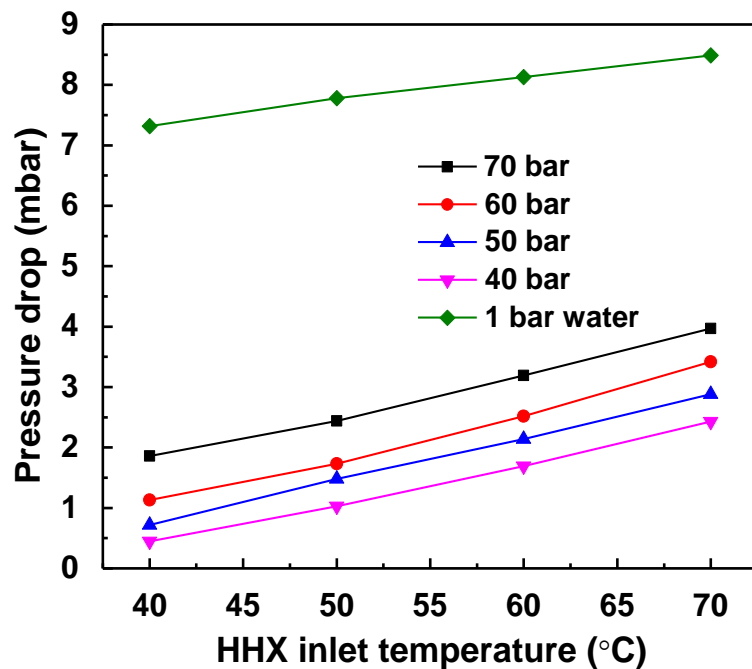


Figure 5.14 Variation of pressure drop for water and subcritical vapour CO₂ at different pressure

5.3 LOOP FLUID IN SUBCRITICAL LIQUID CONDITION

This experimental study is mainly focused on low temperature (below 0 °C) applications such as refrigerators, solar water heater for cold weather, etc. In CHX and HHX, methanol is used as the external fluid in place of water as it becomes solid at sub-zero temperature. The inlet temperature of CHX is maintained constant and HHX temperature is varied. CHX and HHX methanol inlet temperature is considered in the range of -18 to -14 °C and -12 to 15 °C respectively.

5.3.1 Heat transfer rate and pressure drop of CO₂ based NCL at different operating pressures and temperatures

Figure 5.15 shows that as the methanol inlet temperature of HHX increases, the heat transfer rate increases due to the increase in buoyancy effect caused by the increase in temperature difference between CHX and HHX. Even though there is a decrease in density at a higher temperature at a given pressure, which may cause a drop in mass flow rate, but the heat transfer rate does not decrease. It shows the dominancy of the buoyancy force. The heat transfer rate is found to be maximum for the operating pressure of 45 bar.

The effect of operating pressure on the pressure drop at different HHX inlet temperatures (T_H) for a fixed T_C is depicted in Figure 5.15. Results show that with the increase in operating pressure, there is an increase in pressure drop. However, the pressure drop decreases with an increase in HHX inlet temperature. At higher temperatures, there is a decrease in viscosity of a liquid, leads to a lower pressure drop in the loop (shown in Table 5.3).

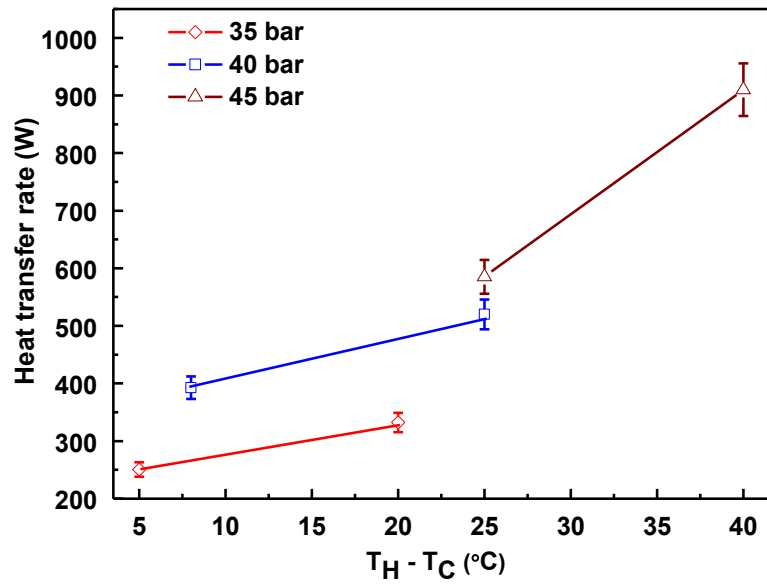


Figure 5.15 Variation of heat transfer rate of CO₂ at different operating pressures and different HHX inlet temperatures

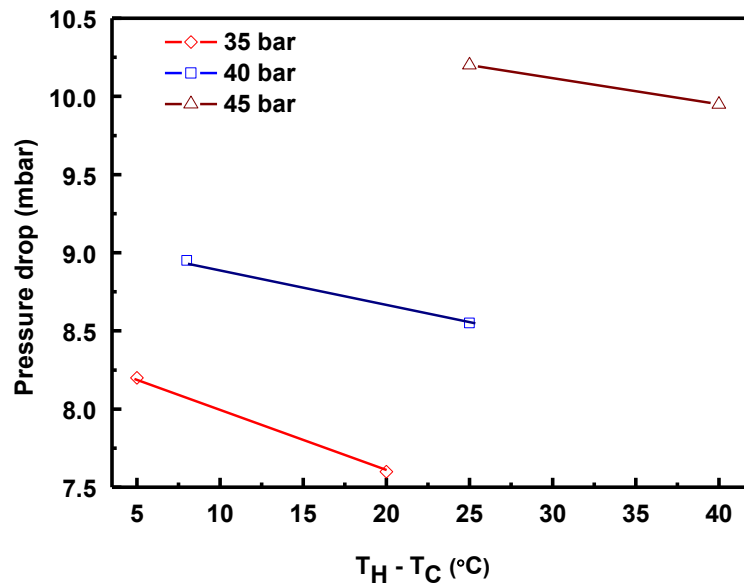
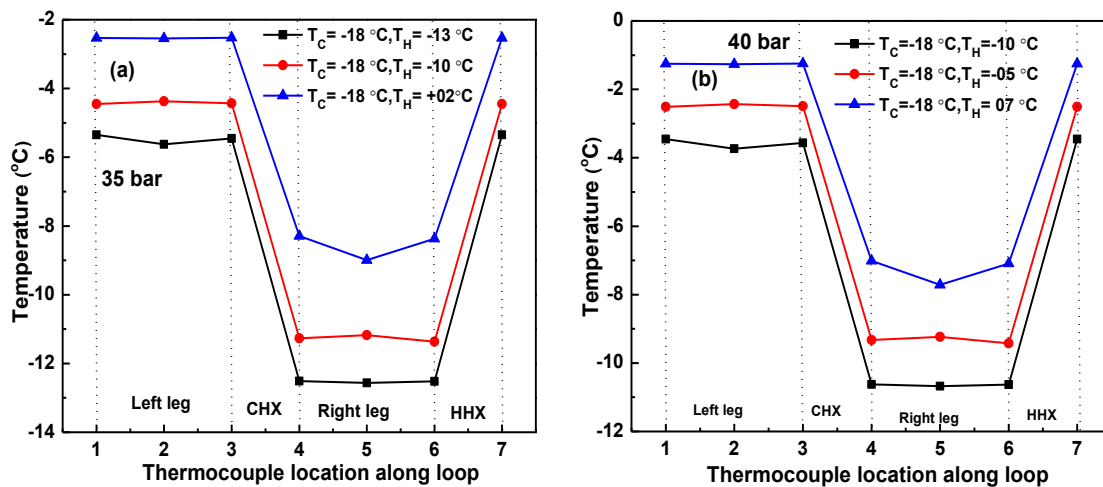


Figure 5.16 Variation of pressure drop of CO₂ at different operating pressures and different HHX inlet temperatures

5.3.2 Temperature distribution of subcritical liquid CO₂ based NCL at different operating pressures

Figures 5.17 (a) to (c) show the temperature variation throughout the loop at different operating pressure (35, 40 and 45 bar) and different HHX inlet temperature. The temperature variation is also recorded for all operating pressures to make sure the loop fluid (CO₂) is in the subcritical state throughout the loop.

Figure 5.17 (a) shows that with the increase in the HHX inlet temperature, the loop fluid temperature difference between the left leg and right leg center also increases along with the increase in overall loop fluid temperature. Similar trends are also observed in Figure 5.17 (b) and (c) for 40 and 45 bar. Results clearly show that as pressure increases, temperature difference decreases, which occurs due to an increase in specific heat (shown in table 5.3) at higher pressure at a particular average operating temperature.



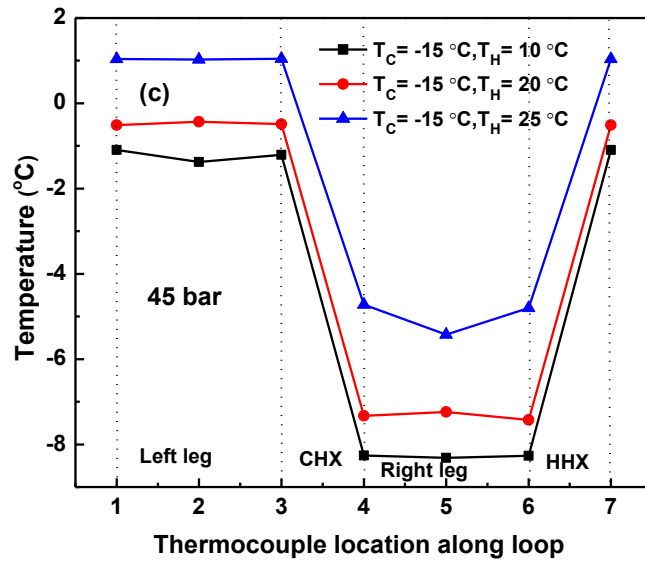


Figure 5.17 Variation of temperature along the loop at different HHX inlet temperatures and different operating pressures (a) 35 bar, (b) 40 bar, and (c) 45 bar.

5.3.3 Effect of tilt angle

In this tilt study, the pressure drop and heat transfer performance of CO₂ based NCL with end heat exchangers, operating under subcritical liquid conditions for various tilt angles (30°, 45°) in XY and YZ planes are investigated.

5.3.3.1 Effect of tilt angle on heat transfer rate at different operating pressures

Figures 5.18 (a) and (b) show the effect of tilt angle on heat transfer rate at different operating pressures in XY (0°, 30°, 45°) and YZ (0°, 30°, 45°) planes, respectively at fixed CHX and HHX methanol inlet temperature difference. The difference between the methanol inlet temperature of HHX and CHX is kept fixed at 25 °C. Average operating temperatures for different pressures are given in Table 5.3. Results show that there is the marginal drop in heat transfer rate after tilting the loop in XY (30°, 45°) as well as in YZ (30°, 45°) planes, which occurs due to lower buoyancy on account of reduction in effective height of the loop between CHX and HHX.

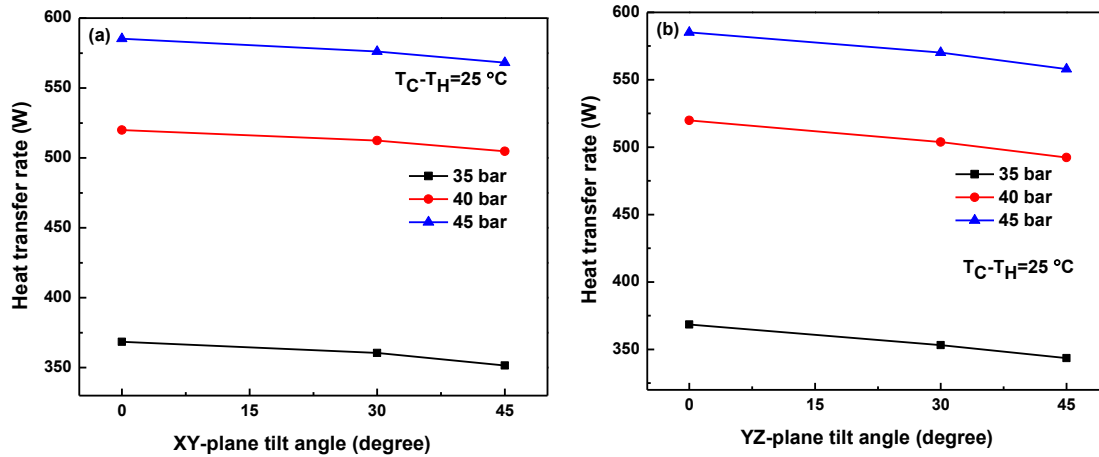


Figure 5.18 Variation of heat transfer rate of CO₂ at different pressures and $T_H - T_C = 25\text{ }^\circ\text{C}$ in (a) XY-plane and (b) YZ-plane

It is also observed that the drop in heat transfer rate due to tilting the loop in YZ plane is slightly higher than the tilting in XY plane (6.4% in YZ plane and 4.8% in XY plane at 45° tilt angle). This occurs due to an additional drop in effective height by tilting loop in YZ plane compared to XY plane. As explained in earlier, the heat transfer rate in YZ plane becomes zero if the loop is tilted by 90° as both the heat exchangers are at the same horizontal plane, which is not the case in XY plane. Hence, tilting of the loop could be a solution for instability with a small reduction of heat transfer rate.

5.3.3.2 Effect of tilt angle on pressure drop at different operating pressures

Figure 5.19 (a) and (b) shows the effect of tilt angle in XY/YZ (0°, 30°, 45°) planes on pressure drop at different operating pressures. The difference between the methanol inlet temperature of HHX and CHX is kept fixed at 25 °C. Results show that, as pressure increases, pressure drop also increases in both cases due to an increase in viscosity at higher pressure. Maximum pressure drop is observed at 90 bar and minimum pressure drop is found at 75 bar. There is a marginal increase in pressure drop in the tilting of the loop in XY plane, whereas decrease in pressure drop is observed while tilting the loop in YZ plane. The maximum change in pressure drop is observed at 45° angle of tilt in XY and in YZ plane.

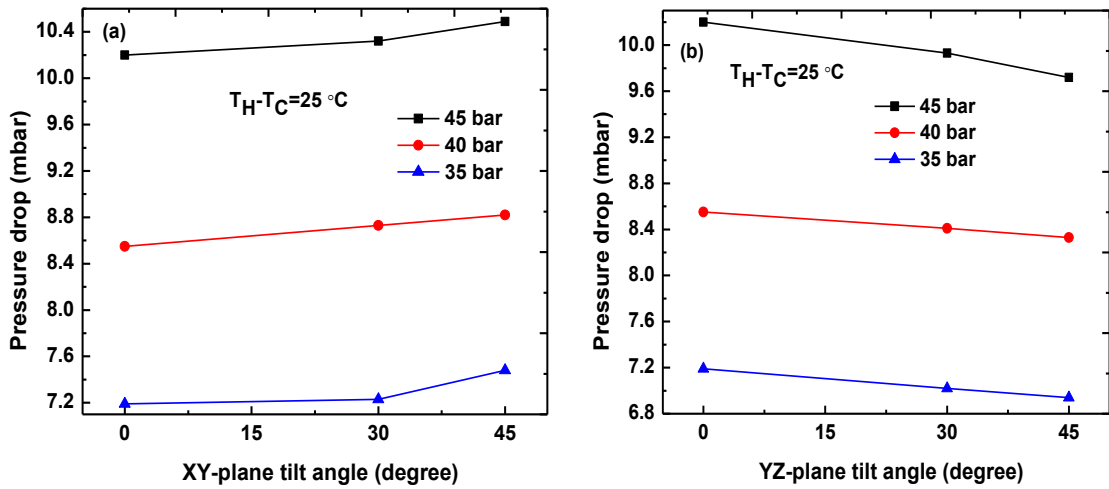


Figure 5.19 Pressure drop comparison of CO₂ at different pressures and $T_H - T_C = 25$ °C in (a) XY-plane and (b) YZ-plane

From the Figure 4.1 it is observed that there is an increase in height between the connecting ends of a differential pressure transducer with increase in tilt angle in XY plane, which causes a rise in additional pressure head. In YZ plane tilting, the connecting ends of differential pressure transducer remain horizontal, but the mass flow rate decreases due to decrease in buoyancy effect, and causes a lower pressure drop.

5.3.3.3 Effect of tilt angle on temperature distribution along the loop at different operating pressures

Figures 5.19 (a) and (b) show the temperature variation throughout the entire loop at 35 bar for loop tilting in XY (0°, 30°, 45°) and YZ (0°, 30°, 45°) planes, respectively for different HHX water inlet temperatures and fixed CHX inlet temperature. Results show that the temperature throughout the loop is below saturation temperature confirming the subcritical liquid condition of the CO₂ inside the loop. Results show that, as HHX temperature increases, the overall loop fluid temperature increases. Tilting the loop in XY plane and YZ plane there causes decrease in loop fluid temperature; maximum decrease in temperature is observed in YZ plane.

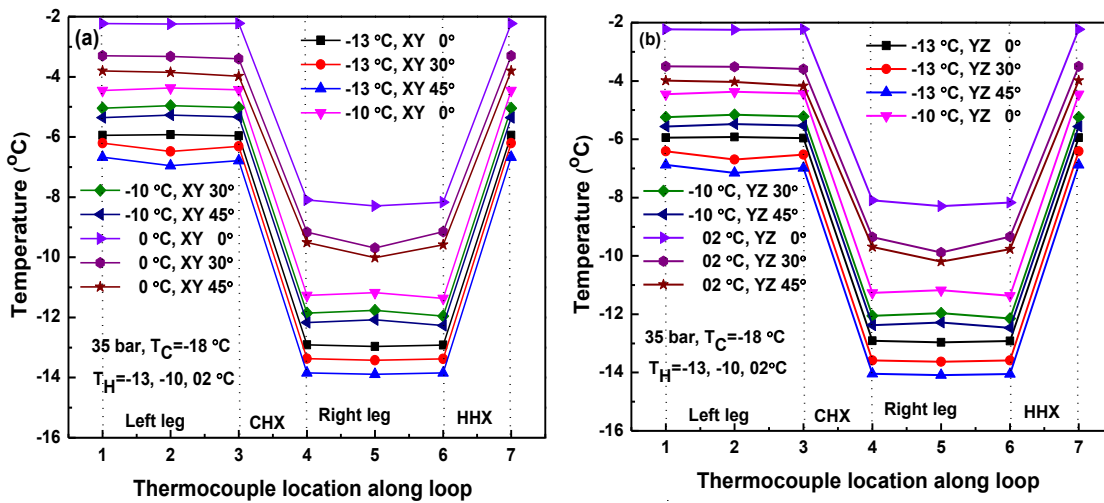


Figure 5.20 Variation of temperature along the loop at 35 bar in (a) XY-plane and (b) YZ-plane

Experiments are also conducted for the operating pressures of 40 bar and 45 bar, and temperature variation throughout the loop is recorded. Figures 5.21 and 5.22 show the temperature variation throughout the entire loop at 40 bar and 45 bar respectively for loop tilting in XY (0°, 30°, 45°) and YZ (0°, 30°, 45°) planes, for different HHX water inlet temperatures and fixed CHX inlet temperature. A similar trend of temperature variation as observed in the case of 35 bar is obtained here.

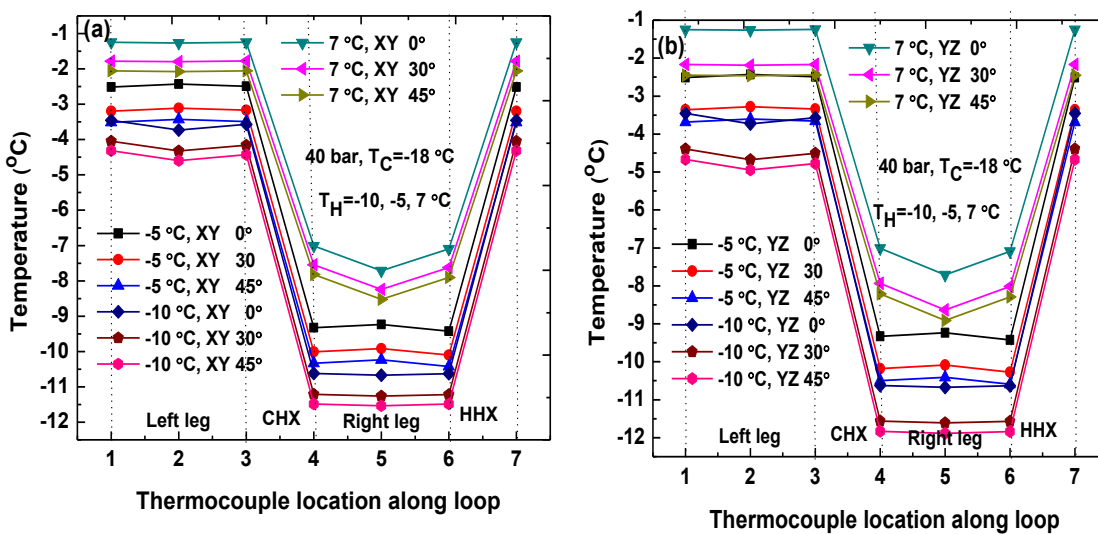


Figure 5.21 Variation of temperature along the loop at 40 bar in (a) XY-plane and (b) YZ-plane

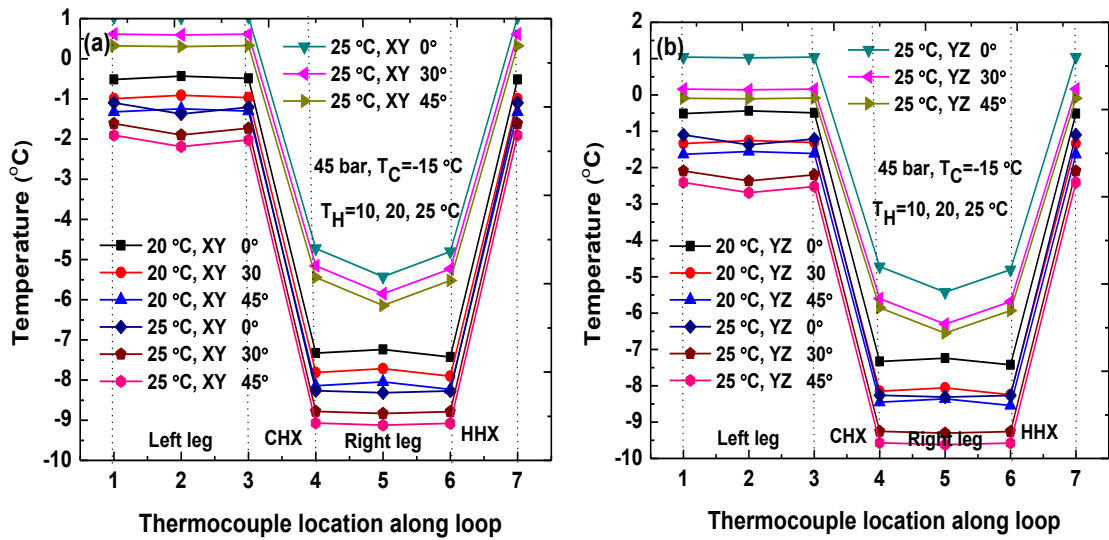


Figure 5.22 Variation of temperature along the loop at 45 bar in (a) XY-plane and (b) YZ-plane

From the above Figures 5.20 to 5.22, it is observed that as HHX inlet temperature increases, the overall loop temperature increases which are obvious, but as tilt angle increases, the drop in temperature in YZ plane case is slightly higher compared to XY plane case.

5.3.4 Heat transfer and pressure drop comparison of subcritical liquid CO₂ based NCL with brine based NCL

The heat transfer rate and pressure drop of supercritical CO₂ based NCL is compared with widely used water/brine based natural circulation loop at the same CHX and HHX temperatures as explained in section 5.1. The operating pressure for brine as loop fluid is kept at 1 atm pressure as the variation of thermophysical properties of brine with operating pressure is insignificant (less than 1%), which in turn does not affect the heat transfer rate significantly Table 5.2.

Table 5.2: Brine properties variation with pressure

Temperature (K)	Pressure (bar)	Density (kg/m ³)	C_p (kJ/kg-K)	Viscosity (μ Pa-s)	Volumetric expansion coefficient 1/K
05	1	1259.09	3.238	790.00	0.00033045
05	45	1204.82	3.190	756.80	0.00030723

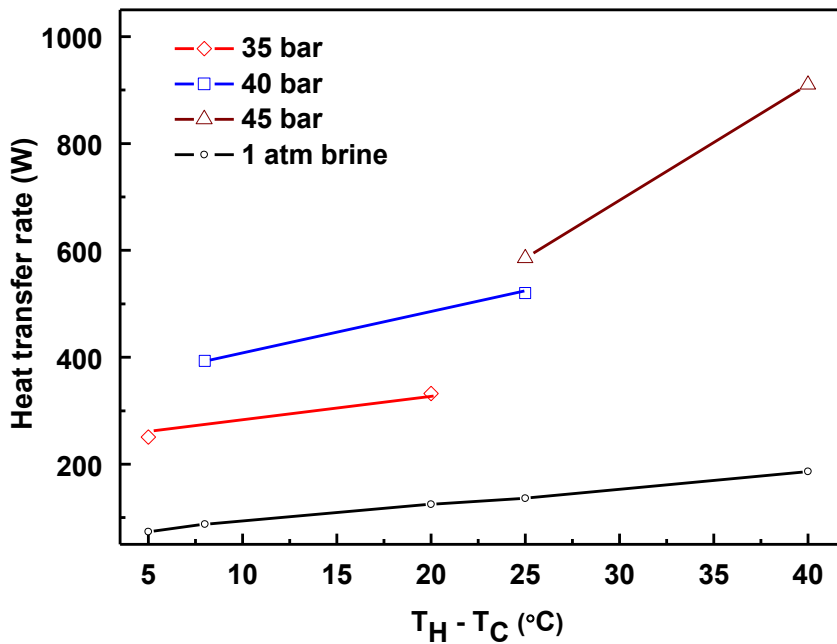


Figure 5.23 Variation of heat transfer rate for brine and subcritical liquid CO₂ at different pressure

Figure 5.23 shows the variation of heat transfer at different operating temperatures and different operating pressures. Results show that an increase in temperature increases the heat transfer rate of brine as well as CO₂ based NCL, the heat transfer rate is found to be maximum for the operating pressure of 45 bar. Due to very low viscosity and very high volumetric expansion coefficient of CO₂ compared to brine (as shown in Table 5.3), we achieved a 500% higher heat transfer rate in this case of liquid CO₂ compared to brine-based NCL.

Figure 5.24 shows the variation of pressure drop at different operating temperatures and different operating pressures. The result shows that the pressure drop increases

with increase in operating pressure, whereas it decreases with increase in HHX inlet temperature. At higher temperatures, there is a decrease in viscosity of liquid leads to a lower pressure drop in the loop. From the results it is clear that maximum pressure is found in brine based NCL compared to CO₂ based NCL, because of the higher viscosity of brine.

Table 5.3: Comparison of the properties of subcritical liquid CO₂ at different pressures with brine at atmospheric pressure for different operating temperatures

Pressure of CO ₂ (bar)	Avg. Temperature, T_{avg} (°C)	Density ratio, ρ_{CO_2}/ρ_{brine}	Specific heat ratio, $C_{p,CO_2}/C_{p,brine}$	Thermal conductivity ratio, k_{CO_2}/k_{brine}	Viscosity ratio, μ_{CO_2}/μ_{brine}	Ratio of volumetric coefficient, $\beta_{CO_2}/\beta_{brine}$
35	-16.5	0.89	0.64	0.25	0.004	16.19
	-14.5	0.89	0.64	0.25	0.004	16.52
40	-9	0.86	0.66	0.23	0.003	17.34
	-14	0.89	0.64	0.23	0.004	16.30
45	-2.5	0.84	0.69	0.21	0.003	18.86
	2.5	0.81	0.73	0.20	0.002	21.27

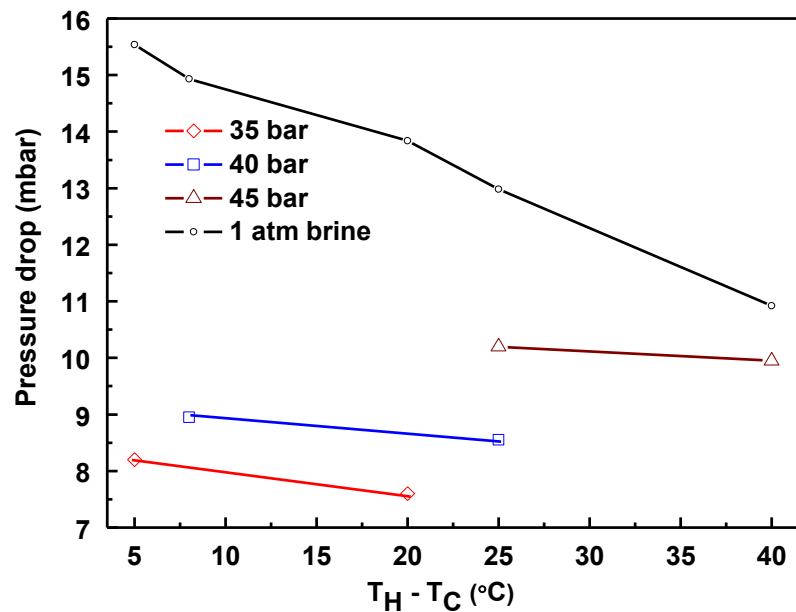


Figure 5.24 Variation of pressure drop for brine and subcritical liquid CO₂ at different pressure

5.4 SUMMARY

An experimental study to find the steady state behavior of a natural circulation loop with end heat exchangers is carried out. The subcritical phase of CO₂ is considered with operating pressures of 35 to 70 bar and operating temperatures in the range of -18 °C to 70 °C. Studies are undertaken in the conditions of XY and YZ planes for various loop tilt angles 0°, 30°, 45°. From this study, the following conclusions emerge:

- In the case of subcritical vapor CO₂ as loop fluid, a 400% higher heat transfer rate is obtained compared to water as loop fluid. After tilting the loop in XY (0°, 30°, 45°) and YZ (0°, 30°, 45°) planes, there is a decrease in heat transfer rate 3.8% for XY plane and 6% for YZ plane.
- For low-temperature applications (below 0 °C), subcritical liquid CO₂ yields a 500% higher heat transfer rate compared to brine solution as loop fluid. After tilting the loop in XY (0°, 30°, 45°) and YZ (0°, 30°, 45°) planes, there is a decrease in heat transfer rate 4.8% for XY plane and 6.4% for YZ plane.
- As a decrease in heat transfer rate is less in the case of loop tilting in the XY plane, it should be preferred over the YZ plane to get better performance.
- Loop tilting could be considered as one of the solution to overcome that reduces the ever challenging instability problem in NCL.

Chapter 6

EXPERIMENTAL INVESTIGATION ON TWO PHASE CO₂ BASED NATURAL CIRCULATION LOOP

6.1 INTRODUCTION

This experimental study covers the operating conditions ranging from -10 °C to 47 °C temperatures and operating pressure from 50 bar to 65 bar in two phase region of CO₂. The heat transfer rate and pressure drop of supercritical CO₂ based natural circulation loop (NCL) is compared with brine based system at the same operating temperatures. The temperature distribution of CO₂ along the loop at different operating temperatures and pressure is studied to ensure the condition/state of the inside the loop fluid.

The present experimental study is conducted to quantify the tilting effect on the heat transfer rate and pressure drop as well. To get the effect at various tilt angle, the entire loop is tilted in XY plane (30°, 45°) as well as in YZ plane (30°, 45°). Results on two phase CO₂ with and without tilting are presented. To check the repeatability of the measured parameter, each experiment is repeated twice.

To ensure turbulent flow conditions in heat exchangers (CHX and HHX), external fluid (water) at a mass flow rate of 0.083 kg/s (5 liters/min) is circulated in annulus. Calculation of heat transfer rate is done by the heat carried away or supplied by external fluid in the heat exchangers.

Heat transfer rate (Q),

$$Q = m \times c_{p-HHX} \times \Delta T_{HHX} = m \times c_{p-CHX} \times \Delta T_{CHX} \quad (1)$$

Where, m = mass flow rate of external fluid in kg/s

c_{p-HHX} = specific heat of HHX in J/kg-K

c_{p-CHX} = specific heat of CHX in J/kg-K

ΔT_{HHX} = HHX temperature difference between inlet and outlet

ΔT_{CHX} = CHX temperature difference between inlet and outlet

Average temperature is calculated by

$$T_{avg} = \frac{T_C + T_H}{2} \quad (2)$$

Where, T_C = CHX inlet temperature in °C

T_H = HHX inlet temperature in °C.

6.2 HEAT TRANSFER RATE AND PRESSURE DROP OF CO₂ BASED NCL AT DIFFERENT OPERATING PRESSURES AND TEMPERATURES

In this study, methanol is employed as the external fluid in both CHX and HHX to achieve two-phase at lower temperature water cannot be used as external fluid since the temperature is going below 0 °C. The operating parameters considered to conduct the experiments are shown in Table 6.1.

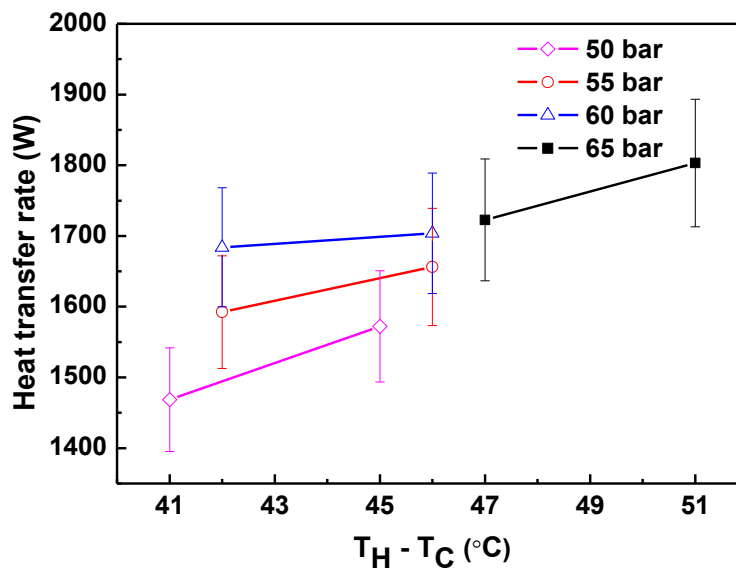


Figure 6.1 Variation of heat transfer rate of CO₂ at different operating pressures and at different HHX inlet temperatures

For different operating pressures of CO₂, i.e., 50, 55, 60, and 65 bar, results are obtained. In this case, achieving two-phase inside the loop maintained at high pressure is quite difficult. With the continuous cooling and recording temperatures at different locations in the loop, we achieved two-phase CO₂ by comparing saturation temperature at a given pressure

Figure 6.1 shows that as the methanol inlet temperature of HHX increases, the heat transfer rate increases due to the increase in buoyancy effect caused by the increase in temperature difference between CHX and HHX. Even though there is a decrease in density at a higher temperature at a given pressure, which may cause in a drop in mass flow rate, but heat transfer rate does not decrease. It shows the dominancy of the buoyancy force. The heat transfer rate is found to be maximum for the operating pressure of 65 bar. As the loop moves into the two-phase region, a large buoyancy effect gets generated causing an increase in the mass flow rate (Reynolds number) of CO₂ and which in turn enhances the heat transfer rate.

As the loop moves into two phase region, buoyancy force increases as long as liquid-vapour mixture at inlet of riser and liquid at the inlet of downcomer are maintained. With increase in buoyancy force mass flow rate of CO₂ increases and which in turn increases the heat transfer rate.

Table 6.1: Operating parameters for two phase CO₂

Pressure (bar)	Saturation temperature (°C)	CHX Inlet temperature (°C)	HHX inlet temperature (°C)	Difference between saturation temperature and HHX inlet temperature (°C)
			35	21
50	14.54	-10	33	19
			31	17
			36	21
55	18.42	-6	38	19
			40	17
			43	21
60	22.13	-3	41	19
			39	17
			47	21
65	25.6	-4	45	19
			43	17

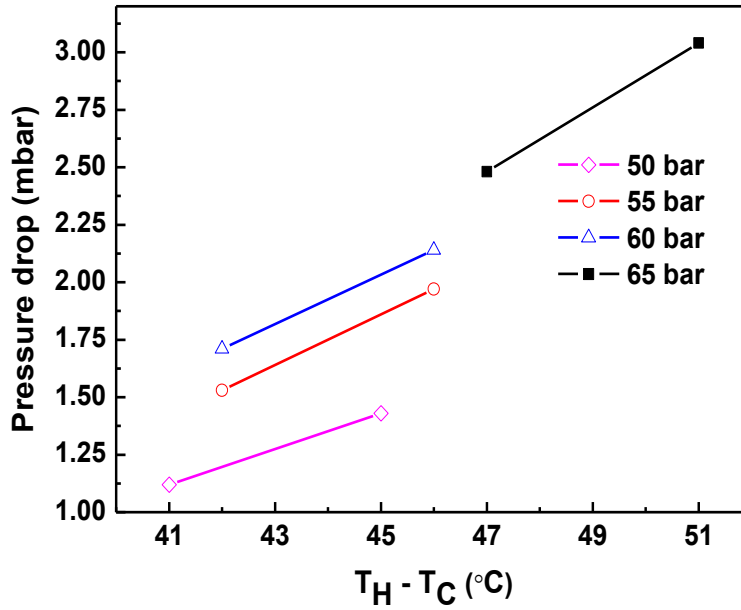


Figure 6.2 Variation of heat transfer rate of CO₂ at different operating pressures and at different HHX inlet temperatures

Figure 6.2 show the effect of HHX methanol inlet temperature on pressure drop at different operating pressures 50, 55, 60, and 65 bar. Results shows that the operating pressure increases, the pressure drop increases which occurs due to an increase in viscosity of carbon dioxide at higher temperature at a fixed operating pressure of 55 bar. HHX inlet temperature increases, pressure drop increases owing to higher buoyancy effect caused by a higher temperature difference between CHX and HHX.

6.3 TEMPERATURE DISTRIBUTION OF TWO PHASE CO₂ BASED NCL AT DIFFERENT OPERATING PRESSURE

Figures 6.3 (a) to (d) show the temperature variation throughout the loop at different operating pressure (50, 55, 60 and 65 bar) and different HHX methanol inlet temperature. The temperature variation is also recorded for all operating pressures to ensure the loop fluid is in the two phase condition of the loop.

Figure 6.3 (a) shows with an increase in the HHX inlet temperature, the loop fluid temperature increases and the loop fluid temperature difference between the left leg center and right leg center also increases. Similar trends also observed in Figure 6.3 (b), (c) and (d) (55, 60, and 65 bar. Figure 6.3 shows the effect of pressure on the loop fluid temperature difference between the left leg center and right leg center. Results

clearly show that as pressure increases, temperature difference decreases, which occurs due to an increase in specific heat at higher pressure at a particular average operating temperature (Table 6.2).

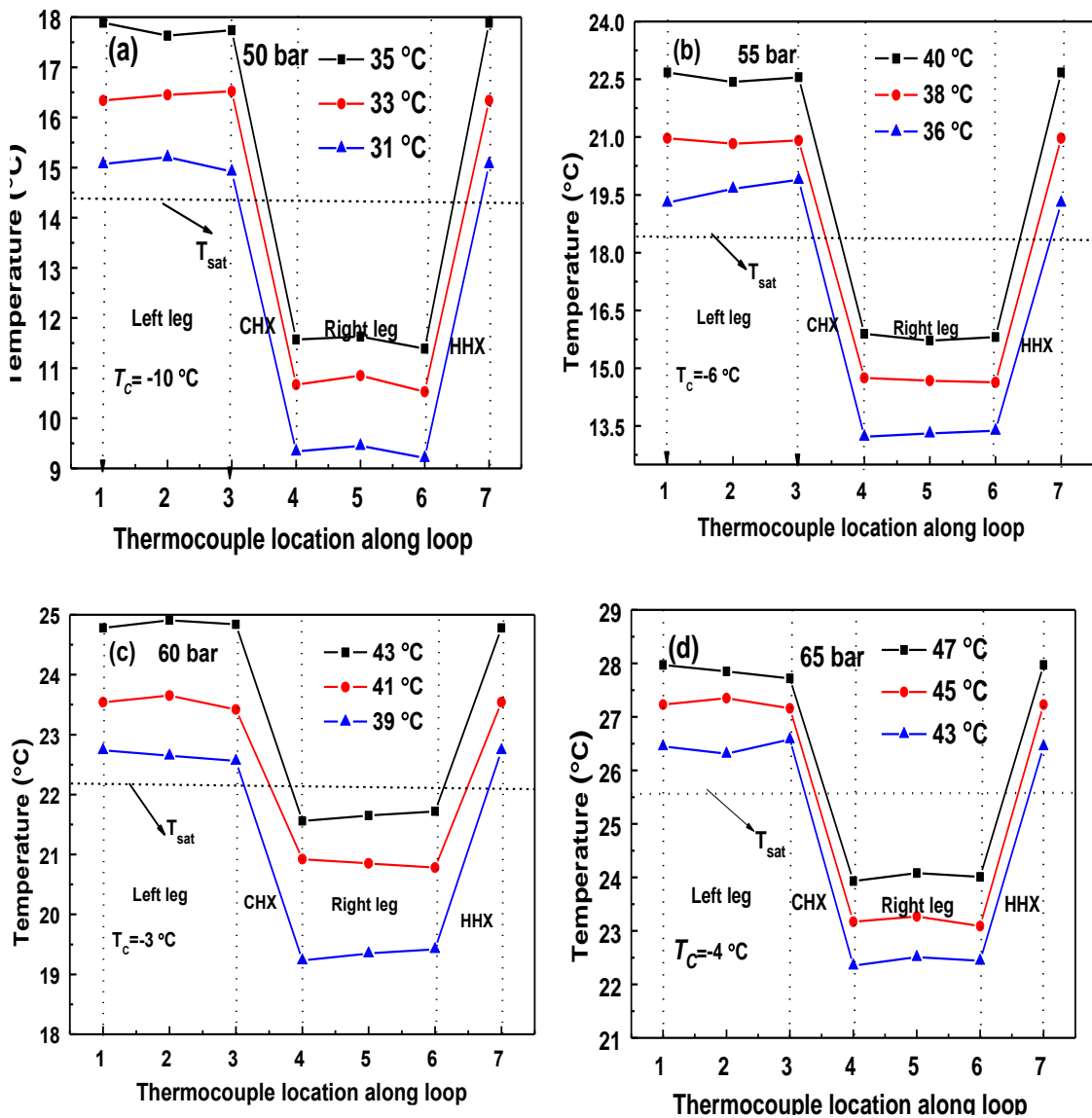


Figure 6.3 Variation of temperature along the loop at different HHX inlet temperatures and different operating pressures (a) 50 bar, (b) 55 bar, (c) 60 bar and (d) 65 bar

6.4 TILT ANGLE EFFECT STUDY ON TWO PHASE CO₂ BASED NCL

Literature survey reveals that a majority of two phase NCL studies deal with water, and only a few experimental works are available on fluids other than water. Due to the high risk involved in handling high operating pressure of CO₂ and to maintain two

phase condition inside the loop, the availability of experimental studies on two phase CO₂ based system is very scant.

6.4.1 Effect of tilt angle on heat transfer rate at different operating pressures

Figures 6.4 (a) and (b) show the effect of tilt angle on heat transfer rate for 50 °C HHX methanol inlet temperature at different operating pressures (50, 60 and 65 bar) in XY/YZ (0°, 30°, 45°) planes and fixed CHX and CHX methanol inlet temperature difference (42 °C). Results show that there is a subsidiary drop in heat transfer rate after tilting the loop in XY (30°, 45°) as well as in YZ (30°, 45°) planes, which occurs due to lower buoyancy on account of a decrease in effective height of the loop between CHX and HHX.

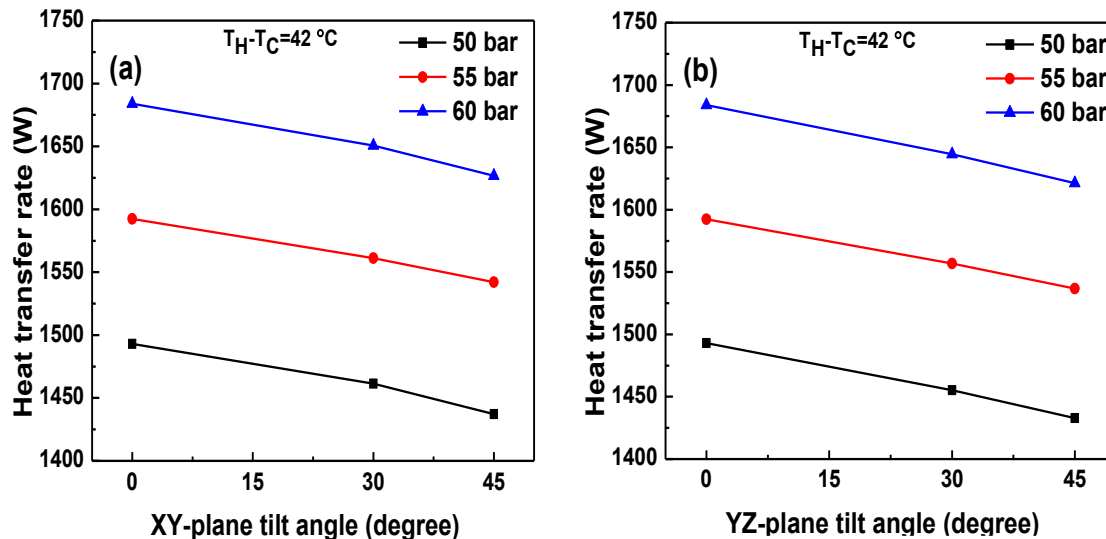


Figure 6.4 Variation of heat transfer rate of CO₂ at different pressures and $T_H - T_C = 42$ °C in (a) XY-plane and (b) YZ-plane

Figure 6.5 (a) and (b) shows the effect of tilt angle on heat transfer rate for 60 °C HHX water inlet temperature at different operating pressures in XY/YZ (0°, 30°, 45°) planes and fixed CHX and CHX methanol inlet temperature difference (46°C). Results show that there is a small marginal drop in heat transfer rate after tilting in XY (30°, 45°) as well as in YZ (30°, 45°) planes, maximum drop in heat transfer rate found in YZ planes.

It is also observed that the drop in heat transfer rate due to tilting the loop in YZ plane is slightly higher than the tilting in XY plane (4% in YZ plane and 3.5% in XY plane

at 45° tilt angle). This occurs due to additional drop in effective height by tilting loop in YZ plane compared to XY plane. Heat transfer rate in YZ plane becomes zero if a loop is tilted by 90° as both the heat exchangers are at a horizontal position, which is not the case in XY plane. Hence, tilting of the loop could be a solution for instability with small reduction of heat transfer rate.

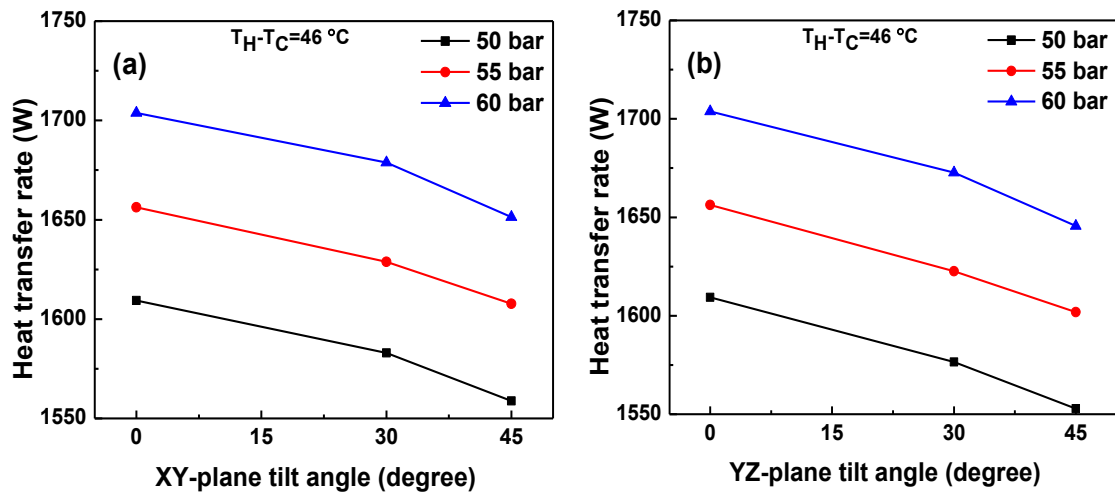


Figure 6.5 Variation of heat transfer rate of CO₂ at different pressures and $T_H - T_C = 46$ °C in (a) XY-plane and (b) YZ-plane

6.4.2 Effect of tilt angle on pressure drop at different operating pressures

Figures 6.6 and 6.7 show the effect of tilt angle on pressure drop at different operating pressures in XY (0°, 30°, 45°) and YZ (0°, 30°, 45°) planes, respectively at fixed CHX and HHX methanol inlet temperature difference of 42 °C and 46 °C. Results show that, as pressure increases, pressure drop also increase in both cases due to an increase in viscosity at higher pressure. A differential pressure transducer is connected across the CHX to measure the pressure drop, as shown in Figure 3.6.

There is an increase in height between the connecting ends of the differential pressure transducer with the increase in tilt angle in XY plane, which causes a rise in the additional pressure head. In YZ plane tilting, the connecting ends of differential pressure transducer remain horizontal, but the mass flow rate decreases due to a reduction in buoyancy effect and causes a lower pressure drop. Results also obtained for the temperature difference between HHX and CHX methanol inlet temperature of

46 °C as shown in Figure 6.7 (a) and (b), a similar trend observed in XY and YZ plane.

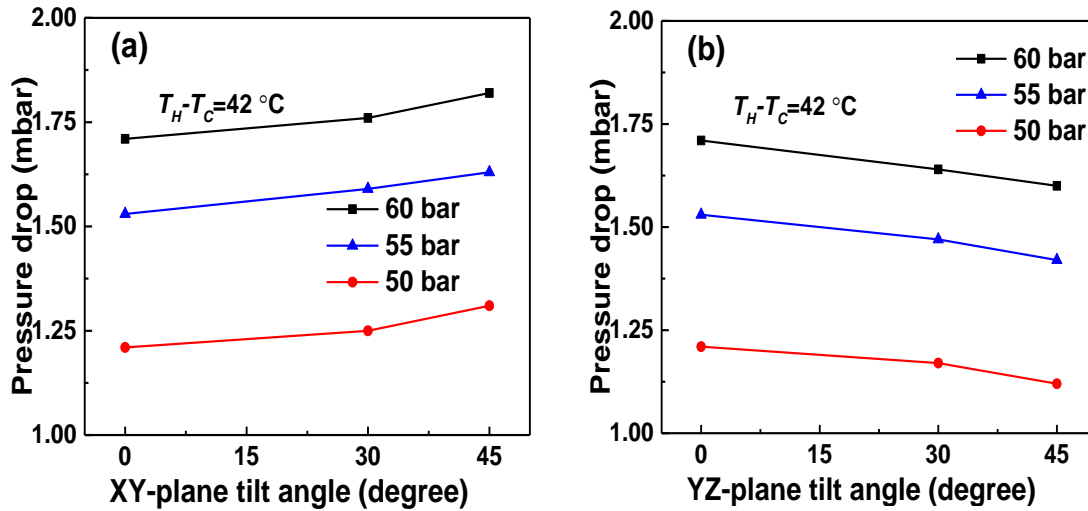


Figure 6.6 Pressure drop comparison of CO₂ at different pressures and $T_H - T_C = 42\text{ °C}$ in (a) XY-plane and (b) YZ-plane

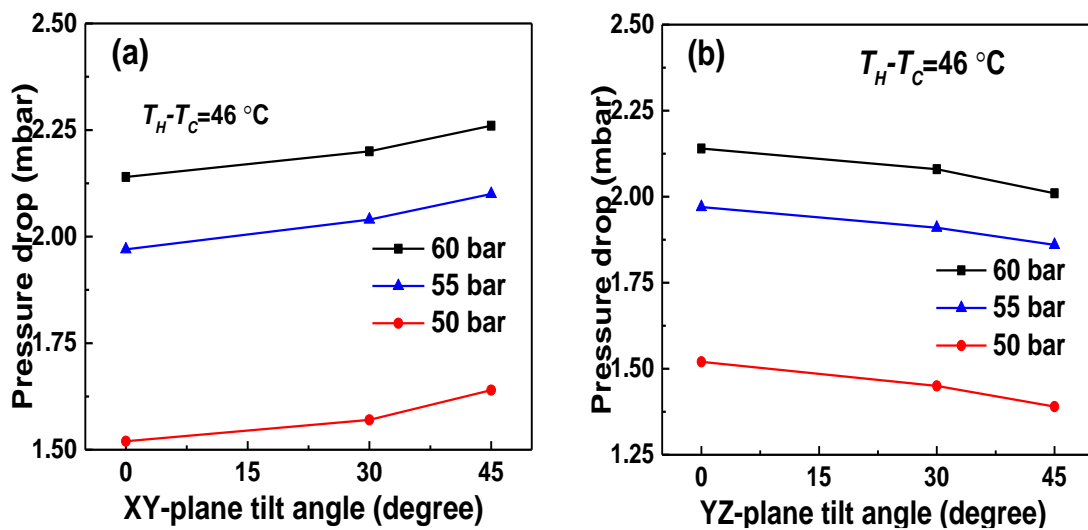


Figure 6.7 Pressure drop comparison of CO₂ at different pressures and $T_H - T_C = 46\text{ °C}$ in (a) XY-plane and (b) YZ-plane

6.4.3 Effect of tilt angle on temperature distribution along the loop at different operating pressures

Figure 6.8 (a) and (b) show the temperature variation throughout the entire loop at 50 bar for loop tilting in XY (0°, 30°, 45°) and YZ (0°, 30°, 45°) planes, respectively for

different HHX methanol inlet temperatures and fixed CHX inlet temperature. Results show that the temperature at left leg and right leg is lies between saturation temperature, confirming the two phase condition of the CO₂ inside the loop and as HHX temperature increases the loop fluid temperature increases. Tilting the loop in XY plane and YZ plane there is a marginal decrease in loop fluid temperature, the maximum decrease in temperature is observed in YZ plane.

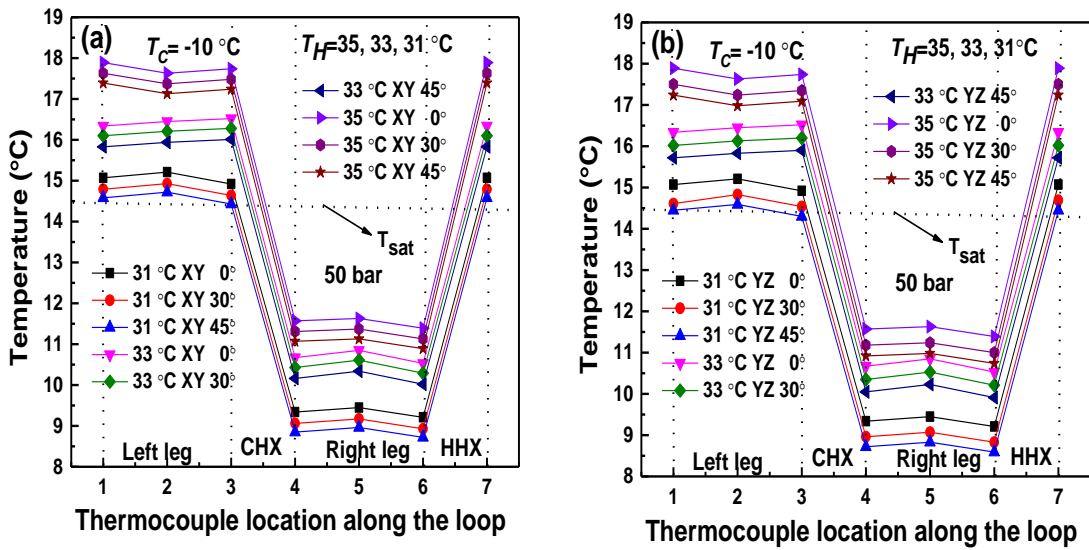


Figure 6.8 Variation of temperature along the loop at 50 bar in (a) XY-plane, and (b) YZ-plane

Figure 6.9 (a) and (b) show the temperature variation throughout the entire loop at 55bar for loop tilting in XY (0°, 30°, 45°) and YZ (0°, 30°, 45°) planes, respectively for different HHX water inlet temperatures and fixed CHX inlet temperature. Tilting the loop in XY plane and YZ plane there is small decrease in loop fluid temperature, the maximum decrease in temperature is found in YZ plane compared to XY plane. Similar trends are observed in Figures 6.10 and 6.11.

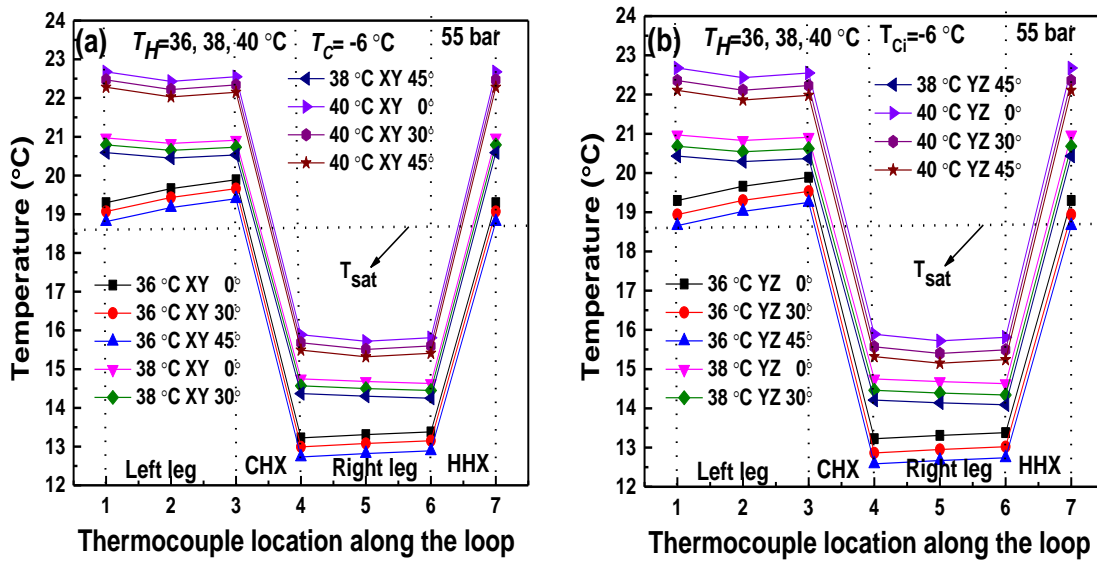


Figure 6.9 Variation of temperature along the loop at 55 bar in (a) XY-plane, and (b) YZ-plane

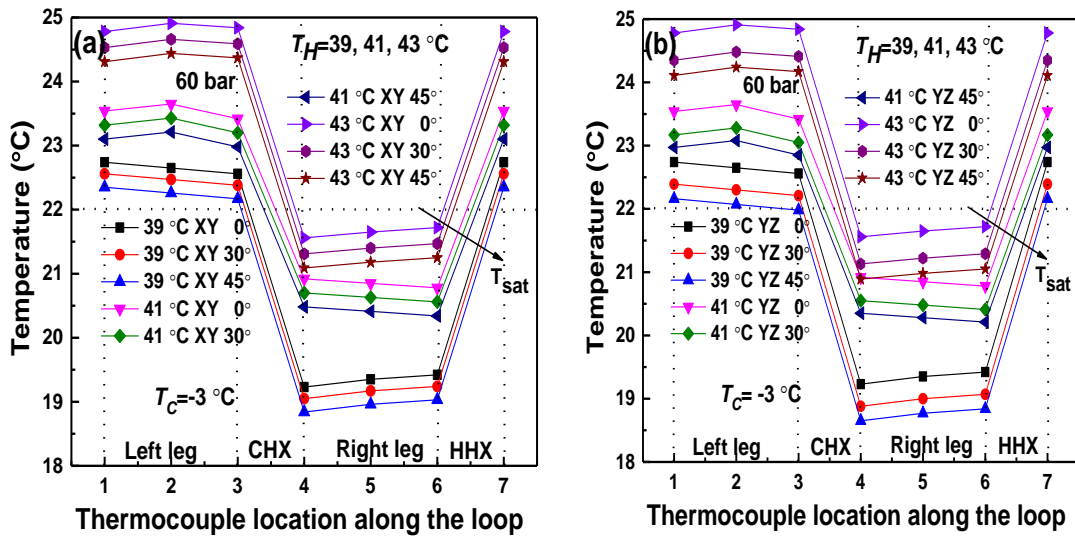


Figure 6.10 Variation of temperature along the loop at 60 bar in (a) XY-plane, and (b) YZ-plane

From above Figures 6.8 to 6.11 it is observed that as HHX inlet temperature increases, the overall loop temperature increases which is obvious, but as tilt angle increases, the drop in temperature in YZ plane case is slightly higher compared to XY plane case.

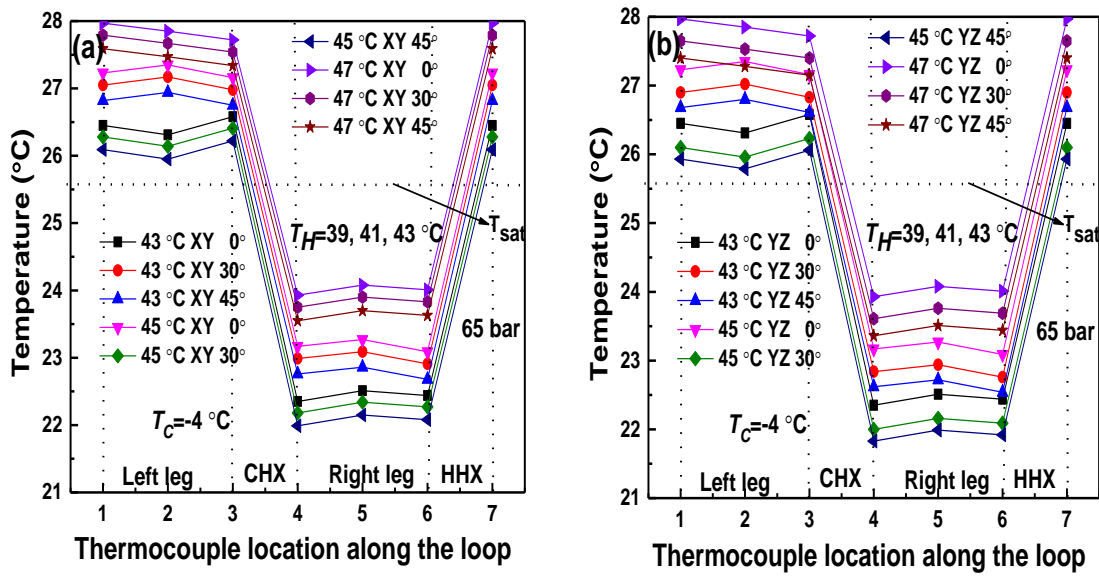
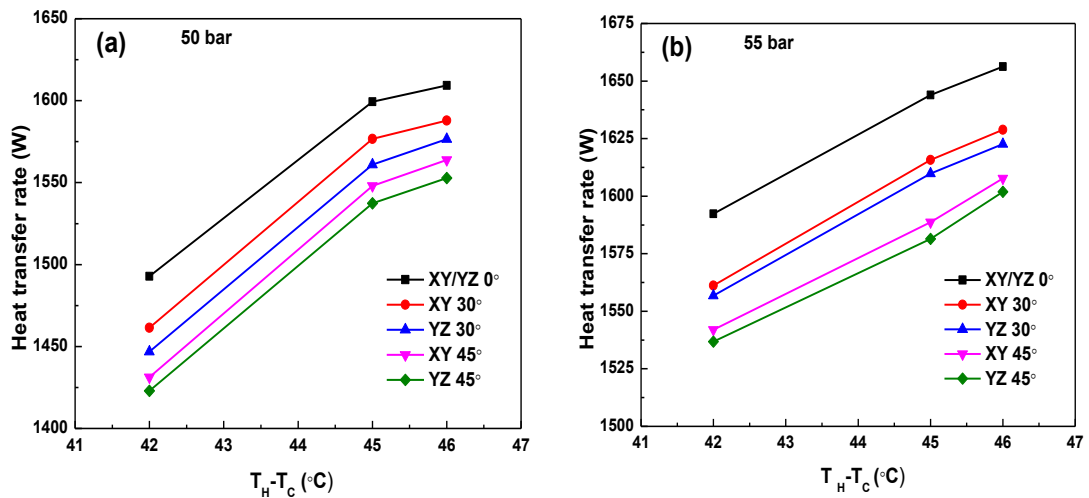


Figure 6.11 Variation of temperature along the loop at 65 bar in (a) XY-plane, and (b) YZ-plane

6.4.4 Effect of HHX water inlet temperature on heat transfer rate at different tilt angles and different operating pressures

Figures 6.12 (a) to (c) show the effect of HHX water inlet temperature and operating pressure on heat transfer rate at different tilt angles at 50, 55 and 60 bar respectively. Results show that as HHX methanol inlet temperature increases, heat transfer rate increases due to a higher buoyancy effect caused by the higher temperature difference between CHX and HHX (explained in section 6.2).



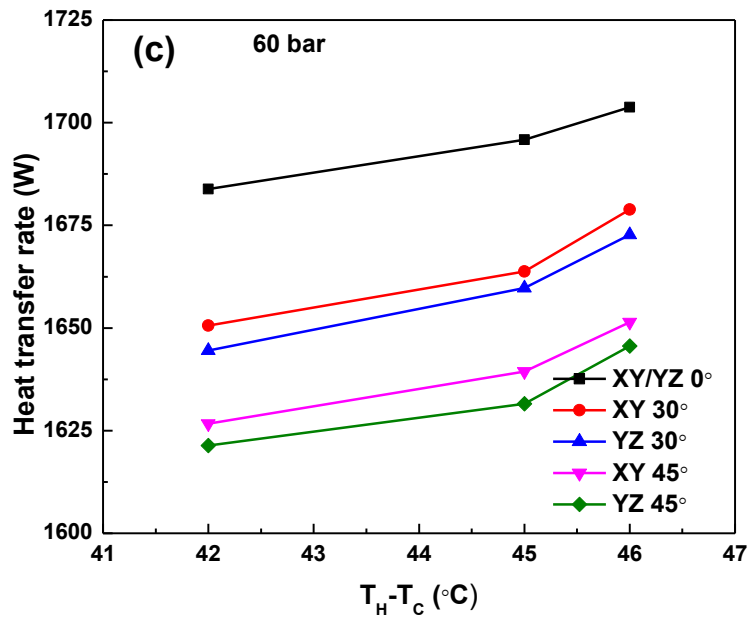


Figure 6.12 Effect of HHX inlet temperature on heat transfer at different operating pressure (a) 50 bar, (b) 55 bar, and (c) 60 bar

Results show that there is a marginal decrease in the heat transfer rate after tilting the loop in XY/YZ (30°, 45°) planes. A maximum drop in heat transfer rate is observed in YZ plane. This occurs due to an additional reduction in effective height by tilting loop in YZ plane compared to XY plane. Heat transfer rate in YZ plane becomes zero if the loop is tilted by 90° as both the heat exchangers are at a horizontal position, which is not the case in XY plane.

6.5 HEAT TRANSFER AND PRESSURE DROP COMPARISON OF TWO PHASE CO₂ BASED NCL WITH BRINE BASED NCL

The heat transfer rate and pressure drop of two phase CO₂ based NCL is compared with widely used brine based natural circulation loop (lower temperature) at the same CHX and HHX temperatures. Brine solution is prepared by using a mixture of water and NaCl (17%) to get a freezing point up to -18 °C. The operating pressure for brine as loop fluid is kept at 1 atm pressure as the variation of thermophysical properties of brine with operating pressure is insignificant (less than 1%), which in turn does not affect the heat transfer rate significantly Table 6.2.

Table 6.2: Brine properties variation with pressure

Temperature (K)	Pressure (bar)	Density (kg/m ³)	Cp (kJ/kg-K)	Viscosity (μPa-s)	Volumetric expansion coefficient 1/K
311	1	1056.78	3.897	720.00	0.00038945
311	75	1073.78	3.834	723.80	0.00037823

Figure 6.13 shows the variation of heat transfer rate at different operating temperatures and pressures. Results show that an increase in temperatures increases the heat transfer rate of brine as well as CO₂ based NCL, the heat transfer rate is found to be maximum for the operating pressure of 65 bar.

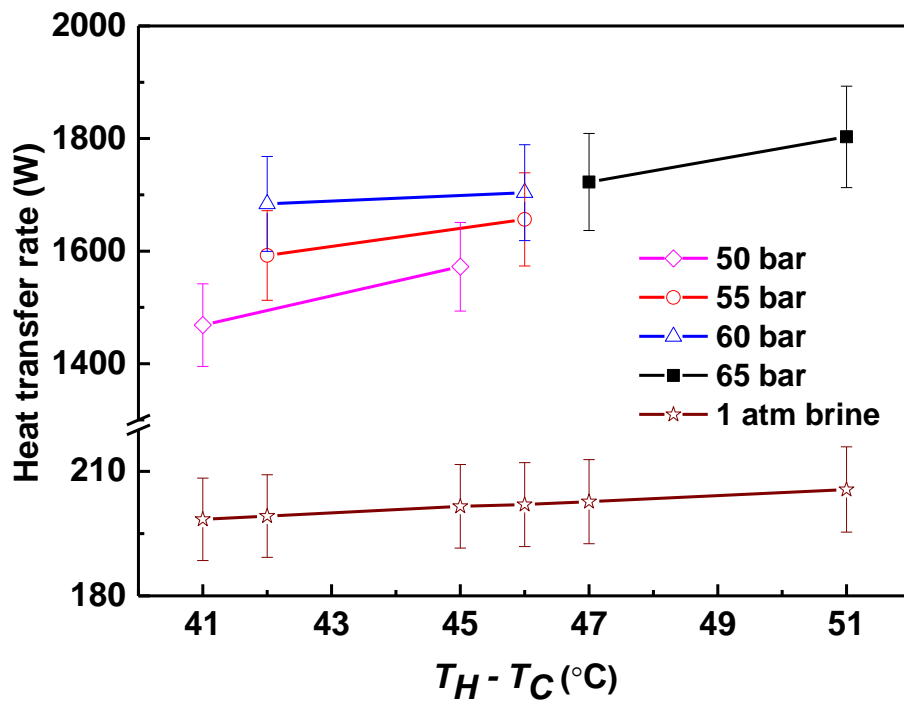


Figure 6.13 Variation of heat transfer rate for brine and two phase CO₂ at different pressure

As the loop moves into the two-phase region, a large buoyancy effect gets generated, causing an increase in the mass flow rate (Reynolds number) of CO₂ and which in turn enhances the heat transfer coefficient. In this case, the heat transfer rate of CO₂ based NCL yields 9 times (900%) higher than the brine solution based NCL for the same operating temperatures as shown in Figure 6.15.

Figure 6.14 shows the variation of pressure drop at different operating temperatures and different operating pressures. Results show that as HHX inlet temperature increases pressure drop of CO₂ increases which occurs due to increase in viscosity of carbon dioxide at a higher temperature at fixed operating pressures. From the results it is clear that maximum pressure is found in brine based NCL compare to CO₂ based NCL, because of the higher viscosity of brine.

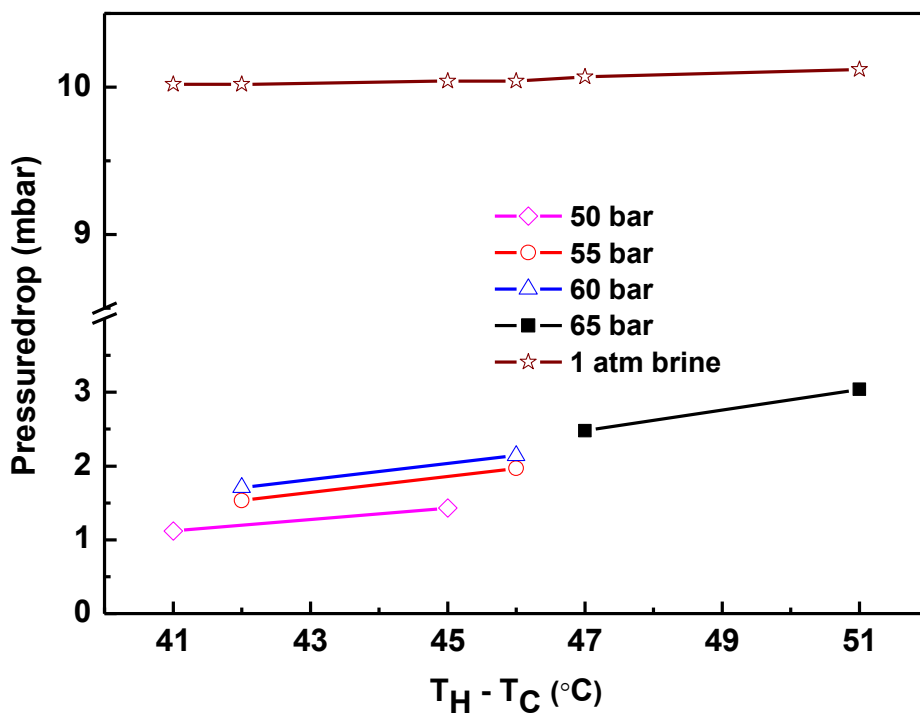


Figure 6.14 Variation of pressure drop for water and supercritical CO₂ at different pressure

6.6 SUMMARY

Steady state analysis has been carried out on the loop with end heat exchangers. two phase of CO₂ was considered with operating pressures of 50 to 65 bar and operating temperatures in the range of -10 °C to 47 °C. Studies were undertaken in the conditions of XY and YZ planes for various loop tilt angles 0°, 30°, 45°. From this study, the following conclusions emerge:

- A much higher heat transfer rate (900%) is obtained in the case of two-phase CO₂ based NCL compared to brine-based NCL. This study is carried out for low-temperature applications (below 0 °C). After tilting the loop in XY (0°,

30°, 45°) and YZ (0°, 30°, 45°) planes, there is a decrease in heat transfer rate 3.5% for XY plane and 4% in YZ plane.

- Heat transfer rate in the two phase is higher due to more buoyancy effect.
- As the decrease in heat transfer rate is less in the case of loop tilting in the XY plane, it should be preferred over the YZ plane to get better performance.

Chapter 7

CONCLUSIONS AND SCOPE OF FUTURE WORK

7.1 CONCLUSIONS

This dissertation presents an array of experimental investigations carried out to study the steady-state behavior of a CO₂ based natural circulation loop (NCL). Subcritical (liquid, vapor, and two-phase) and supercritical phases of the CO₂ are considered with an operating pressure in the range of 35-90 bar and an operating temperature in the range of -18 to 70 °C. Results are obtained for the tilt angle 0°, 30°, 45° in XY and YZ planes for the CO₂ as loop fluid. The heat transfer rate of CO₂ based NCL is compared with widely used loop fluid i.e., water (for above 0 °C) and brine (for below 0 °C). To give a comprehensive overview of the dissertation, all the investigations are summarized briefly, and the remarkable observations are reiterated in the following sections.

7.1.1 Experimental analysis of supercritical CO₂ with end heat exchangers

Steady state analysis is carried out on the loop with end heat exchangers. The supercritical phase of CO₂ is considered with operating pressures of 75, 80 and 90 bar and operating temperatures in the range of 40 °C to 70 °C. Studies are undertaken for various loop tilt angles 0°, 30° and 45° in XY and YZ planes conditions. The following conclusions are drawn from this study:

- In the case of supercritical CO₂ as loop fluid, an 800% higher heat transfer rate is obtained compared to water as loop fluid.
- After tilting the loop in XY (0°, 30°, 45°) and YZ (0°, 30°, 45°) planes, there is a decrease in heat transfer rate i.e., 4.3% for XY plane and 6.2% in YZ plane.
- After tilting the loop in XY (0°, 30°, 45°) and YZ (0°, 30°, 45°) planes, there is an increase in pressure drop for XY plane and a decrease in pressure drop YZ plane.

7.1.2 Experimental analysis of subcritical CO₂ (liquid, vapor, and two-phase) with end heat exchangers

Steady state analysis is carried out on the loop with end heat exchangers. The supercritical phase of CO₂ is considered with operating pressures of 35 to 70 bar and operating temperatures in the range of -18 °C to 70 °C. Studies are undertaken with the tilting conditions of XY and YZ planes for various loop tilt angles 0°, 30°, 45°. From this study, the following conclusions emerge:

- In the case of subcritical vapor CO₂ as loop fluid, a 400% higher heat transfer rate is obtained compared to water as loop fluid. After tilting the loop in XY (0°, 30°, 45°) and YZ (0°, 30°, 45°) planes, there is a decrease in heat transfer rate, i.e., 3.8% for XY plane and 6% for YZ plane.
- For low-temperature applications (below 0 °C), subcritical liquid CO₂ yields a 500% higher heat transfer rate compared to brine solution as loop fluid. After tilting the loop in XY (0°, 30°, 45°) and YZ (0°, 30°, 45°) planes, there is a decrease in heat transfer rate i.e., 4.8% for XY plane and 6.4% for YZ plane.
- A much higher heat transfer rate (900%) is obtained in the case of two-phase CO₂ based NCL compared to brine-based NCL. This study is carried out for low temperature applications (below 0 °C). After tilting the loop in XY (0°, 30°, 45°) and YZ (0°, 30°, 45°) planes, there is a decrease in heat transfer rate i.e., 3.5% for XY plane and 4% in YZ plane.
- Heat transfer rate in the subcritical liquid and vapor case is lower than that for the supercritical CO₂ scenario. To achieve the maximum heat transfer rate, operating conditions should be chosen near the pseudocritical region in supercritical zone.
- Heat transfer rate in the two phase CO₂ is higher than that supercritical case, subcritical liquid and subcritical vapor scenario due to more buoyancy effect.
- As the decrease in heat transfer rate is less in the case of loop tilting in the XY plane, it should be preferred over the YZ plane to get better performance.
- Loop tilting is one of the solution to reduces the ever challenging instability problem in NCL.

7.2 SCOPE FOR FUTURE WORK

The present dissertation analyses several aspects of subcritical (liquid, vapor, and two-phase)/supercritical CO₂ based NCLs. A few areas have been studied in the course of the present study which deserves further attention, as few explained below:

- i. Further studies to see and understand the flow reversal phenomenon are to be planned with better control of the operating parameters.
- ii. Transient studies can be done for the tilting effect on the loop with end heat exchangers
- iii. Studies can be carried out on different orientations of the heat exchangers and also loops with parallel risers and downcomers.
- iv. Performance enhancing techniques such as the use of integrally finned surfaces and employing a nanofluid as the loop fluid can be explored in greater detail.

REFERENCES

- Aarlien, R., and Frivik, P. E. (1998). Comparison of practical performance between CO₂ and R-22 reversible heat pumps for residential use, *Proceedings of the Natural Working Fluids, IIR-Gustav Lorentzen Conference, Oslo, Norway*.
- Adriansyah, and Willy (2004). “Combined Air Conditioning and Tap Water Heating Plant Using CO₂ as Refrigerant.” *Energy Build.*, 36(7), 690–695.
- Agrawal, N. (2008). Transcritical carbon dioxide heat pumps: studies on multi staging and capillary tube systems, *Ph.D. Thesis, Indian Institute of Technology, Kharagpur*.
- Aittomiiki, A., and Lahti, A. (1997). “Potassium formate as a secondary refrigerant.” *Int. J. Refrig.*, 20(4), 276–282.
- Altamush Siddiqui, M. (1997). “Heat transfer and fluid flow studies in the collector tubes of a closed-loop natural circulation solar water heater.” *Energy Convers. Manage.*, 38(8), 799-812.
- Bhatti, M. (1997). A critical look at R-744 and R-134a mobile air conditioning systems, *SAE paper no. 970527*.
- Brown, J. S., Yana-Motta, S. F., and Domanski, P. A. (2002). “Comparative analysis of an automotive air conditioning systems operating with CO₂ and R134a.” *Int. J. Refrig.*, 25(1), 19-32.
- Cammarata, L., Fichera, A., and Pagano, A. (2003). “Stability maps for rectangular circulation loops.” *Appl. Therm. Eng.*, 23(8), 965–977.
- Chen, K. S. (1985a). “On the oscillatory instability of closed-loop thermosyphons.” *J. Heat Transfer*, 107(4), 826-832.
- Chen, K. S. (1985b). “The optimal configuration of natural convection loops.” *Sol. Energy*, 34, 407-416.

Chen, K. S., Chen, Y. Y., Shiao, S. W., and Wang, P. C. (1991). "An experimental study of steady state behavior of a two phase natural circulation loop." *Energy Convers. Manage.*, 31(6), 553-569.

Chexal, V. K., and Bergles, A. E. (1973). "Two phase instabilities in a low pressure natural circulation loop." *AIChE Symposium*, 69, 37-45.

Cho, H., Ryu, C., Kim, Y., and Kim, H. Y. (2005). "Effects of refrigerant charge amount on the performance of a transcritical CO₂ heat pump." *Int. J. Refrig.*, 28(8), 1266-1273.

Christensen, K. G. (1999). Use of CO₂ as primary and secondary refrigerant in supermarket applications. *20th International Congress of Refrigeration, IIF/IIR, Sydney*.

Close, D. J. (1962). "The Performance of Solar Water Heaters with Natural Circulation." *Sol. Energy*, 6(1), 30-40.

Cohen, H., and Bayley, F. J. (1955). "Heat Transfer Problems of Liquid Cooled Gas Turbine Blades." *Proceedings of Institution of Mechanical Engineers*, 169, 1063-1080.

Da Silva, A. K., and Mantelli, M. B. H. (2004). "Thermal applicability of two phase thermosyphons in cooking chambers-experimental and theoretical analysis." *Appl. Therm. Eng.*, 24(5-6), 717-733.

Delmastro, D. F., Clausse, A., and Converti, I. (1991). "The influence of gravity on the stability of boiling flows." *Nucl. Eng. Des.*, 127(1), 129-139.

Elias, G., Fantini, L., Ferrari, E., and Sala, R. (2000). "Theoretical study and experimental verification of the behavior of passive conditioning system for electronic components." *Heat Mass Transfer*, 36(11), 505-510.

Faramarzi, R. T., and Walker, D. H. (2004). Investigation of secondary loop supermarket refrigeration systems. *California Energy Commission (Public Interest Energy Research Program), Consultant Report*.

Finn, D. P., Cabello, Portoles, A., and Smyth, S. (2008). Evaluation of defrost options for secondary coolants in multi-temperature indirect transport refrigeration part I: experimental results. *Proceeding of 8th IIR Gustav Lorentzen Conference on natural working fluids, Denmark*.

Forbes, D., and Pearson (2004). Development of carbon dioxide as a volatile secondary heat transfer fluid to replace glycols. *IIR-Gustav conference on natural working fluids, Glasgow*.

Garibaldi, P., and Misale, M. (2008) “Experiments in single phase natural circulation mini loops with different working fluids and geometries.” *J. Heat Transfer*, 130(10).

Georgi, S., Kazachki, David, K., and Hinde (2006). Secondary coolant system for supermarkets. *ASHRAE*, 35-46.

Giroto, S., Minetto, S., and Petter Neksa (2004). “Commercial refrigeration system using CO₂ as the refrigerant.” *Int. J. Refrig.*, 27(7), 717–723.

Grief, R. (1988). “Natural Circulation Loops.” *J. Heat Transfer*, 110(4b), 1243-1257.

Gupta, C. L., and Garg, H. P. (1968). “System design in solar water heaters with natural circulation.” *Sol. Energy*, 12(2), 163-182.

Hafner, A. (2002). Experimental study on heat pump operation of prototype CO₂ mobile air conditioning system. *Preliminary proceedings of the 5th IIR-Gustav Lorentzen Conference on Natural Working Fluids, Guangzhou*.

Haider, S. Joshi, Y., and Nakayama, W. (2002). “A natural circulation model of the closed loop two phase thermosyphon for electronic cooling.” *J. Heat Transfer*, 124(5), 881-890.

Hinde, D., Zha, S., and Lan, L. (2008). Experience in North America super markets. *Proceedings of 8th IIR Gustav Lorentzen Conference on Natural working fluids, Denmark*.

- Hirao, T., Mizukami, H., Takeuchi, M., and Taniguchi, M. (2002). Development of air conditioning system using CO₂ for automobile. *Preliminary Proceedings of the 5th IIR-Gustav Lorentzen Conference on Natural Working Fluids, Guangzhou.*
- Horton, W. T., and Groll, E. A. (2003). Secondary loop refrigeration in supermarket applications: A case study. *International Congress of Refrigeration, ICR0434, Washington DC.*
- Hsieh, C. C., Wang, S. B., and Pan, C. (1997). “Dynamic visualization of two phase flow patterns in a natural circulation loop.” *Int. J. Multiphase Flow*, 23(6), 1147–1170.
- Huang, B. J. (1980). “Similarity theory of solar water heater with natural circulation.” *Sol. Energy*, 25(2), 105-116.
- Hussein, H. (2002). “Transient investigation of a two phase closed thermosyphon flat plate solar water heater.” *Energy Convers. Manage.*, 43(18), 2479-2492.
- Hussein, H. (2003). “Optimization of a natural circulation two phase closed thermosyphon flat plate solar water heater.” *Energy Convers. Manage.*, 44(14), 2341–2352.
- Jabbar, A., and Khalifa, N. (1998). “Forced versus natural circulation solar water heaters: a comparative performance study.” *Renewable Energy*, 14(1-4), 77-82.
- Jain, K. C., Petrick, M., Miller, D., and Bankoff S, G. (1966). “Self sustained hydrodynamic oscillations in a natural circulation boiling water loop.” *Nucl. Eng. Des.*, 4(3), 233–252.
- Jain, P. K., and Rizwan-uddin, (2008). “Numerical analysis of supercritical flow instabilities in a natural circulation loop.” *Nucl. Eng. Des.*, 238(8), 1947–1957.
- Japikse, D. (1973). “Advances in thermosyphon technology.” *Adv Heat Transfer*, 9(C), 1(C)–111.

Jong M Kim, Sang Y Lee, Experimental observation of flow instability in a semi-closed two phase natural circulation loop, *Nuclear Engineering and Design*, V 196, pp. 359-367, 2000.

Joshi, J. B. (2001). "Computational Flow Modeling and Design of Bubble Column Reactors." *Chem. Eng. Sci.*, 56(01), 5893–5933.

Juei, T., Hsu, Mamoru Ishii, and Takashi Hibiki. (1998). "Experimental study on two phase natural circulation and flow termination in a loop." *Nucl. Eng. Des.*, 186(3), 395–409.

Kaga, S., Nomura, T., Seki, K., and Hirano, A. (2008). Development of compact inverter refrigerating system using R600a/CO₂ by "Thermo-siphon", *Proceedings of 8th Gustav Lorentzen Natural Working Fluids Conference, Copenhagen*.

Kang, Y. K., Kang, M. C., and Chun, W. C. (2003). "On thermal characteristics of the solar collector made with closed loop thermosiphon." *Int. commun. heat mass*, 30(7), 955-964.

Keller, J. B. (1966). "Periodic oscillations in a model of thermal convection." *J. Fluid Mech.*, 29(3), 599–606.

Khandekar, S., and Gupta, A. (2007). Embedded Pulsating Heat Pipe Radiators. *Proceedings of 14th International Heat Pipe Conference, Florianópolis, Brazil*.

Kim, J., and Lee, S. (2000). "Experimental observation of flow instability in a semi-closed two phase natural circulation loop." *Nucl. Eng. Des.*, 196(3), 359-367.

Kim, M. H., Pettersen, J., and Bullard, C. W. (2004). "Fundamental process and system design issues in CO₂ vapor compression systems." *Prog. Energy Combust. Sci.*, 30(10), 119–174.

Kiran Kumar, K., and Ram Gopal, M. (2009). Carbon dioxide as secondary fluid in natural circulation loops. *Proceedings of the Institution of Mechanical Engineers, Part E: Journal of Process Mechanical Engineering*, 223, 189–194.

Kreitlow, D. B., Reistad, G., M., Miles C. R., and Culver G. G. (1978). "Themosyphon models for down hole heat exchanger application in shallow geothermal systems." *J. Heat Transfer*, 100(4), 713–719.

Kruse, H. (2004). "Refrigerant use in Europe." *ASHRAE J.*, 42(9), 16-24.

Kyung, I. S., and Lee, S. Y. (1994). "Experimental observation on flow characteristics in an open two phase natural circulation loop." *Nucl. Eng. Des.*, 159(1), 163–176.

Lawrence, S. A., and Tiwari, G. N. (1990). "Theoretical evaluation of solar distillation under natural circulation with heat exchanger." *Energy Convers. Manage.*, 30(3), 205-213.

Lee, Y. S., and Ishii, M. (1990). "Characteristics of two phase natural circulation in Freon-113 boiling loop." *Nucl. Eng. Des.*, 121(1), 69–81.

Lorentzen, G. (1995). "The use of natural refrigerants: a complete solution to the CFC/HCFC predicament." *International Journal of Refrigeration*, 18(3), 190–197.

Lorentzen, G., and Pettersen, J. (1993). "A new efficient and environmentally benign system for car air-conditioning." *Int. J. Refrig.*, 16(1), 4–12.

Luca, C., Marco, C., Fornasieri, E., and Zamboni, L. (2005). "Carbon dioxide as refrigerant for tap water heat pumps: A comparison with the traditional solution." *International Journal of Refrigeration*, 28(8), 250–1258.

Mao, C., Lin, J., Chun, Wen, S., Lee, Sih Li, and Chen. (2003). "Thermal performance of a two phase thermosyphon energy storage system." *Sol. Energy*, 75(4), 295-306.

Mathur, G. D. (2000). "Carbon dioxide as an alternative refrigerant for automotive air conditioning systems." *American institute of aeronautics and astronautics*, 28, 371–380.

- McKee, H. R. (1970). "Thermosyphon reboilers: A review." *J. Ind. Eng. Chem.*, 62(12), 76–82.
- Melinder, A. (2007). Choosing secondary working fluid for two common types of indirect system applications. *International Congress of Refrigeration Beijing*.
- Melinder, A. (1998). A Critical review on thermophysical properties of liquid secondary refrigerants. *IIR–Gustav Lorentzen Natural Working Fluids Conference, Oslo*.
- Melinder, A. (2004). "Secondary fluids for low operating temperatures" 6th *IIR-Gustav Lorentzen Natural Working fluids, Glasgow*.
- Mertol, A., Place, W., Webster, T., and Greif, R. (1981). "Detailed loop model (DLM) analysis of liquid solar thermosiphons with heat exchangers." *Sol. Energy*, 27(5), 367–386.
- Milanovic, P., Jacimovic, B., and Genic, S. (2004). "The influence of heat exchanger performances on the design of indirect geothermal heating system." *Energy Build.*, 36(1), 9–14.
- Minea, V. (2007). "Supermarket refrigeration system with completely secondary loops." *ASHRAE J.I.*, 49(9), 40.
- Minea, V. (2008). Low charge and low emission super market refrigeration systems. *Proceedings of 8th IIR Gustav Lorentzen Natural working fluids Conference, Denmark*.
- Misale, M., and Frogheri, M. (2001). "Stabilization of single phase natural circulation loop by pressure drops." *Exp therm fluid sci.*, 27(5), 277–282.
- Misale, M., Garibaldi, P., Passos, J. C., and Bitencourt, G. D. (2007). "Experiments in a single phase natural circulation mini-loop." *Exp therm fluid sci.*, 31(8), 1111–1120.
- Morrison, G. L., and Ranatunga, D. (1980). "Thermosyphon circulation in solar collectors." *Sol. Energy*, 24(2), 191-198.

- Mousavian, S.K., Misale, M., D'Auria, F., and Salehi, M. A. (2004). "Transient and stability analysis in single-phase natural circulation." *Ann. Nucl. Energy*, 31(10), 1177–1198.
- Nayak, A. K., Gartia, M. R., and Vijayan, P. K. (2008). "An experimental investigation of single phase natural circulation behavior in a rectangular loop with Al₂O₃ nano fluids." *Exp therm fluid sci.*, 33(1), 184–189, 2008.
- Neeraj Agarwal, (2008). Transcritical carbon dioxide heat pumps: studies on multistaging and capillary tube systems Ph.D., Thesis. *Indian Institute of Technology, Kharagpur*.
- Neksa, P. (2002). "CO₂ heat pump systems." *Int. J. Refrig.*, 25(4), 421-427.
- NIST Standard Reference Database REFPROP, 2013, Version 9.1.
- Norton, B., and Probert, S. D. (1983). "Recent advances in natural circulation in solar energy water heater designs." *Appl. Energy*, 15(1), 15-42.
- Nottenkamper, R., Stieff, A., and Weinspach, P. M. (1983). "Experimental investigation of hydrodynamics of bubble columns." *Ger. Chem. Eng.*, 6, 147–155.
- Ong, K. S. (1974). "A finite-difference method to evaluate the thermal performance of a solar water heater." *Sol. Energy*, 16(3-4), 137-147.
- Pal, A., Yogendra, K., Joshi, Monem, H., Beitelmal, Chandrakant, D., Patel, Todd, M., and Wenger (2002). "Design and performance evaluation of a compact thermosyphon." *IEEE transactions on Components and Packaging Technologies*, 25(4), 601-607.
- Palm, B. (2007). "Refrigeration systems with minimum charge of refrigerant." *Appl. Therm. Eng.*, 27(10), 1693–1701.
- Pearson, A. (2005). "Carbon dioxide- new uses for old refrigerant." *Int. J. Refrig.*, 28(5), 1140-1148.

- Pettersen, J., Hafner, A., Skaugen, G., and Rekstad, H. (1998). "Development of compact heat exchanger for CO₂ air conditioning systems." *Int. J. Refrig.*, 21(3), 180-193, 1998.
- Pin, C. C. (2001). "The application of capillary pumped loop for cooling of electronic components." *Appl. Therm. Eng.*, 21(17), 1739-1754.
- Preissner, M., Cutler, B., Singanamalla, S., Hwang, Y., and Radermacher, R. (2002). Comparison of automotive air conditioning systems operating with CO₂ and R134a, Preliminary. *Proceedings of 5th IIR-Gustav Lorentzen Natural Working Fluids Conference, Guangzhou.*
- Rahmatollah, K. (2005). "Pressure drop in riser and evaporator in an advanced two phase thermosyphon loop." *Int. J. Refrig.*, 28(5), 725–734.
- Rasmussen, P. (2008). Use of CO₂ in free cooling systems. *Proceedings of 8th Gustav Lorentzen Natural Working Fluids Conference, Copenhagen.*
- Richard Clarke, Donal, P., and Finn. D. (2008). "The influence of secondary refrigerant air chiller U-bends on fluid temperature profile and downstream heat transfer for laminar flow conditions." *Int. J. Heat Mass Transfer*, 51(3-4), 724-735.
- Richter, M. R., Song, S. M., Yin, J. M., Kim, M. H., Bullard, C. W., and Hrnjak, P. S. (2003). "Experimental results of transcritical CO₂ heat pump for residential application." *Energy*, 28(10), 1005–1019.
- Rieberer, R., Karl, M., and Hermann, H. (2004). CO₂ two-phase thermosyphon as a heat source system for heat pumps. *Proceedings of 6th IIR-Gustav natural working fluids conference, Glasgow.*
- Rieberer. R. (2005). "Naturally circulation probes and collectors for ground-coupled heat pumps." *Int. J. Refrig.*, 28(8), 1308-1315.
- Riffat, S. B., Afonso, C. F., Oliveira, A. C., and Reay, D. A. (1997). "Natural refrigerants for refrigeration and air-conditioning systems." *Appl. Therm. Eng.*, 17(1), 33–42.

Samuel Luna Abreu, and Sergio Colle (2004). “An experimental study of two phase closed thermosyphons for compact solar domestic hot water systems.” *Sol. Energy*, 76(1-3), 141–145.

Sarkar, J., Bhattacharyya, S., and Ram Gopal, M. (2004). “Optimization of a transcritical CO₂ heat pump cycle for simultaneous cooling and heating applications.” *Int. J. Refrig.*, 27(8), 830–838.

Sarma, N. V. L. S., Reddy, P. J., and Murti, P. S. (1973). “A computer design method for vertical thermosyphon reboilers, Industrial and Engineering.” *Ind Eng Chem Process Des Dev.*, 12(3), 278–290.

Shitzer, A., and Kalomonviz, D. (1979). “Experiments with a flat plate solar water heating system in thermo symphonic flow.” *Solar Energy*, 22(1), 27–35.

Soo Ick, K., Sang and Lee, Y. (1994). “Experimental observations on flow characteristics in an open two phase natural circulation loop.” *Nucl. Eng. Des.*, 159(1), 163-176.

Sung, C., Kim, Jong, P., Won, Min, S., and Kim (2009). “Effects of operating parameters on the performance of a CO₂ air conditioning system for vehicles.” *Appl. Therm. Eng.*, 29(11-12), 2408–2416.

Tahsin, B., and Serhan, K. (2007). “Flow through rectangular thermosyphon at specified wall temperatures.” *Heat Mass Transfer*, 43(12), 1293-1302.

Thomas, L., Webster, Pascal Coutier. J., Wayne Place, J., Mehdi Tavana (1987). “Experimental evaluation of solar thermosyphons with heat exchangers.” *Sol. Energy*, 38(4), 219-231.

Tomoichiro, T., Yuuichi, Y., and Fumitoshi, N. (2005). “Experimental study on automotive cooling and heating air conditioning system using CO₂ as a refrigerant.” *Int. J. Refrig.*, 28(8), 1302–1307.

Tong, B. Y., Wong, T. N., and Ooi, K. T. (2001). “Closed-loop pulsating heat pipe.” *Appl. Therm. Eng.*, 21(18), 1845–1862.

- Torrance, K. E. (1979). "Open-loop thermosyphons with geological application." *J. Heat Transfer*, 100(4), 677–683.
- Tuma, P. E., and Mortazavi, H. R. (2006). "Indirect thermosyphons for cooling electronic devices." *Electronic Cooling*, 12 (1), 26–32.
- Van Riessen, G. (2004). NH₃/CO₂ Supermarket refrigeration system with CO₂ in the cooling and freezing section. *Proceedings of 6th IIR-Gustav Lorentzen Natural Working Fluids Conference, Glasgow*.
- Verhoef, P. J., and Verhoef, B. V. (2004). Opportunities for CO₂ in supermarket refrigeration. *6th IIR-Gustav Lorentzen Natural Working Fluids Conference, Glasgow*.
- Vijayan, P. K. (2002). "Experimental observations on the general trends of the steady state and stability behaviour of single phase natural circulation loops" *Nucl. Eng. Des.*, 215(1-2), 139–152.
- Vijayan, P. K. (2007). Natural circulation systems: advantages and challenges, IAEA course on natural circulation in water-cooled nuclear power plants. *ICTP, Trieste, Italy*.
- Vladimir, G., Pastukhov, Yury, F., and Maydanik (2007). "Low-noise cooling system for PC on the base of loop heat pipes." *Appl. Therm. Eng.*, 27(5-6), 894-901.
- Wang, K., Magnus Eisele, Yunho Hwang, and Radermacher, R. (2010). "Review of secondary loop refrigeration system." *Int. J. Refrig.*, 33, 212–234.
- Welander, P. (1967). "On the oscillatory instability of a differentially heated fluid loop." *J. Fluid Mech.*, 29(1), 17–30.
- Winkler, H., Theobald, and Quack (2007). The extraordinary properties of carbon dioxide as a secondary refrigerant. *International Congress of Refrigeration, Beijing*.

Wu, C. Y., Wang, S. B., and Pan, C. (1996). "Chaotic oscillation in a low pressure two phase natural circulation loop under low power and high inlet subcooling conditions." *Nucl. Eng. Des.*, 162(2-3), 223-232.

Yadav, A. K., Bhattacharyya, S., and Ram Gopal, M. (2012). "On the suitability of carbon dioxide in forced circulation type loop." *Int. J. Low Carbon Technol.*, 9(1), 85-09.

Yadav, A. K., Bhattacharyya, S., and Ram Gopal, M. (2016). "Optimum operating conditions for subcritical/supercritical fluid-based natural circulation loops." *J. Heat Mass Transf.*, 138(11), 112501.

Yadav, A. K., Ramgopal, M., and Bhattacharyya, S. (2017). "Transient analysis of subcritical/supercritical carbon dioxide based natural circulation loop with end heat exchangers: experimental study." *Heat Mass Transf.*, 53, 2951-2960.

Yadav, A.K., Ramgopal, M., and Bhattacharyya, S. (2016). "Effect of tilt angle on subcritical/supercritical carbon dioxide based natural circulation loop with isothermal source and sink." *J. Thermal Science Engg. Appln.*, 8(1), 1-8.

Yanagisawa, Y., Fukuta, M., Ogura, N., and Kaneo, H. (2004). Operating characteristics of natural circulating CO₂ secondary loop refrigeration system working with NH₃ primary loop. *Proceedings of 6th IIR-Gustav Lorentzen Natural Working Fluids Conference.*

Yin, J. M., Park, Y. C., Boewe, D. E., McEnaney, R. P., Beaver, A., Bullard, C. W., and Hrnjak, P. S. (1998). Experimental and model comparison of transcritical CO₂ versus R134a and R410a system performance. *Proceedings of IIR Conference Gustav Lorentzen, Oslo.*

Yoshikawa, S., Richard, L., Smith, Jr., Hiroshi, I., Yukihiro, M. (2005). "Performance of a natural convection circulation system for supercritical fluids." *J. Supercrit. Fluids*, 36(1), 70–80.

Zerrouki, A., Boumedien, A., and Bouhadeif, K. (2002). “The natural circulation solar water heater model with linear temperature distribution.” *Renewable Energy*, 26(4), 549-559.

Zhang, X. R., and Yamguchi, H. (2007). “An experimental study on evacuated tube solar collector using supercritical CO₂.” *Appl. Therm. Eng.*, 28(10), 1225–1233.

Zimmermann, A. J. P., Melo, C. (2008). “Analysis of a R744 two phase loop thermosyphon applied to the cold end of a Stirling cooler. *Proceedings of 8th Gustav Lorentzen Natural Working Fluids Conference, Copenhagen.*

Zvirin, Y. (1981). “A review of natural circulation loops in pressurized water reactors and other systems.” *Nucl. Eng. Des.*, 67(2), 203–225.

Zvirin, Y., Shitzer, A., and Grossman, G. (1977). “The natural circulation solar heater-models with linear and nonlinear temperature distributions.” *International J. Heat Mass Transfer*, 20(9), 997–999.

List of Publications based on Ph.D. Research Work

Sl. No.	Title of the paper	Authors (in the same order as in the paper. Underline the Research Scholar's	Name of the Journal/ Conference/ Symposium, Vol., No., Pages	Month & Year of Publication	Category *
1	Heat transfer enhancement using CO ₂ in a natural circulation loop	<u>Thippeswamy L.R.</u> Ajay Kumar Yadav	Scientific Reports (SCI IF-4). 10, 1570 https://doi.org/10.1038/s41598-020-58432-6 (Nature publications)	January 2020	1
2	Effect of Loop Tilting on the Heat Transfer and Pressure Drop in Two Phase CO ₂ based Natural Circulation Loop: an Experimental Study	<u>Thippeswamy L.R.</u> Ajay Kumar Yadav	Journal of Thermal Science and Engineering application (SCI IF-1.6) (ASME) 10(2):021021 https://doi.org/10.1115/1.4047820	July 2020	1
3	Computational fluid dynamics analysis of nanofluids based natural circulation loop with end heat exchangers	<u>Thippeswamy L.R.</u> Ajay Kumar Yadav, Venkatesh Lamani	5th International and 41 st National Conference on Fluid Mechanics and Fluid Power.	IIT Kanpur, 2014, Dec 11-14.	3
4	Experimental Investigation of Subcritical/Supercritical CO ₂ Based Natural Circulation Loop with End Heat Exchanger	<u>Thippeswamy L.R.</u> Ajay Kumar Yadav	24th National and 2 nd International ISHMT-ASTFE Heat and Mass Transfer Conference (IHMTTC-2017).	December 27-30, 2017, BITS Pilani, Hyderabad, India.	3
5	Heat transfer performance of CO ₂ based NCL with and without tilting: an experimental study	<u>Thippeswamy L.R.</u> Ajay Kumar Yadav, Tabish Wahidi	11 th International Exergy, Energy and Environment Symposium (IEEES-11).	July 14-18, 2019, SRM, Chennai, India.	3
6	Effect of tilting on heat transfer performance of subcritical liquid CO ₂ based natural circulation loop	<u>Thippeswamy L.R.</u> Ajay Kumar Yadav	Proceedings of IMEC 2019 International Mechanical Engineering Congress (IMEC-2019).	29th November-1st December 2019, NIT Tiruchirappalli, India.	3

7	Heat transfer performance of subcritical liquid CO ₂ based natural circulation loop with end heat exchangers: an experimental study	<u><i>Thippeswamy L.R.</i></u> Ajay Kumar Yadav	Proceedings of the 46 th National Conference on Fluid Mechanics and Fluid Power (FMFP)	December 9-11, 2019, PSG College of Technology, Coimbatore, India.	3
---	--	--	---	--	---

- * Category: 1: Journal paper, full paper reviewed
2: Journal paper, Abstract reviewed
3: Conference/Symposium paper, full paper reviewed
4: Conference/Symposium paper, abstract reviewed
5: others (including papers in Workshops, NITK Research Bulletins, Short notes etc.)

(If the paper has been accepted for publication but yet to be published, the supporting documents must be attached.)

Research Scholar	Research Guide
Name & Signature, with Date Thippeswamy L.R.	Name & Signature, with Date Dr. Ajay Kumar Yadav

BIODATA

NAME: THIPPESWAMY L R
DATE OF BIRTH: 07-07-1985
Mobile No.: +91 9743135140
Email:thippesh.lr@gmail.com



ADDRESS:
THIPPESWAMY L R
S/O RUDRAPPA L T
CHIKKAGONDANAHALLY(P)
CHITRADURGA(T) (D)
PIN-577502

QUALIFICATION:

Examination	Board/Institute	Year	Percentage/ CGPA
Ph. D (course work)	NITK, Surathkal	2014	8.5
M.Tech (Thermal Engg.)	UVCE, Bangalore	2008-10	85%
B.E. (Mechanical Engg)	BMSCE, Bangalore	2004-08	68%

EXPERIENCE:

Sr. no	Name of the college/Institute	Designation	From	To
1.	Dayananda Sagar College of Engg. Bangalore.	Assistant Professor	10 th September, 2010	25 th May, 2013